NATIONAL ADVISORY COMMITTEE FOR AERONAUTICS

REPORT No. 396

HYDRAULICS OF FUEL INJECTION PUMPS FOR COMPRESSION-IGNITION ENGINES

By A. M. ROTHROCK

1931

For sale by the Superintendent of Documents, Washington, D. C. - - - - - - - - - - - - Price 25 cents

AERONAUTICAL SYMBOLS

1. FUNDAMENTAL AND DERIVED UNITS

	Symbol	Metric		English	
		Unit	Symbol	Unit	Symbol
Length	l	meter	m	foot (or mile)	ft. (or mi.)
Time	t	second	s	second (or hour)	sec. (or hr.)
Force	F	weight of one kilogram	kg	weight of one pound	lb.
Power	P	kg/m/s		horsepower	hp
Speed		km/h	k. p. h.	mi./hr.	m. p. h.
		m/s	m. p. s.	ft./sec.	f. p. s.

2. GENERAL SYMBOLS, ETC.

W, Weight $= mg$

g, Standard acceleration of gravity $= 9.80665$ m/s^2 $= 32.1740$ ft./sec.^{2}

m, Mass $= \frac{W}{g}$

ρ, Density (mass per unit volume).

Standard density of dry air, 0.12497 (kg-m^{-4} s^2) at 15° C. and 750 mm $= 0.002378$ (lb.-ft.$^{-4}$ sec.^{2}).

Specific weight of "standard" air, 1.2255 kg/m^3 $= 0.07651$ lb./ft.^{3}.

mk^2, Moment of inertia (indicate axis of the radius of gyration k, by proper subscript).

S, Area.

S_w, Wing area, etc.

G, Gap.

b, Span.

c, Chord.

$\frac{b^2}{S}$, Aspect ratio.

μ, Coefficient of viscosity.

3. AERODYNAMICAL SYMBOLS

V, True air speed.

q, Dynamic (or impact) pressure $= \frac{1}{2}\rho V^2$.

L, Lift, absolute coefficient $C_L = \frac{L}{qS}$

D, Drag, absolute coefficient $C_D = \frac{D}{qS}$

D_o, Profile drag, absolute coefficient $C_{D_o} = \frac{D_o}{qS}$

D_i, Induced drag, absolute coefficient $C_{D_i} = \frac{D_i}{qS}$

D_p, Parasite drag, absolute coefficient $C_{D_p} = \frac{D_p}{qS}$

C, Cross-wind force, absolute coefficient $C_C = \frac{C}{qS}$

R, Resultant force.

i_w, Angle of setting of wings (relative to thrust line).

i_t, Angle of stabilizer setting (relative to thrust line).

Q, Resultant moment.

Ω, Resultant angular velocity.

$\rho\frac{Vl}{\mu}$, Reynolds Number, where l is a linear dimension.

e. g., for a model airfoil 3 in. chord, 100 mi./hr. normal pressure, at 15° C., the corresponding number is 234,000;

or for a model of 10 cm chord 40 m/s, the corresponding number is 274,000.

C_p, Center of pressure coefficient (ratio of distance of c. p. from leading edge to chord length).

α, Angle of attack.

ϵ, Angle of downwash.

α_o, Angle of attack, infinite aspect ratio.

α_i, Angle of attack, induced.

α_o, Angle of attack, absolute. (Measured from zero lift position.)

γ Flight path angle.

REPORT No. 396

HYDRAULICS OF FUEL INJECTION PUMPS FOR COMPRESSION-IGNITION ENGINES

By A. M. ROTHROCK
Langley Memorial Aeronautical Laboratory

63287—31——1

NATIONAL ADVISORY COMMITTEE FOR AERONAUTICS

NAVY BUILDING, WASHINGTON, D. C.

(An independent Government establishment, created by act of Congress approved March 3, 1915, for the supervision and direction of the scientific study of the problems of flight. Its membership was increased to 15 by act approved March 2, 1929 (Public, No. 908, 70th Congress). It consists of members who are appointed by the President, all of whom serve as such without compensation.)

EXECUTIVE COMMITTEE

PREFACE

During the last few years there has been a decided increase in the number of organizations working on the development of the compression-ignition engine for aircraft service. The advantages of the compression-ignition engine are threefold: It operates at a high-compression ratio, from 11 : 1 to 16 : 1, which results in a higher cycle efficiency and consequently a lower fuel consumption than the carburetor engine with a compression radio of 5 : 1 to 7 : 1; radio interference caused by an electrical ignition system is eliminated without shielding; the fire hazard is considerably lessened, because of the low volatility of the fuel. There are two disadvantages to the compression-ignition engine: Because of the high cylinder pressures the parts of the engine are more highly stressed than in the carburetor engine; the allowable time for the injection and its mixture with the air in the combustion chamber is extremely short, so that it is difficult to obtain a high combustion efficiency.

One of the important problems in the design of a high-speed compression-ignition engine suitable for aircraft service is the design of the fuel injection system. There has been considerable work done both here and abroad to determine the operating characteristics of several types of systems. Until the latter part of 1929, however, there was little material available on the theory of fuel injection systems. Since then Doctor Sass has published material on the adaptation of the Allievi theory of water hammer to fuel injection pumps for compression-ignition engines. Before the publication of Doctor Sass's work, a series of tests had been made at the Langley Memorial Aeronautical Laboratory in which the instantaneous discharge pressures from a fuel injection pump were measured. With the data obtained in these tests and the theory presented by Doctor Sass, as well as additional analyses, it was thought advisable to write a report incorporating this material for use in the design of injection systems for high-speed compression-ignition engines.

In presenting this material in such a manner that it can be used in actual design, the author has attempted to give the mathematical analyses in such a way that they will be readily understood. Numerical examples are presented in considerable detail and emphasis is laid on the necessity of having all equations satisfied dimensionally. Although at times it may seem as though too much detail is included, the author felt that it was better to present some material that may seem obvious than to shorten the work so that the derivations could not be easily followed.

REPORT No. 396

HYDRAULICS OF FUEL INJECTION PUMPS FOR COMPRESSION-IGNITION ENGINES

By A. M. Rothrock

SUMMARY

Formulas are derived for computing the instantaneous pressures delivered by a fuel pump. The first derivation considers the compressibility of the fuel and the second, the compressibility, elasticity, and inertia of the fuel. The second derivation follows that given by Sass; it is shown to be the more accurate of the two. Additional formulas are given for determining the resistance losses in the injection tube. Experimental data are presented in support of the analyses. The report is concluded with an application of the theory to the design of fuel pump injection systems for which sample calculations are included.

INTRODUCTION

With the introduction of the high-speed compression-ignition engine, it became necessary to devise a method for injecting minute quantities of liquid fuel into the combustion chamber of the engine in extremely short time intervals. For slow-speed engines the mechanically operated injection valve had proved itself to be satisfactory. However, controlling the amount of fuel injected by the lift of a mechanically operated injection valve did not prove satisfactory for the higher speeds and the smaller fuel quantities required for automotive and aircraft engines, because of the difficulty of keeping the lift adjusted properly while in operation. Consequently, investigations were made to determine the possibility of accurately controlling the timing of injection and the quantity of fuel injected by means of a displacement pump. It was found that such pumps provided an accurate method of injecting the small fuel quantities required.

The use of direct injection from the fuel pump for automotive compression-ignition engines has steadily gained in favor, particularly in Germany, and at present the use of a common-rail injection system, with a mechanically operated injection valve, is rare for engine speeds of over 1,000 r. p. m. Of the aeronautical compression-ignition engines that have been successfully flight tested, the Packard, the Junkers, the Clerget, and the Fiat all use direct pump injection.

The different types of fuel pumps that have been employed are numerous. They have been described by several writers (references 1, 2, 3, and 4) according to the mechanical details of the pumps and the methods of regulating the fuel quantity delivered. The pumps can, in general, be divided into two classes: pumps in which the fuel quantity delivered is controlled by the stroke of the pump, and pumps in which the fuel quantity delivered is controlled by valves which by-pass the fuel for a certain part of the stroke. In the first class can be mentioned the Dorner system, as used on the Packard Aircraft Diesel (reference 5), and the Motorenfabrik Deutz pump (reference 4). Examples of the second class are the Bosch pump (reference 1), the N. A. C. A. single-cylinder pump (reference 6), and the Linke-Hofmann-Busch-Werke pump (reference 4). With pumps of the first class either a lever arm of variable length, as is used on the Dorner pump, or a bevel flank cam, as is used on the Motorenfabrik Deutz pump, may be employed. With the constant-stroke pump the by-pass valves may be port valves as employed on the Bosch pump, poppet valves as employed on the N. A. C. A. single-cylinder pump, or a combination of a poppet and a needle valve as employed on the Linke-Hofmann-Busch-Werke pump.

Two other types of pumps might be mentioned: pumps in which the fuel quantity delivered is controlled by a valve which by-passes part of the fuel during the injection stroke; and pumps in which the fuel quantity delivered is controlled by limiting the fuel drawn into the pump on the suction stroke. The former can be classed with the variable-stroke pumps and the latter with the constant-stroke pumps.

The construction of fuel injection pumps has been perfected to a high degree. Machining methods have progressed so that the pumps can be made reliable and sturdy at a cost that is not prohibitive. Too little attention has been paid, however, to the hydraulics of the system. Although it is known that pumps will meter minute quantities of fuel accurately, the manner in which the fuel is injected has been very much open to question. Unfortunately, there has not been sufficient experimental work done on the effect of the rate of fuel injection on engine performance to allow definite rules to be formed as to the rates of injection to be

employed. Ricardo (reference 7) has stated that the rate of combustion can be controlled by the rate of injection after combustion has been started. Neumann (reference 8) has made computations of the theoretical cycle efficiencies which should be obtained for various rates of fuel combustion. Wild (reference 1) has stated that for efficient combustion the fuel must be injected at an increasing velocity, so that, as injection proceeds, the unburned fuel entering the combustion chamber will penetrate through the burned gases into fresh air. However, Rheim (reference 9) and Schweitzer (reference 10) have both shown that the maximum penetration of the fuel spray is independent of the rate at which it leaves the nozzle, although as shown by Miller and Beardsley (reference 11) and Gelalles (reference 12), the rate of penetration for the first 0.002 or 0.003 second is affected by the rate at which the fuel leaves the nozzle. If the injection system is to be designed so that the rate of injection is controlled by the fuel pump, it is necessary to determine the effect of the rate of displacement of the fuel-pump plunger on the rate of fuel discharge from the discharge orifice. In such a determination there are several factors that must be taken into consideration. The most important of these are the compressibility, the elasticity, the inertia of the fuel column between the pump plunger and the discharge orifice, and the resistance to fuel flow through the injection system. Because of these factors, the fuel quantity discharged is generally less than the fuel quantity displaced at the fuel pump, even though the volumetric efficiency of the pump may be as high as 100 per cent. The resistance to flow can be made negligible by the use of flow passages of the correct internal diameter. The other factors mentioned must be considered in the design of the fuel pump and the injection valve. They do not constitute any disadvantage to the injection of the fuel once their effect is known and compensated for.

To design correctly a fuel-pump injection system that will inject the fuel according to a predetermined method, it is necessary to study the hydraulics of the injection system from the pump plunger to the discharge orifice. There are sufficient data on hydraulics available to permit an analysis to be made that will lead to certain principles to be used in pump design. It is the purpose of this report to present such an analysis based on the available data and formulas of hydraulics, as applied to fuel-pump injection systems, and to present experimental data to show how closely the analysis corresponds to actual pump operation.

The research was conducted at the Langley Memorial Aeronautical Laboratory, Langley Field, Va.

ANALYSIS

The instantaneous pressures p at the discharge orifice of a fuel injection system operated by a displacement pump are, at any pump angle θ, controlled by:

V—Velocity of the pump plunger at the angle θ, in units of length per degree of pump rotation.
A—Area of the pump plunger.
n—Pump speed, r. p. m.
T—Cross-sectional area of injection tube.
L—Length of the injection tube.
γ—Density of the fuel oil.
μ—Viscosity of the fuel at the pressure p.
E—Bulk modulus of the fuel.
R_θ—Total volume between the pump plunger and the discharge orifice at the angle θ.
a—Area of discharge orifice or area of sum of discharge orifices if a multiorifice nozzle is used.
c—Coefficient of discharge of discharge orifice or orifices.
p_i—Opening pressure of injection valve.
p_k—Pressure maintained in the injection tube between successive injections.

There are two methods of computing the instantaneous pressures at the discharge orifice from these variables. The first is to consider the fuel as compressible but to neglect pressure waves that occur in the system because of the compressibility of the fuel; that is, to assume that all pressures are transmitted instantaneously throughout the injection system. The method is applicable when the pressure-wave energy is small; that is, for low fuel velocities through the injection tube. The second method considers the pressure-wave energy, and is based on Allievi's theory of water hammer as adapted by Sass to the design of fuel injection systems for compression-ignition engines. (Reference 13.) The second method is the more accurate. The first is the simpler, but can be used only under the above conditions.

(a) ANALYSIS CONSIDERING COMPRESSIBILITY BUT NEGLECTING PRESSURE WAVES

The maximum pressure p_m which a fuel injection pump can deliver for a given pump-plunger velocity V is obtained by equating the rate of displacement at the fuel pump to the rate of discharge through the discharge orifice.

$$6AnV = ac\sqrt{\frac{2p_m}{\rho}} \tag{1}$$

in which ρ is equal to γ/g. The velocity V is multiplied by $6n$ because the velocity in units of distance traversed per second is equal to $6n$ times the velocity in units of distance traversed per degree of pump rotation. Solving for p_m

$$p_m = \frac{18(AnV)^2\rho}{(ac)^2} \tag{2}$$

It is seen that the maximum pressure at any given pump angle varies directly as the square of pump-plunger speed at that angle, and inversely as the fourth power of the discharge-orifice diameter. When pump injection is used for variable-speed engine operation, this variation of p_m with pump speed is an important factor. With a closed nozzle the injection-valve stem will remain lifted during the whole injection period at and above the speed which gives values of p_m for the injection period equal to or greater than $p_i a'/a''$. Here a' is the area of the injection valve stem exposed to the hydraulic pressure when the injection valve is closed, and a'' the area exposed to the hydraulic pressure when the valve is opened. At speeds below this the valve stem will oscillate, opening and closing the injection valve, unless there is sufficient volume of fuel under pressure to maintain the value of $p_i a'/a''$ due to the fluid compression.

The effect of engine speed on the instantaneous pressures which appear in both methods of computation, as will be seen later, presents one of the most serious difficulties in fuel-pump operation. Since the pressures vary with speed, the rate of fuel injection must also vary with speed. Consequently, the distance traversed by the fuel in the combustion chamber of the engine during the time available for combustion (reference 12) varies with the engine speed. Furthermore, according to the work of Triebnigg (reference 14), Woltjen (reference 15), Kuehn (reference 16), and Sass (reference 17), the atomization of the fuel spray varies with the injection pressure. It is seen, therefore, that with fuel-pump injection systems, the rate of penetration and the atomization of the fuel spray vary with engine speed. As a result, it can not be expected that the combustion characteristics will be the same at all speeds. This variation can be compensated for to a certain extent by the use of a variable rate-of-lift cam in the fuel pump, and by so designing the pump that the low rate-of-lift portion is used for high speeds and the high rate-of-lift portion for the low speeds, in which the rate of lift is considered with respect to pump degrees.

The maximum pressures given in equation (2) are seldom realized in operation because of the resistance to flow through the injection system, the inertia of the fuel, and the compressibility of the fuel. Consequently, the instantaneous pressures at any given pump angle vary as some power of the speed less than the square. The effect of the compressibility of the fuel can be treated in the following manner.

When the by-pass valve of the injection pump closes, or, if no by-pass valve is used, when the pump plunger starts its stroke, the displacement of the pump plunger starts to compress the fuel between the pump plunger and the discharge orifice, and, if an open nozzle is used, starts to discharge the fuel. If a closed nozzle is used, no discharge takes place until the fuel pressure is raised to the injection valve opening pressure. If the injection valve opening pressure is less than p_m, the pressure in the injection tubes continues to rise while discharge is taking place. If it be assumed that all pressures are transmitted instantaneously throughout the injection system and that the resistance to flow in the injection tube is neglible, the rate at which the fuel is displaced at the pump will be equal to the rate at which it is discharged at the injection valve plus the rate at which the fuel between the pump plunger and the injection valve is compressed. The rate at which the fuel is displaced at the pump plunger is given by the left-hand member of equation (1). The rate at which the fuel is discharged from the injection valve is given by the right-hand member of equation (1), in which p_m now becomes p. The rate at which the fuel is compressed is equal to the rate of change of pressure $6n\frac{dp}{d\theta}$, divided by the bulk modulus of the fuel, multiplied by the volume of fuel between the pump plunger and the discharge orifice at the angle θ. Therefore,

$$6AnV = ac\sqrt{\frac{2p}{\rho}} + 6n\frac{dp}{d\theta}\frac{R_\theta}{E} \tag{3}$$

Any system of units can be used in equation (3) provided that each unit chosen is used consistently throughout. For instance, assume that the units are pounds, inches, and seconds. Then, remembering that $6n$ has the units of degrees per second,

$$\text{deg. sec.}^{-1}\,\text{in.}^2\,\text{in. deg.}^{-1} = \text{in.}^2\sqrt{\frac{\text{lb. in.}^{-2}}{\frac{\text{lb. in.}^{-3}}{\text{in. sec.}^{-2}}}} + \text{deg. sec.}^{-1}\,\frac{\text{lb. in.}^{-2}}{\text{deg.}}\,\frac{\text{in.}^3}{\text{lb. in.}^{-2}}$$

$$\text{in.}^3\,\text{sec.}^{-1} = \text{in.}^3\,\text{sec.}^{-1} + \text{in.}^3\,\text{sec.}^{-1}.$$

It is seen that the units of the left-hand member of the equation are identical with the units of the right-hand member, so that equation is satisfied dimensionally. Equation (3) is the general pump equation, neglecting pressure-wave phenomena, which expresses the instantaneous pressures at the discharge orifice in terms of the dimensions of the injection system and the physical properties of the fuel.

If the value of V in equation (3) is constant, that is, if the fuel pump has a constant-velocity plunger motion, equation (3) can be integrated to

$$\frac{E}{6AnV}\log\left(\frac{R-AV\theta}{R}\right) = \frac{\rho}{ac}\left(\sqrt{\frac{2p}{\rho}} - \sqrt{\frac{2p_i}{\rho}}\right) + \frac{6AnV\rho}{a^2c^2}\times\log\left(\frac{6AnV - ac\sqrt{\frac{2p}{\rho}}}{6AnV - ac\sqrt{\frac{2p_i}{\rho}}}\right) \tag{4}$$

in which R is the total fuel volume at the start of injection, and is measured relative to the start of injection. The term $R-AV\theta$ represents the volume at any angle θ. The logarithms are with respect to the natural base e. The value of ρ is considered to be constant. The error introduced by this assumption

is negligible. The value of the constant of integration in equation (4) is obtained by letting $p=p_i$ when $\theta=0$. As θ is increased, the values of p approach the value of p_m, equation (2), as a limit. Consequently, it can be concluded that with a constant-velocity pump plunger varying instantaneous pressures can be obtained at the discharge orifice of the fuel-injection valve.

If the velocity of the pump plunger is a function of the pump angle θ, the integration of equation (3) is not so simple. A sufficiently accurate solution can be obtained by substituting for $\frac{dp}{d\theta}$ the expression $(p_b-p_a)/(\theta_b-\theta_a)$. The angles θ_b and θ_a are taken close enough together so that the error introduced by the approximation is small. Equation (3) now becomes

$$6AnV=ac\sqrt{\frac{2p_b}{\rho}}+6n\frac{p_b-p_a}{\theta_b-\theta_a}\frac{R_\theta}{E} \tag{5}$$

In solving equation (5) the initial value of p_a is taken as the injection valve opening pressure p_i. The value of p_b is obtained either by substituting trial values of p_b until the equation is satisfied, or by solving the equation as a quadratic in $\sqrt{p_b}$.

$$\sqrt{p_b}=\frac{-ac\sqrt{\frac{2}{\rho}}+\sqrt{\frac{2a^2c^2}{\rho}+\frac{144n^2AVR_\theta}{(\theta_b-\theta_a)E}+\frac{144n^2R_\theta^2}{(\theta_b-\theta_a)^2E^2}p_a}}{\frac{12n}{(\theta_b-\theta_a)}\frac{R_\theta}{E}} \tag{6}$$

By expanding and retaining only first powers of $(\theta_b-\theta_a)$ equation (6) can be simplified to

$$\sqrt{p_b}-\sqrt{p_a}=\frac{E(\theta_b-\theta_a)}{2R_\theta}\left(\frac{AV}{\sqrt{p_a}}-\frac{ac}{6n}\sqrt{\frac{2}{\rho}}\right) \tag{7}$$

Equation (7) can be used when the rate of change of the pump plunger velocity is small. When the value of R remains virtually constant, that is, when the volume of fuel in the injection tube is considerably greater than the total volume displaced by the fuel pump during injection, the use of equations (6) or (7) is recommended, since all the terms in the right-hand members can be considered constant except p_a and V. When the volume of fuel in the injection tube is not considerably greater than the volume displaced by the fuel pump, the solution by trial values of p_b is recommended.

If no check valve is employed between the pump and injection valve, the discharge stops with the opening of the cut-off valve or with the end of the pump stroke when a variable-stroke pump is used. Under these conditions the total fuel discharged is given by the equation

$$Q=Q_D-\frac{p_2-p_1}{E}R_2 \tag{8}$$

in which Q_D is the fuel quantity displaced by the pump, p_2 is the pressure at the end of injection, and R_2 the total volume of fuel under compression at the end of injection. Equation (8) shows that the total fuel quantity displaced may be considerably greater than the total fuel quantity discharged, even though the volumetric efficiency of the pump is 100 per cent. When a check valve is used, some of the fuel under pressure in the injection tube may be trapped, so that discharge continues after cut-off at the pump. The research on the common-rail system (reference 18) showed that, under certain conditions the rate of pressure drop in the injection tube when cut-off occurs may be even more rapid than the closing of the injection valve. Consequently, it can not be expected that a check valve will close so rapidly when cut-off occurs that the fuel in the injection line will continue to discharge through the discharge orifice until the injection valve closing pressure is reached. However, the maximum time during which discharge can take place after cut-off occurs can be obtained by assuming that the check valve closes instantaneously. In this case the discharge through the orifice after cut-off is at every instant equal to the rate of decompression of the fuel in the injection tube,

$$a\,c\sqrt{\frac{2p}{\rho}}=\frac{-R_2}{E}\frac{dp}{dt}. \tag{9}$$

The complete integral of equation (9) is

$$t=\frac{R_2}{Eac}\sqrt{2\rho}\left(\sqrt{p_3}-\sqrt{p}\right) \tag{10}$$

in which p_3 is the pressure in the injection tube at the instant cut-off occurs, and p is the instantaneous pressure t seconds after cut-off. Solving equation (10) for p

$$p=\left[\sqrt{p_3}-\frac{tEac}{R_2\sqrt{2\rho}}\right]^2 \tag{11}$$

(b) ANALYSIS CONSIDERING PRESSURE WAVES

Equations (6) and (11) are based on consideration of the static pressure phenomena in the fuel injection system. While the compressibility of the liquid fuel has been considered, the effects of the elasticity and inertia of the fuel have been omitted. Consequently, the equations fail when the effect of inertia and elasticity becomes appreciable. The phenomenon is now the same as that discussed by Allievi (reference 19) in his treatment of the flow of water under high pressure. Sass (reference 13) has adapted the Allievi theory to fuel pumps. Although at first the mathematics involved may seem complicated, a study of it shows that they are comparatively simple, and that the method is easily adapted to actual working conditions.

Following the method employed by Allievi, Sass shows that the differential equations representing the conditions in the fuel injection system (fig. 1) are:

$$\left.\begin{aligned}\frac{\partial v}{\partial t} &= -\frac{1}{\rho}\frac{\partial p}{\partial x}\\ \frac{\partial v}{\partial x} &= -\frac{1}{\rho s^2}\frac{\partial p}{\partial t}\end{aligned}\right\} \tag{12}$$

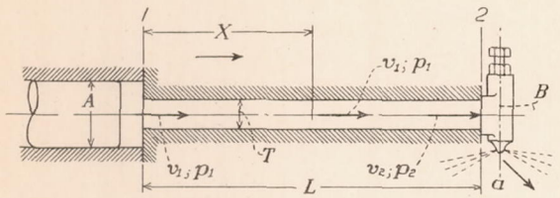

FIGURE 1.—Fuel pump for explanation of Sass's method

in which v is the velocity of the fuel at any time t and at any point x in the injection system between the pump plunger and discharge orifice, measured from the pump plunger; ρ is, as before, the density of the fuel divided by g; and s is the velocity of pressure waves in the system and is equal to $\sqrt{\frac{E}{\rho}}$.

The differential equations (12) are satisfied by the particular integral (see reference 13 for proof).

$$\left.\begin{aligned}p &= p_k + F\left(t-\frac{x}{s}\right)\\ v &= v_k + \frac{1}{\rho s}F\left(t-\frac{x}{s}\right)\end{aligned}\right\} \tag{13}$$[1]

wherein F is a function having the dimensions of pressure, ML^{-2}, determined by the boundary conditions and acting in the direction from the pump plunger towards the discharge orifice. As is shown later, F represents the pressure wave originating at the pump plunger, owing to the motion of the plunger. The argument of the function $t-x/s$ indicates that the pressure wave F reaches the point x in x/s seconds after the wave originated at the plunger. The quantities p_k and v_k represent the pressure and velocity in the system before the start of the injection. Consequently, v_k is equal to zero. When a check valve is used between the pump plunger and the injection tube, or when a high primary pressure is used to feed the injection pump, p_k has a value greater than zero. In fact, as will be shown later, it often exceeds $F(t-x/s)$. If the injection valve is so constructed that the disturbing pressure wave F is completely expended in forcing the fuel through the discharge orifice, the disturbance is completely determined by means of equations (13). In general, however, this is not the case, and a partial reflection of the wave F takes place at the discharge orifice, so that the reflected portion of F runs back from the discharge orifice toward the pump plunger. The function denomination of this reflected wave will be designated $-W$. The negative sign is used for W since it contains within itself the correct algebraic sign. This back-rushing wave on reaching the pump plunger is reflected again, and traverses the tube toward the discharge orifice. In general, there is a series of reflecting waves in the injection system caused by the partial reflection or, in some cases, the complete reflection of each successive wave at the discharge orifice. The form of all the waves is the same, and they differ only in amplitude. The phenomena consist, therefore, of two series of waves, one traversing the system from the injection pump to the discharge orifice, and the other traversing the system from the discharge orifice to the pump. The series do not interfere with each other, consequently the total pressure at any point in the injection system is the algebraic sum of the instantaneous pressures at that point.

Sass designates the symbol of the back-rushing wave as $-W\left(t+\frac{x}{s}\right)$, since the wave reaches the point x in x/s seconds before it reaches the pump where $x=0$.

Throughout his treatment, all the symbols of the waves are represented as the time interval between the wave passing the point x and reaching the pump plunger. Consequently, all waves in the positive direction of x have the symbol $t+x/s$ and all waves in the negative direction have the symbol $t+x/s$. With this system of notation all waves are considered as originating at the last reflecting surface. If all waves are considered as originating at the pump plunger, the symbol becomes $t-\eta L/s-\frac{(L-x)}{s}$ or $t-\frac{(\eta+1)L-x}{s}$ for waves traveling in the negative direction, and $t-\eta\frac{L}{s}-\frac{x}{s}$ or $t-\frac{\eta L+x}{s}$ for waves traveling in the positive direction, where η represents the number of reflections of the wave, and also designates the time at which the wave originated at the pump plunger, and L is the distance between the pump plunger and the discharge orifice.

The general integral of equation (12) can now be written, according to Sass's notation

$$\left.\begin{aligned}p_x &= p_k + F\left(t-\frac{x}{s}\right) - W\left(t+\frac{x}{s}\right) + U\left(t-\frac{x}{s}\right)\\ &\quad - V\left(t+\frac{x}{s}\right), \text{ etc.}\\ v_x &= \frac{1}{\rho s}\left[F\left(t-\frac{x}{s}\right) + W\left(t+\frac{x}{s}\right) + U\left(t-\frac{x}{s}\right)\right.\\ &\quad \left. + V\left(t+\frac{x}{s}\right), \text{ etc.}\right]\end{aligned}\right\} \tag{14}$$

[1] The term $F(t-x/s)$ is read F of $(t-x/s)$. It represents a quantity dependent on the conditions at the fuel pump x/s seconds earlier than the time under consideration

or using the author's notation

$$\left.\begin{aligned} p_x &= p_k + F\left(t-\frac{x}{s}\right) - W\left(t-\frac{2L-x}{s}\right) \\ &\quad + U\left(t-\frac{2L+x}{s}\right) - V\left(t-\frac{4L-x}{s}\right), \text{ etc.} \\ v_x &= \frac{1}{\rho s}\left[F\left(t-\frac{x}{s}\right) + W\left(t-\frac{2L-x}{s}\right)\right. \\ &\quad \left. + U\left(t-\frac{2L+x}{s}\right) + V\left(t-\frac{4L-x}{s}\right), \text{ etc.}\right] \end{aligned}\right\} \quad (15)$$

Consider the injection system shown in Figure 1. Let the pressures and velocities at the tube entrance be designated by the subscript 1, and those at the discharge orifice, by the subscript 2. Let the velocity of the pump plunger be represented by v_o. All velocities are considered with respect to time, and not pump degrees. For convenience consider the injection process divided into time intervals equal to L/s — the time required for a pressure wave to traverse the injection tube. Consider also that the injection process is divided into phases such that:

Phase I from $t=0$ to $t=L/s$.
Phase II from $t=L/s$ to $t=2L/s$.
Phase III from $t=2L/s$ to $t=3L/s$, etc.

In equation (15) the phase under consideration when x is equal to L is represented by the greatest value of $\eta+1$. As the equation is written, the greatest value of $\eta+1$ is 4. Consequently, the equation represents the conditions in the fourth phase. The F term represents the wave originating at the pump plunger at $t-L/s$ seconds. The W term is the reflected portion of the wave originating $\frac{2L-x}{s}$ seconds before the time under consideration; it is, consequently, the reflected portion of $F\ (t-2L/s)$. The U term represents the wave originating $\frac{3L-x}{s}$ seconds before the time under consideration. It is the reflected portion of $F\ (t-3L/s)$, and has, consequently, reached the pump plunger and is starting back toward the discharge orifice. The V term represents the reflected portion of the wave originating $\frac{4L-x}{s}$ seconds before the time under consideration. This wave, since its origin, has traversed the tube from the pump plunger to the discharge orifice, has been partially reflected traversing the tube back again to the pump plunger, where the partially reflected wave has been wholly reflected, and traversed the tube again to the discharge orifice, where a second partial reflection has taken place; and the second partially reflected wave has started back again toward the pump plunger and reached the point x. It is seen that the total number of reflections that any wave has experienced at the time under consideration is represented by the number η for that particular wave.

The total time since the start of injection is represented in equation (15) by setting the last symbol equal to zero and solving for t, or in this particular case

$$t=\frac{4L-x}{s}$$

The disturbance taking place during the first phase, that is, from the beginning of the injection at the fuel pump until the arrival of the initial wave at the discharge orifice, is expressed by equations (13) in which $v_k=0$.

$$\left.\begin{aligned} &I. \quad p_x = p_k + F\left(t-\frac{x}{s}\right) \\ &I. \quad v_x = \frac{1}{\rho s} F\left(t-\frac{x}{s}\right) \end{aligned}\right\} \quad (16)$$

in which the Roman numerals indicate the phase under consideration. Following Sass's treatment, consider the conditions at the pump plunger where $x=0$.

$$\left.\begin{aligned} &I. \quad p_1 = p_k + F(t) \\ &I. \quad v_1 = \frac{1}{\rho s} F(t) \end{aligned}\right\} \quad (17)$$

The fuel in the immediate vicinity of the pump plunger must move with the velocity of the pump plunger v_o, and at the entrance to the injection tube the velocity is equal to v_o multiplied by the ratio of the pump plunger area A to the injection tube area T.

$$v_1 = v_o\ A/T \quad (18)$$

For the first period, therefore

$$I. \quad v_1 = \frac{1}{\rho s} F\ (t) = v_o \frac{A}{T} \quad (19)$$

$$F\ (t) = \rho s\ v_1 = \rho s\ v_o \frac{A}{T} \quad (20)$$

From the pump speed and from the shape of the pump cam v_o, v_1, and consequently, $F\ (t)$ can be determined for all phases of the injection period. It is seen that F is a continuous function extending through the whole injection period.

The primary wave reaching the discharge orifice is also determined from equations (13) in which x is equal to L.

$$\left.\begin{aligned} &I. \quad p_2 = p_k + F\left(t-\frac{L}{s}\right) \\ &I. \quad v_2 = \frac{1}{\rho s} F\left(t-\frac{L}{s}\right) \end{aligned}\right\} \quad (21)$$

The value of the function $F(t-L/s)$ is identical with the function $F(t)=s\rho v_1$ except that it occurs L/s seconds

later than $F(t)$, the time L/s seconds representing the interval required for the wave to traverse the distance L between the pump plunger and the discharge orifice. Equations (21) may now be written

I.

$$\left.\begin{aligned} p_2 &= p_k + s\rho v_{1\,t-\frac{L}{s}} \\ v_2 &= v_{1\,t-\frac{L}{s}} \end{aligned}\right\} \qquad I. \qquad (22)$$

It is seen that the pressure at any point in the system during the first phase is equal to the initial pressure in the tube plus the wave energy from the motion of the pump plunger. Since $s\rho v_1$ represents a pressure, it must have the dimensions $M\,L^{-2}$. Writing the factors in dimensional form

$$\begin{aligned} s &= L\ T^{-1} \\ \rho &= \frac{M\ L^{-3}}{L\ T^{-2}} \\ v_1 &= L\ T^{-1} \\ s\rho v_1 &= L\ T^{-1}\ M\ L^{-3}\ L^{-1}\ T^2\ L\ T^{-1} \\ &= M\ L^{-2} \end{aligned}$$

If the pressure p_2 given in equations (22) is equal to or greater than the pressure required to open the injection valve, when an automatic injection valve is used, the pressure wave is in general partially reflected. The portion of the wave F which is reflected, designated $-W$, appears in the second phase. The pressure and velocity now prevailing in the injection tube are, consequently, of the order of the general equations (14) or (15).

II.

$$\left.\begin{aligned} p^2 &= p_k + F\left(t-\frac{L}{s}\right) - W\left(t-\frac{L}{s}\right) \\ v_2 &= \frac{1}{\rho\, s}\left[F\left(t-\frac{L}{s}\right) + W\left(t-\frac{L}{s}\right)\right] \end{aligned}\right\} \qquad II. \qquad (23)$$

multiplying the second equation by ρs and adding to the first

II.

$$p_2 + s\rho v_2 = p_k + 2\ F\left(t-\frac{L}{s}\right) \qquad (24)$$

Substituting for $F\ (t-L/s)$ its value $\rho s\ v_{1\,t-\frac{L}{s}}$

II.

$$p_2 + s\rho v_2 = p_k + 2\ \rho s\ v_{1\,t-\frac{L}{s}} \qquad (25)$$

which also represents the pressure conditions at the discharge orifice through the third phase. The quantity $\rho s\ v_2$ represents the portion of the wave $\rho s\ v_{1\,t-\frac{L}{s}}$, which is not reflected but is absorbed in the discharge of the liquid fuel from the discharge orifice. The velocity v_2 is the vector sum of the velocity of the oncoming wave $\rho s\ v_{1\,t-\frac{L}{s}}$ plus the velocity of its reflected portion $W\left(t-\frac{L}{s}\right)$. Consequently, v_2 must be equal to the velocity of the fuel through the discharge orifice multiplied by the ratio of the discharge orifice area a times its coefficient of discharge c to the tube area T.

$$v_2 = v_a \frac{a\ c}{T} \qquad (26)$$

in which v_a is the velocity through the discharge orifice. From the conservation of energy

$$p_2 + \frac{\rho}{2} v_2^2 = \frac{\rho}{2} v^2{}_a + p_z \qquad (27)$$

in which p_z is the pressure in the engine cylinder into which the discharge takes place. Substituting from equation (26)

$$p_2 = \frac{\rho}{2} v_2^2 \left[\left(\frac{T}{ac}\right)^2 - 1\right] + p_z \qquad (28)$$

Since in practice the ratio $(T/ac)^2$ is large, equation (28) can be simplified to

$$p_2 - p_z = \frac{\rho}{2} v_2^2 \left(\frac{T}{ac}\right)^2 \qquad (29)$$

Equations 25 and 29 both contain the parameter v_2 which can be eliminated between them, resulting in a quadratic equation in p_2 which can be solved for p_2. In which case

$$p_2 - p_z = \frac{1}{4}\left[-\rho\frac{sac}{T}\sqrt{\frac{2}{\rho}} + \sqrt{\left(\rho\frac{sac}{T}\sqrt{\frac{2}{\rho}}\right)^2 + 4(p_k + 2\rho s\ v_1 - p_z)}\right]^2 \qquad (30)$$

Since $\left(\rho\frac{sac}{T}\sqrt{\frac{2}{\rho}}\right)^2$ is generally small, equation (30) can be simplified to

$$p_2 - p_z = \frac{1}{4}\left[-\rho\frac{sac}{2T}\sqrt{\frac{2}{\rho}} + \sqrt{p_k + 2\rho s\ v_1 - p_z}\right]^2 \qquad (31)$$

A second method of obtaining p_2 is the graphical method employed by Sass using equations (25) and (29). From the cam contour determine the range of values for v_1. Substituting in equation (29) values of v_2 equal to the values of v_1, plot a curve of p_2 against $p_2 + s\rho v_2$. Since from equation (25), $p_2 + s\rho v_2 = p_k + 2s\rho v_{1\,t-\frac{L}{s}}$, this is also a curve of p_2 against $p_k + 2s\rho v_{1\,t-\frac{L}{s}}$. From the values of $p_k + 2s\rho v_{1\,t-\frac{L}{s}}$ the corresponding values of p_2 are obtained from the curve. Consequently, the instantaneous pressures are determined at the discharge orifice for the second phase. In the same manner, the quantity $s\rho v_2$ can be determined. It represents the portion of the wave that is lost because of the discharge through the discharge orifice.

If the first equation of (23) is subtracted from equation (24), the value of the back-rushing wave $-W$ is obtained.

$$\rho s v_2 - \rho s v_{1_{t-\frac{L}{s}}} = W\left(t-\frac{L}{s}\right) \tag{32}$$

Equation (32) shows that the reflected wave is equal to the oncoming wave less the wave energy lost to discharge. Had the pressure p_2 been less than the valve opening pressure, v_2 would be equal to zero, since no discharge could take place, and the oncoming wave would be completely reflected. Consequently, for the case of complete reflection

II.

$$p_2 = p_k + 2\rho s v_{1_{t-\frac{L}{s}}} \tag{33}$$

It is difficult to determine the exact conditions existing during the start of discharge from the injection valve when a closed nozzle is used. Sass undertakes, at this point in the analysis, to consider the movement of the injection valve stem. He assumes that the lift of the stem is at all times equal to the lift that would be obtained with a static pressure equal to the computed instantaneous pressures. This method does not consider the inertia of the injection valve stem and spring; consequently, the results are in error, unless the frequency of the stem and spring is extremely high. In commercial injection valves this is seldom true, the frequencies being of the order of 500 cycles per second for injection valves designed for high-speed engine operation. (Reference 18.) If the injection valve is so designed that a small fraction of the total lift of the stem presents a flow area considerably greater than the flow area of the discharge orifice, the effect of the stem motion may be neglected. If this is not the case, the oscillations of the stem will affect the discharge of the fuel and may, in some cases, cause the stem to strike the injection valve seat, causing momentary stopping of the discharge. (See fig. 42.) As will be shown later by the experimental records, when the injection tube is of sufficient size to insure laminar flow through it, the lift of the injection valve stem required to present a flow area equal to the discharge orifice is reached in an extremely short time. Consequently, the effect of the injection valve stem movement is neglected, and the flow is assumed to start instantaneously when the injection valve opening pressure is reached.

In Sass's computations he considers that the initial wave reaching the discharge orifice is completely reflected, since reflection takes place instantaneously. The author has assumed that partial reflection takes place because of the difficulty of accurately analyzing the conditions that take place during the small time interval between the start of opening of the injection valve and the time when the stem has reached a lift sufficient to permit unrestricted flow around it.

The back-rushing wave $-W$ reaches the pump plunger $2\,L/s$ seconds after the wave of which it is the partial reflection originated at the pump plunger, and it is completely reflected, reaching the discharge orifice L/s seconds later, which is the end of the third phase. The interpretation of equations (14) and (15) is now fully explained. For the conditions at the pump where $x=0$ and considering t equal to $2\,L/s$

III.

$$p_1 = p_k + F(t) - W\left(t-\frac{2L}{s}\right) + U\left(t-\frac{2L}{s}\right)$$

III.

$$v_1 = \frac{1}{\rho s}\left[F(t) + W\left(t-\frac{2L}{s}\right) + U\left(t-\frac{2L}{s}\right)\right] \tag{34}$$

It is seen that the argument of $-W$ is the same as that of U. This is because W is instantaneously reflected. Since no wave energy is lost during reflection at the pump plunger, U is equal to W but opposite in sign. Equations (34) can, therefore, be written

III.

$$p_1 = p_k + F(t) - 2W\left(t-\frac{2L}{s}\right)$$

III.

$$v_1 = \frac{1}{\rho s} F(t) \tag{35}$$

As was the case for complete reflection at the discharge orifice, the velocities of W and U are identical but opposite in sign, so that V_1 during the third phase is equal to $\frac{1}{\rho s} F(t)$ which is equal to $v_o A/T$. The onrushing wave of the third phase $\rho s v_{1_{t-\frac{L}{s}}}$ is now reenforced by the reflection of the reflected wave of the first phase, that is, by U. These two waves reach the discharge orifice together at the end of the third phase. Equation (15) now becomes for $x=L$

III.

$$p_2 = p_k + F\left(t-\frac{L}{s}\right) - W\left(t-\frac{L}{s}\right) + U\left(t-\frac{3L}{s}\right) - V\left(t-\frac{3L}{s}\right)$$

III.

$$v_2 = \frac{1}{\rho s}\left[F\left(t-\frac{L}{s}\right) + W\left(t-\frac{L}{s}\right) + U\left(t-\frac{3L}{s}\right) + V\left(t-\frac{3L}{s}\right)\right] \tag{36}$$

which represents the conditions during the third phase. In equations (36) F represents the wave originating at the pump plunger during the third phase, W represents the reflected portion of it, U represents the reflected portion of the wave originating during the first phase, and V represents the reflected portion of U. The equation can be simplified by combining the two reflected portions W and V into a single reflected wave W'.

$$\left.\begin{aligned} &III.\\ &p_2 = p_k + F\left(t-\frac{L}{s}\right) + U\left(t-\frac{3L}{s}\right) - W'\left(t-\frac{L}{s}\right)\\ &III.\\ &v_2 = \frac{1}{\rho s}\left[F\left(t-\frac{L}{s}\right) + U\left(t-\frac{3L}{s}\right) + W'\left(t-\frac{L}{s}\right)\right] \end{aligned}\right\} \quad (37)$$

It has already been shown that U is equal to, but opposite in sign to the reflected portion of the preceding phase, and is therefore equal to

$$\rho s v_{1\,t-\frac{3L}{s}} - \rho s v_{2\,t-\frac{2L}{s}}$$

Substituting in equation (37)

$$\left.\begin{aligned} &III.\\ &p_2 = p_k + \rho s v_{1\,t-\frac{L}{s}} + \left(\rho s v_{1\,t-\frac{3L}{s}} - \rho s v_{2\,t-\frac{2L}{s}}\right) - W'(t-\frac{L}{s})\\ &III.\\ &v_2 = v_{1\,t-\frac{L}{s}} + \left(v_{1\,t-\frac{3L}{s}} - v_{2\,t-\frac{2L}{s}}\right) + \frac{1}{\rho s}W'(t-\frac{L}{s}) \end{aligned}\right\} \quad (38)$$

All the values in equations (38) are known with the exception p_2, v_2, and W'. They are determined in the same manner as was used in the derivation of equation 32. If the graphical method is employed, the same curve of p_2 against $p_2 + psv_2 = p_k + 2s\rho v_{1\,t-\frac{L}{s}}$ can be used, since the two oncoming waves can be considered as a single wave.

By the use of equations (38) the general equations (14) or (15) can be simplified into

$$\left.\begin{aligned} {}^{t}_{p_2} &= p_k + F\left(t-\frac{L}{s}\right) - W\left(t-\frac{2L}{s}\right) - W'\left(t-\frac{L}{s}\right)\\ {}^{t}_{v_2} &= \frac{1}{\rho s}\left[F\left(t-\frac{L}{s}\right) + W\left(t-\frac{2L}{s}\right) + W'\left(t-\frac{L}{s}\right)\right] \end{aligned}\right\} \quad (39)$$

in which W represents the reflection of all waves reaching the discharge orifice 2 L/s seconds before the time t under consideration, and W' represents the reflected portion of both F and W. The use of equations (39) results in the computations for actual cases being much shorter than the use of equations (14) or (15) which Sass employs because equations (39) consider all waves in the positive direction as a single wave, and all waves in the negative direction as a single wave, whereas equations (14) or (15) consider each wave individually.

The first equation in equations (39) may also be written

$$p^{t}_{2} = p_k + 2\left(s\rho v_{1\,t-\frac{L}{s}} + s\rho v_{1\,t-\frac{L}{s}}'\right) - s\rho v_2 \quad (40)$$

in which v_1' represents the sum of all reflected waves leaving the pump plunger at $t-\frac{L}{s}$.

In reference 13 Sass has applied the general equations (14) to a numerical example. He has, however, made an error in computing the tertiary wave U. He has correctly shown that the pressure at the pump plunger for values of t equal to and greater than $2L/s$ is given by equations (35). He has, however, incorrectly assumed that the onrushing wave is now equal to $F(t-L/s)-2\,W(t+L/s)$. Consequently, although he correctly computes the values of $p_k+2\left[F\left(t-\frac{L}{s}\right)-W\left(t+\frac{L}{s}\right)\right]$ from which the values of p_2 for the various phases are computed, the values of his back-rushing waves are incorrect after the start of the third phase. He considers them as being equal to

$$W'\left(t-\frac{L}{s}\right) = p_2 - \left[p_k + F\left(t-\frac{L}{s}\right) - 2W\left(t+\frac{L}{s}\right)\right]$$

This results in the final pressures being computed to be greater than they actually are. Actually they are given, from the substitution of equation (32), in equation (23) by

$$W'\left(t-\frac{L}{s}\right) = p_2 - \left[p_k + F\left(t-\frac{L}{s}\right) - W\left(t+\frac{L}{s}\right)\right]$$

Since the motion of the fuel injection pump plunger is considered as being transmitted instantaneously to the fuel in the injection tube, the curve for the pressures at the discharge orifice jumps instantaneously from p_k to $p_k + 2s\rho v_{1\,t-\frac{L}{s}} - s\rho v_2$. This is not the case in actual operation since an appreciable time lag must elapse between the start of the closing of the by-pass valve of the injection pump and its complete closure. This jump in the curve occurs again when the reflected portion of the initial wave again reaches the discharge orifice at $t=3L/s$ and for all values of $t=\eta L/s$ for which η is an odd number. However, each time this wave reaches the discharge orifice it loses some of its intensity to the discharging fuel. Consequently, the wave continually decreases in intensity, and finally disappears.

As has been stated, under certain conditions no reflection of the pressure waves takes place. This is true when all the wave energy is absorbed in the discharge of fuel through the discharge orifice. Under this condition v_2 is equal to $v_{1\,t-\frac{L}{s}}$ Substituting the value of p_2 obtained in equation (29) in equation (25) and setting v_2 equal to $v_{1\,t-\frac{L}{s}}$

$$v_{1\,t-\frac{L}{s}} = s\left(\frac{ac}{T}\right)^2 + \sqrt{s^2\left(\frac{ac}{T}\right)^4 + \frac{2}{\rho}\left(\frac{ac}{T}\right)^2 p_k} \quad (41)$$

which represents the value of v_1 for which no reflection of the wave takes place. For any values of v_1 less than this the reflected wave will be one of rarefaction and W will be positive in sign and $-W$ will become negative in value.

(c) DETERMINATION OF VELOCITY OF PRESSURE WAVES

In all the computations presented in this report, the value of s has been computed from the value of E given by Hersey (reference 20), 284,000 pounds per square inch. This value was chosen from fuels of similar properties to that used in the experimental work. The corresponding value of s is 59,600 inches per second. Sass (reference 13) uses the value of E determined experimentally for Diesel oil by Alexander (reference 21) 296,000 pounds per square inch. The corresponding value of s is 60,000 inches per second. The author has determined directly, in the investigation of the time lags of injection systems (reference 22) the approximate value of s. Using the injection system shown in Figure 2, he measured the time lag between the release of pressure at the timing value and the appearance of the fuel spray from the discharge orifice. Figure 3 shows the effect of injection tube length on the time lag. It is seen that the difference in time lag between a 70-inch tube and a 10-inch tube is 0.0012 second. Dividing this time into the difference in tube length, 60 inches, the value of s is found to be 50,000 inches per second, which checks the values computed from E to a reasonable degree of accuracy.

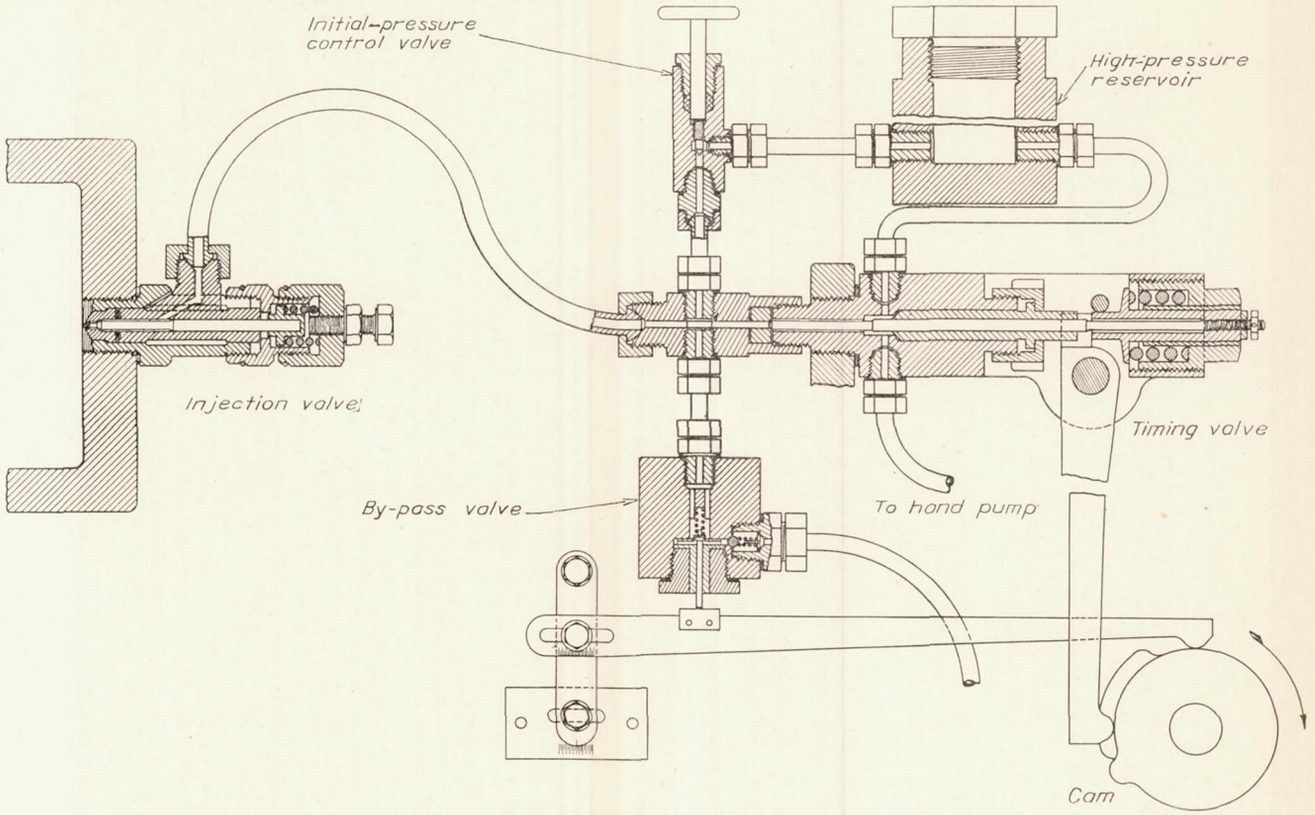

FIGURE 2.—Fuel spray injection system

(d) EFFECT OF EXPANSION OF INJECTION TUBE

According to Sass, any expansion of the injection tube will decrease the velocity of the pressure waves in the tube. He shows, however, that the decrease is negligible. The equation for the velocity in a tube in which expansion takes place is given by Sass (reference 13) as

$$s' = \sqrt{\frac{1}{\left(\frac{1}{E} + \frac{1}{\epsilon}\frac{D'}{D}\right)\rho}}$$

in which ϵ is the bulk modulus of the injection tube material, D' the outside diameter of the injection tube, and D the inside diameter. When ϵ becomes infinite

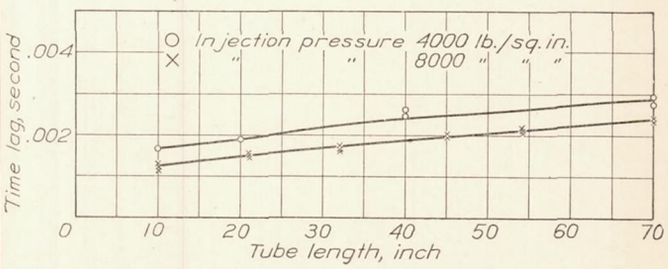

FIGURE 3.—Effect of tube length on time lag. Initial pressure, 1,000 lb./sq. in.; valve opening pressure, 4,000 lb./sq. in.

the equation becomes $s = \sqrt{\frac{E}{\rho}}$. The equation for s' can be rewritten as

$$s' = \sqrt{\frac{E}{\rho}}\sqrt{\frac{\epsilon D}{\epsilon D + ED'}}$$

In practice D' is equal to approximately $2D$. The

value of ϵ is approximately 30,000,000 pounds per square inch, so that

$$\sqrt{\frac{\epsilon D}{\epsilon D+ED'}}=\sqrt{\frac{\epsilon}{\epsilon+2E}}$$
$$=\sqrt{\frac{3\times10^7}{3\times10^7+0.057\times10^7}}$$
$$=0.99$$

Therefore,

$$s'=0.99\,s,$$

a decrease of 1 per cent, which is negligible.

The steel injection tubes used in the tests, the results of which are presented in the next section, had outside diameters of approximately twice the inside diameters. Consequently, the effect of the injection tube expansion was neglected.

e) INVESTIGATION OF RESISTANCE TO FLOW IN THE INJECTION SYSTEM

In both the preceding analyses it has been considered that the resistance to flow in the injection tube is negligible. This is true only when the injection tube is of sufficient size to insure small resistance losses. The resistance depends on the type of flow through the injection tube. For low velocities the flow is laminar and the resistance varies as the first power of the velocity and the viscosity. It is expressed in units of pressure by the relationship

$$p=32v_1\mu L/D^2. \tag{42}$$

For a pump plunger of a given diameter and for a given plunger velocity the value of v_1 is given from equation (19) as

$$v_1=\frac{v_oA}{\frac{\pi}{4}D^2}=\frac{24nVA}{\pi D^2} \tag{43}$$

in which $v_o=6nV$ and D is the injection tube diameter. Substituting in equation (42)

$$p=\frac{768nVA}{\pi D^4}\mu L \tag{44}$$

Therefore, other conditions remaining the same, the resistance in the injection tube, with laminar flow, varies inversely as the fourth power of the injection tube diameter.

As the velocity through the tube is increased, owing to an increase in the pump plunger velocity, the flow changes from laminar to turbulent. The lowest velocity at which this transformation begins is termed the lower critical velocity. It is that velocity for which Reynolds Number $\frac{vD}{\nu}$ is equal to approximately 2,000, and is, therefore, expressed by the relationship

$$v_k=2000\frac{\nu}{D} \tag{45}$$

in which ν is the kinematic viscosity and is equal to μ/ρ. The maximum velocity through the injection tube is expressed by equation (43). Equating v_1 in equation (43) to v_k in equation (45),

$$\frac{6nVA}{\frac{\pi}{4}D^2}=2000\frac{\nu}{D},$$

and

$$D_k=\frac{6nVA}{500\pi\nu} \tag{46}$$

which expresses the tube diameter for the critical velocity in terms of the pump speed and the kinematic viscosity, and determines the minimum injection tube diameter to be used at any pump speed. From equation (46) and a knowledge of the pump dimensions the injection tube diameter for the critical velocity can be determined for all speeds of the pump. Since ν varies as some power of p_m greater than one, and p_m varies as the square of n, the curve of D_k against n may show a maximum. (See fig. 29, Appendix III.)

For turbulent flow the resistance varies as the square of the velocity and as the density. It is expressed in units of pressure by the equation

$$p=fL\frac{v_1^2\rho}{2D} \tag{47}$$

in which f is the coefficient of friction and is given by Hopf (reference 23) as

$$f=0.00714+0.6104\left(\frac{v_1D}{\nu}\right)^{-0.35} \tag{48}$$

It is noticed that f is a function of Reynolds Number, v_1D/ν and consequently is a function of both the density and viscosity of the fluid. However, since Reynolds Number is raised to the -0.35 power, the value of f shows little variation with either the viscosity or the density. Substituting the value of v_1 from equation (43) in equation (47)

$$p=8\,fL\rho\frac{v_o^2A^2}{\pi^2D^5} \tag{49}$$

Therefore, other conditions remaining the same, the resistance to flow through the injection tube when the flow is turbulent varies inversely as the fifth power of the injection tube diameter.

Since in both the analyses for determining the instantaneous pressures the resistance to flow was neglected, the analyses hold only for those injection tube diameters equal to or greater than the values given in equation (46). The values of pressure used in determining the equation for the critical diameter are obtained from equation (2) which is only a first approximation of the actual pressures; consequently, the values of D_k obtained from equation (46) are not exact. The method is, however, accurate enough for practical use. The general rule to follow is not to use injection tubes of diameters smaller than those given in equation (46), using the method of evaluation employed in Appendix III. In evaluating these equa-

tions extreme care must be used to obtain all functions in the correct units.

In adapting the above method to the design of a fuel injection system, it is well to remember that temperature has a marked effect on the viscosity of the fuel. (Reference 20.) An increase of 20° F. may decrease the viscosity 100 per cent. If the flow in the injection tube is in the laminar range, this decrease will decrease the resistance (equation (42)), but if the flow is in the turbulent range, this decrease will increase the resistance (equation (48)).

EXPERIMENTAL DETERMINATION OF DISCHARGE PRESSURES

(a) METHODS AND APPARATUS

The fuel pump used in the tests to determine the applicability of the analyses is shown diagrammatically in Figure 4. The load control was obtained by rotating the pump plunger by means of the ratchet. This varied the position at which the slot in the pump

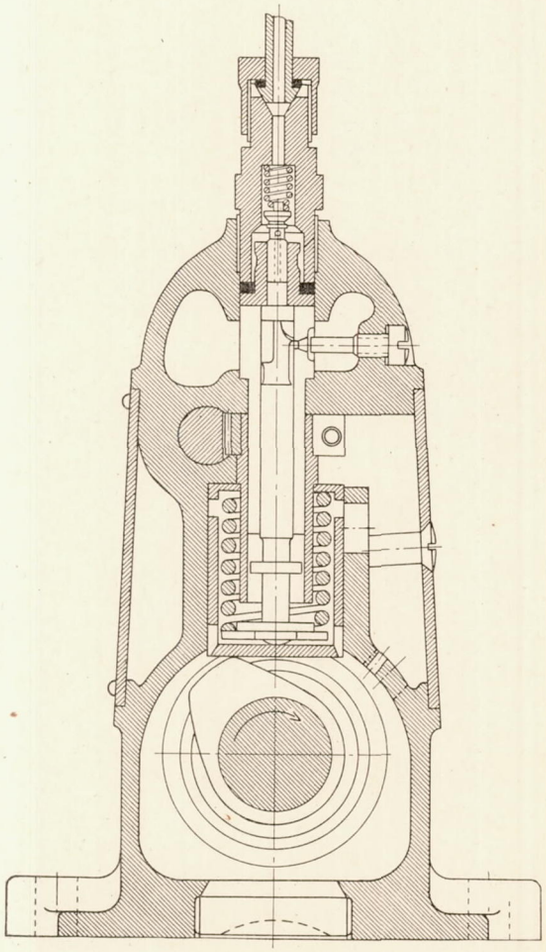

FIGURE 4.—Diagrammatic sketch of fuel pump used in tests

plunger came in contact with the ports in the sleeve. No primary fuel pressure was used other than a head of approximately 1½ feet of fuel. The pump plunger had a diameter of 0.354 inch. The lift and velocity of the pump plunger are shown in Figure 5. The lift data were obtained by means of an extensometer gage, accurate to 0.0005 inch. The velocity curve was obtained by drawing tangents to the lift curve at 2.5° intervals. Although the pump was not necessarily designed for injection over the decreasing velocity portion of the cam, this portion was used in the tests in order to determine the instantaneous

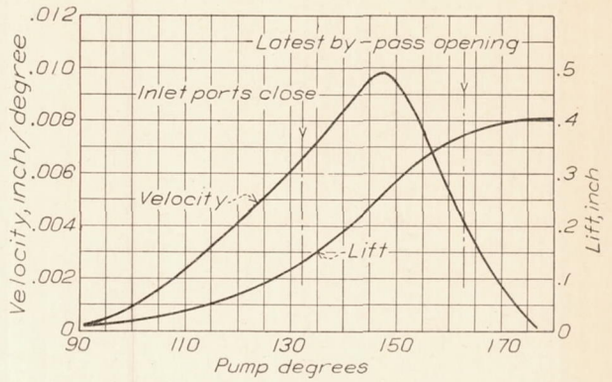

FIGURE 5.—Plunger velocity and lift curves for fuel pump used in tests

pressures delivered by the pump after the maximum velocity was reached.

The injection valve was the same as that used in the tests on the pressure fluctuations in a common-rail fuel injection system. (Reference 18.) The instantaneous pressures at the discharge orifice were determined experimentally by the same method as used in the investigation of the common-rail system from an analy-

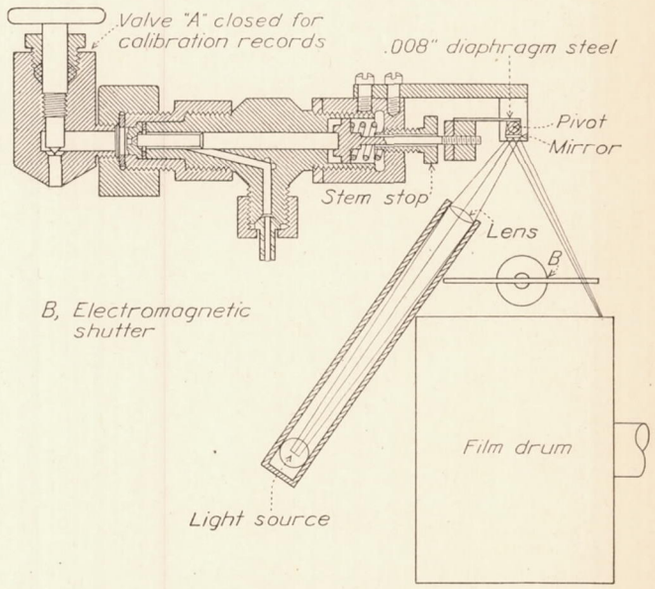

FIGURE 6.—Automatic injection valve and apparatus for recording valve stem movement

sis of photographic records of the movement of the injection valve stem. (Reference 18.) The injection valve and the apparatus for recording the injection valve stem movement are shown in Figure 6. The image of the light source was reflected from the pivoted mirror and focused on the film drum. The film drum was rotated by a synchornous motor at a peripheral

speed of approximately 1,000 inches per second. Any motion of the injection valve stem caused the reflected light beam to traverse the photographic film on the drum and record the stem movement. The electromagnetic shutter was controlled so that the light beam fell on the drum during only one revolution of the pump. Consequently, the record of the stem was obtained for one injection only, although the pump was operating continuously.

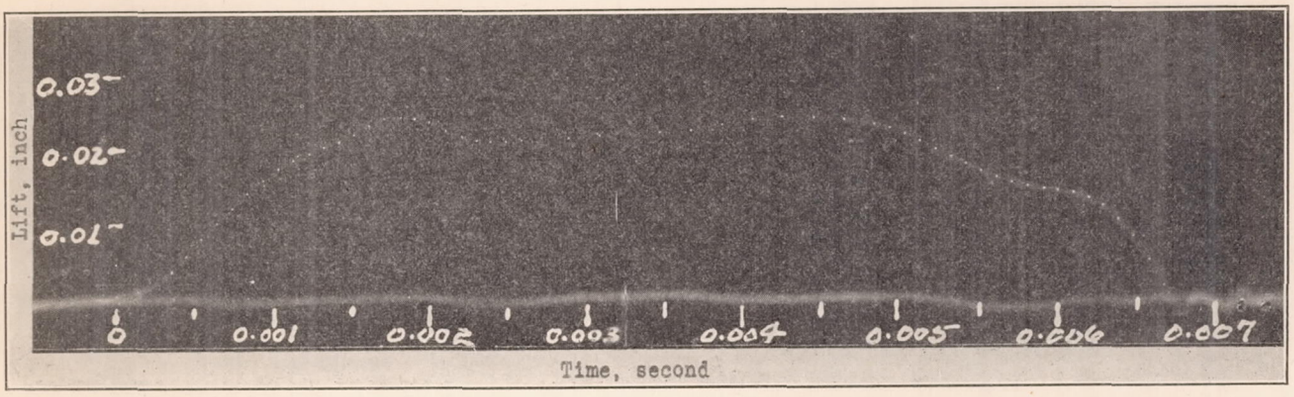

FIGURE 7.—Record of injection valve stem movement. (Small points indicate intervals at which lift was taken from record for analysis)

The method of obtaining the instantaneous pressures on the valve stem from the stem record has been described in detail in reference 18. It consisted of determining the hydraulic pressure from the force equilibrium equation

$$Pa = \lambda S + ma$$

in which P is the mean instantaneous pressure across the stem at any time t, a the area of the stem, λ the spring scale, S the stem lift at the time t, m the mass of the moving parts, and a the acceleration at the time t. The values of S and a were determined from the stem-movement record. The records were calibrated by the method described in reference 18, except in this case it was necessary to disconnect the injection tube from the injection valve and connect the injection valve to a hand-operated high-pressure pump for the calibration of the records. This was done without changing either the position of the injection valve or the recording light. A typical record of the injection valve stem motion is shown in Figure 7. The discharge orifice was one of those used by Gelalles in his investigation of the coefficient of discharge. (Reference 24.) It had a discharge coefficient of 0.94 when installed in the injection valve. (Reference 24.)

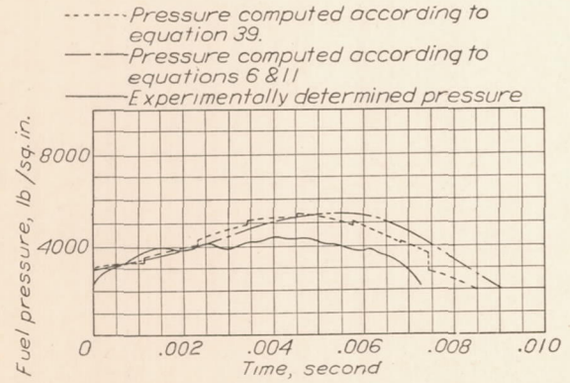

FIGURE 8.—Comparison of test pressures with computed pressures

(b) RESULTS AND DISCUSSION

Modifications to equations (6) and (39).—If the experimental results obtained under the same conditions as the computed results (see Appendices I and II) are compared (fig. 8), zero time refers to the arrival of the initial wave at the discharge orifice, it is seen that both the computed curves give pressures in excess of the experimental curve. It is now necessary to determine in what manner the analyses of the general equations differ from the experimental conditions.

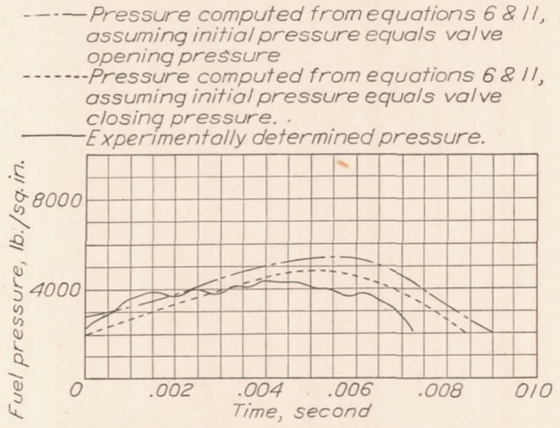

FIGURE 9.—Comparison of test pressures with pressures computed from equations (6) and (11) assuming initial pressure equals the valve closing pressure and the valve opening pressure

In equation (6) it was assumed that the initial pressure at the discharge orifice for the start of injection was equal to the injection valve opening pressure. The recorded lift of the injection valve stem indicates that the effective pressure was actually lower than this, otherwise the initial rate of lift would have been

greater. As has been mentioned before, the conditions existing during the start of injection are difficult to analyze. The assumption will now be made that the initial pressure at the start of injection is not the injection valve opening pressure but the injection valve closing pressure, in order to take care of the unstable conditions at the discharge orifice when the injection valve starts to open. With this assumption the results are again computed, and the resulting curve is shown in Figure 9. It is seen that it more closely fits the experimental curve.

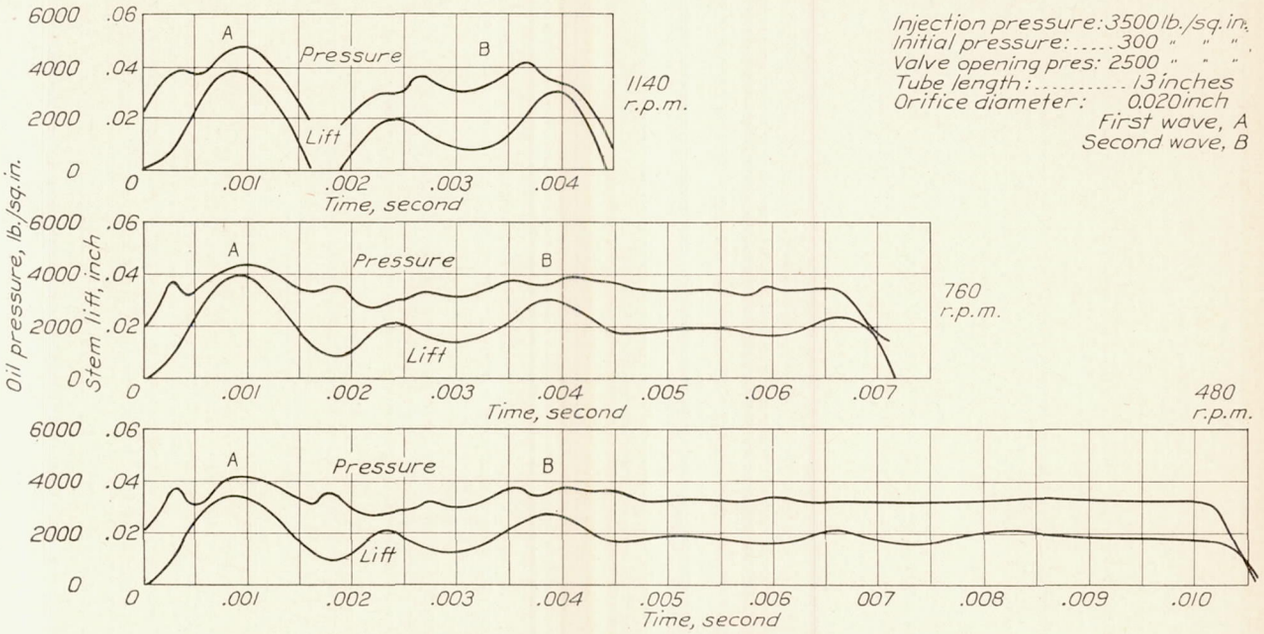

FIGURE 10.—Effect of timing valve cam shaft speed and injection period on stem lift and oil pressure

In the adaptation of equation (39) to the experimental results, it is necessary to make an assumption regarding the damping of the pressure waves. An indication of the damping (fig. 10) is obtained from the investigation of the common-rail system. (Reference 18.) Although the experimental conditions were different from those experienced with a pump, in that the injection was caused by fuel in a reservoir under a high pressure instead of the displacement fuel in a pump, both systems operated under conditions which gave pressure-wave phenomena. Referring to Figure 10, it is seen that the pressure-wave oscillations in the system illustrated in Figure 2 did not occur after the second wave. Consequently, the same assumption will be made in the application of equation (39). The results of the computation, neglecting all reflected waves after the second reflection, are shown in Figure 11. It is seen that under this assumption the results from equation (39) fit the experimental curve more closely than those from equations (6) and (11), indicating that the pressure waves in the system exert the controlling effect on the injection characteristics.

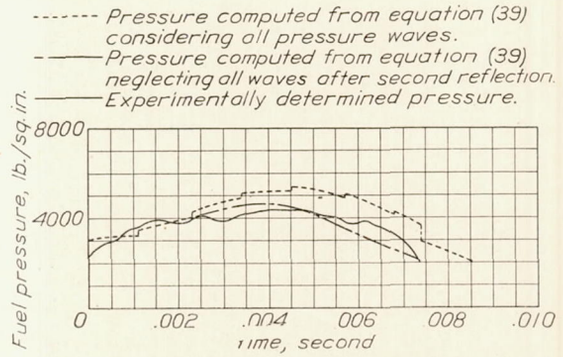

FIGURE 11.—Comparison of test pressures with pressures computed from equation (39) assuming all pressure waves destroyed after second reflection at the discharge orifice

The conclusions are drawn that in adapting equation (6) to the computation of the instantaneous pressures the initial pressure at the start of injection is considered to be the injection valve closing pressure, and that in adapting equation (39) to the computation of the instantaneous pressures, all pressure waves after the second reflection are considered to be destroyed by the damping effects of the system.

Effect of injection valve closing pressure.—Figures 12 and 13 show the effect of the injection valve closing pressure on the injection valve stem lift and on the instantaneous pressures. The solid pressure-curve represents the pressure determined from the experimentally recorded stem lift record, and the broken curves represent the pressures computed from equations (6), (11), and (39) with the modifications discussed in the preceding paragraphs. The injection valve closing pressure can be more accurately determined by the use of the calibration records (reference 18) than the opening pressure, since the opening pressure is obtained by observing the pressure at which the spray first issues from the nozzle as the pressure in the injection valve

is built up by means of a hand pump. The ratio of the stem area exposed to the hydraulic pressure before the stem lifted to the area exposed after the stem lifted was 0.70 for the injection valve used in the tests.

At 750 r. p. m. the injection period at the fuel pump was 0.0071 second. At 470 r. p. m. the injection period at the pump was 0.0113 second. Consequently, when the injection period covers a greater interval than the above time intervals at the respective speeds, the injection is continued because of the fuel under compression in the injection tube when equation (6) is used, or by the continued oscillations of the pressure waves in the injection tube when equation (39) is used. Equation (11) is used to complete the computations of the injection process when the pressure given by equation (6) is greater than the injection valve closing pressure at cut-off at the fuel pump.

At 750 r. p. m. it is seen that at the lowest valve closing pressure the injection period is greater than the time interval during which the by-pass valve at the pump is closed (0.0071 second). As the valve closing pressure was increased, the injection period decreased

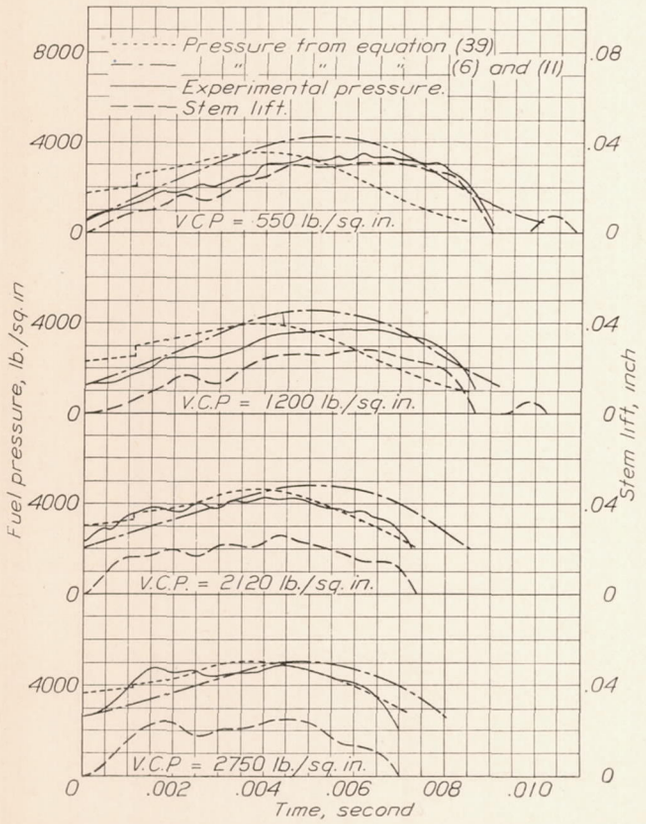

FIGURE 12.—Effect of valve closing pressure on stem lift and fuel pressure. Pump speed=750 r. p. m.; tube length=34 inches; inside tube diameter=0.138 inch

until, at the highest value, the period was slightly less than 0.0071 second. At the lower closing pressures both the computed pressure curves also show the long injection period. At the higher closing pressures the curve from equation (39) shortens correspondingly while the curve based on equations (6) and (11) show an injection period greater than the recorded period. At the lower closing pressures the curve of equations (6) and (11) fit the experimental results more closely, while at the higher closing pressures the curve according to equation (39) shows the closer agreement with the experimental results. It can be concluded that for

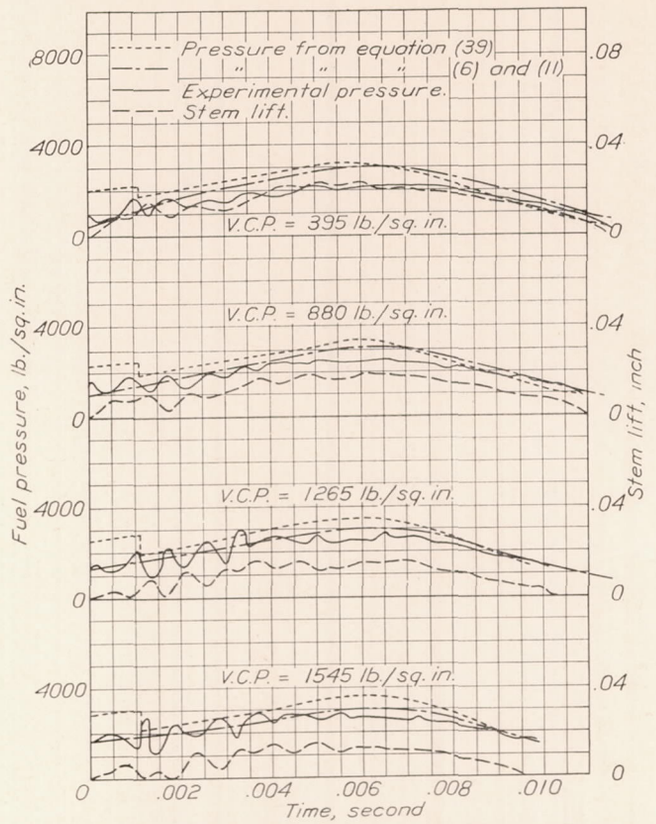

FIGURE 13.—Effect of valve closing pressure on stem lift and fuel pressure at low pump speed. Tube length=34 inches; inside tube diameter=0.076 inch; pump speed=470 r. p. m.; orifice diameter=0.020 inch

high pump speeds at low injection valve closing pressures, and, consequently, lower initial pressures in the injection tube, the actual conditions are closely approximated by computing the instantaneous pressures from a consideration of the compressibility but not the pressure-wave phenomena of the fuel; while at the higher valve closing pressures, and consequent higher initial pressures, the actual conditions are more closely approximated by computing the instantaneous pressures from a consideration of the pressure-wave phenomena. It is well to mention at this time that injection periods at the injection valve which are in excess of the injection period at the pump may be caused by pressure waves set up in the system before the by-pass valve of the pump is closed. In this case, injection would appear earlier than L/s seconds after the closing of the by-pass valve. It is possible that these phenomena did occur with the low injection valve closing pressures.

It is noticed that at the injection valve closing pressures of 550 and 1,200 pounds per square inch secondary discharges occurred. These were not due to the

mechanical bouncing of the injection valve stem, as was the case in the investigation on the common-rail system (reference 18), because in this case the secondary lift would have been jagged and closer to the end of the initial lift. Secondary discharges can be explained from the analysis, according to Sass, in the derivation

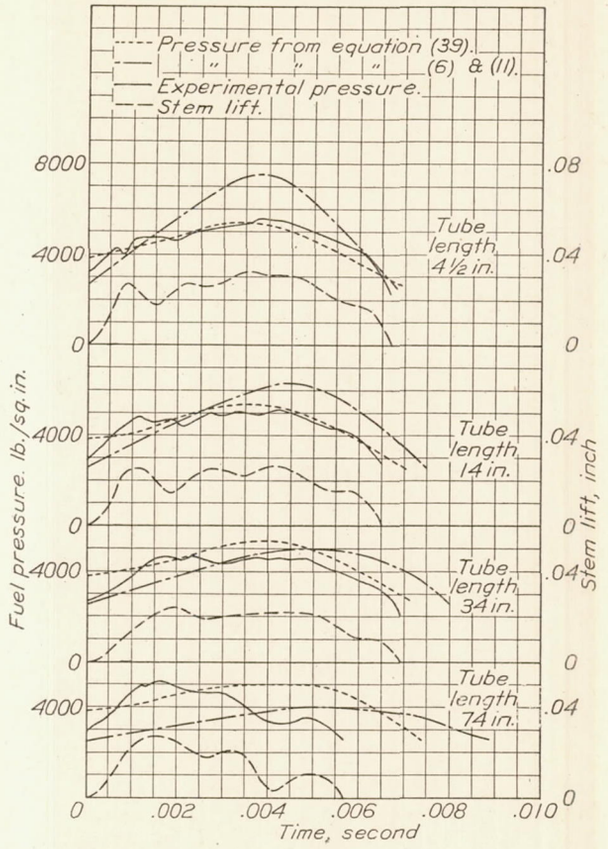

FIGURE 14.—Effect of tube length on stem lift and fuel pressure. Pump speed =750 r. p. m.; inside tube diameter=0.125 inch; valve closing pressure= 2,650 lb./sq. in.

of equation (39) on the assumption that the by-pass valve closes sufficiently rapidly so that the oscillations continue in the injection tube. Under this circumstance the waves can cause several openings and closings of the injection valve. It is difficult to compute the cases under which secondary discharge will take place because of the lack of knowledge of the closing process of the by-pass valve. At the higher valve closing pressures, if such pressure waves did occur, they were not of sufficient intensity to reopen the injection valve.

At the lower pump speed (470 r. p. m.) both methods of computing the instantaneous pressures show good agreement with the experimentally determined values. In this case, the injection period for the lowest injection valve closing pressure was equal to the period at the pump, but as the closing pressure was increased the injection period decreased. The bouncing of the stem during the start of injection was caused by the tube. diameter being less than the critical diameter. (See fig. 29, Appendix III.) This bouncing will be discussed in detail in the section on the effect of injection tube diameter.

Analysis of the two figures indicates that the check valve at the entrance to the injection tube did not permit the pressure in the injection tube to drop to atmospheric but maintained the pressure at a value approaching the injection valve closing pressure.

The general conclusion to be drawn from the figures is that the injection valve closing and opening pressures materially affect the injection characteristics of a fuel pump injection system, and that increasing the injection valve opening and closing pressures decreases the injection period but increases the instantaneous pressures.

Effect of injection tube length.—The effect of the injection tube length on the instantaneous pressures is shown in Figure 14. It is seen that up to tube lengths of 34 inches there is little change in the injection characteristics according to the experimental records and

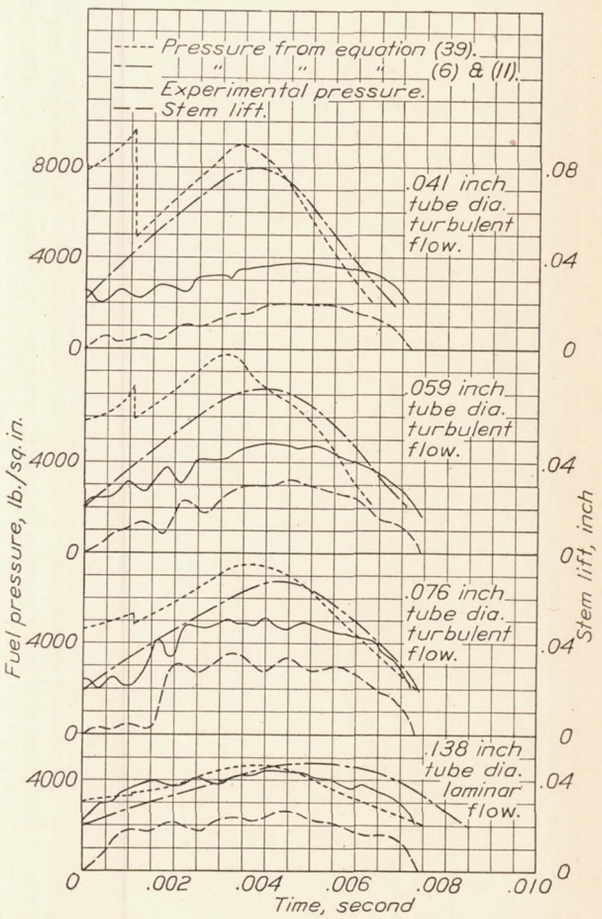

FIGURE 15.—Effect of inside tube diameter on stem lift and fuel pressure. Tube length=34 inches; valve closing pressure=2,000 lb./sq. in.; pump speed=750 r. p. m.

according to the pressures computed from an analysis of the pressure waves. For the longest tube the computed pressures are at considerable variance with the actual pressures, owing possibly to the effect of the by-pass valve or to resistance in the injection tube, which became excessive because of the tube length.

The computation neglecting the pressure waves fails for the short tube lengths. The explanation of the small effect of the tube length is seen from an analysis of Table VII, Appendix II. The values of the reflected waves for the first reflection shown in column 15 reach a maximum of 480 pounds per square inch. Assuming that only these pressure waves reenforce the waves caused by the pump plunger motion, it is seen that the injection tube length can have little effect on the instantaneous pressures, since the addition of the reflected waves to the waves originating at the pump amount to a maximum of only 480 pounds per square inch. Lengthening the injection tube changes the time at which the reflected waves are added to the wave originating at the pump.

The general conclusion to be drawn from the figure is that short injection tubes do not materially aid the injection characteristics of fuel pumps and that consequently the fuel pumps for all cylinders in multicylinder operation may be constructed as a single unit connected by suitable tubing to the injection valve.

Effect of injection tube diameter.—Figure 15 shows the effect of the injection tube diameter on the instantaneous pressures. According to Figure 29, Appendix III, the critical tube diameter for the pump tested at a speed of 750 r. p. m. is 0.094 inch. For tube diameters greater than this the injection pressures should decrease because of the fuel lost to compression according to equation (6) and because of the lesser intensity of the pressure waves according to equation (39). The experimental results presented substantiate this. It is seen that the maximum pressures occur between the 0.076 and 0.138 inch diameter tubes. During the taking of the experimental records it was noticed that for the smaller tube diameters the tubes heated considerably, indicating the resistance losses caused by the

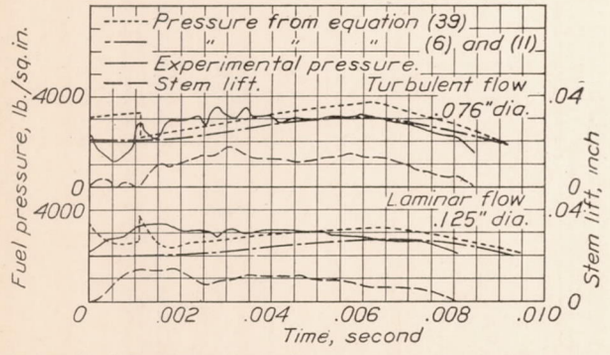

FIGURE 16.—Effect of inside tube diameter on stem lift and fuel pressure Pump speed=470 r. p. m.; tube length=34 inches; valve closing pressure=2,000 lb./sq. in.

turbulent flow. Wires were inserted in the injection tubes in one series of tests, and it was observed that the heating was even more marked and the pressures lower than with an injection tube of the same flow area but without the wire. For the tube diameters below the critical diameter the start of the motion of the injection valve stem is ragged; this is caused by the unsteady flow conditions as a result of the high resistance to flow.

It is noticed that the initial reflected wave changes from a positive value for a tube diameter of 0.138 inch to a negative value for a tube diameter of 0.076 inch.

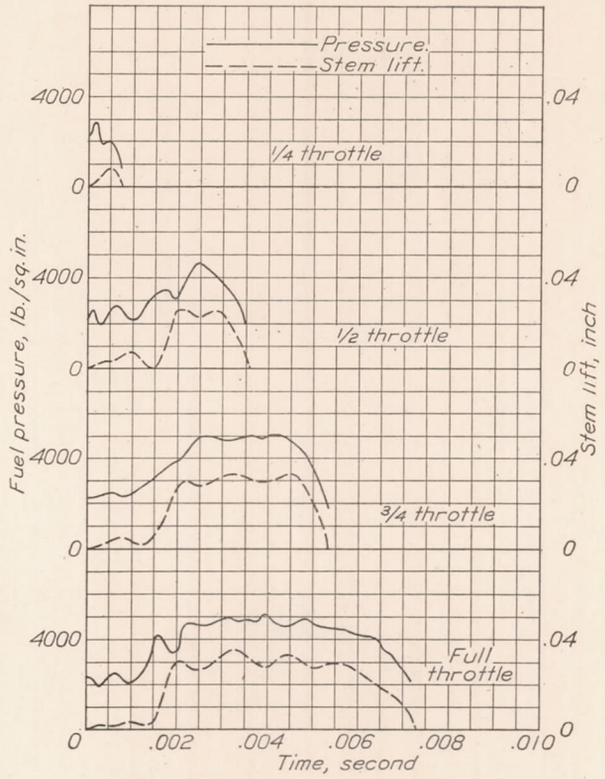

FIGURE 17.—Effect of throttle setting on stem lift and fuel pressures. Injection tube length=34 inches; diameter=0.076 inch; pump speed=750 r. p. m.; valve closing pressure=2,000 lb./sq. in.

Substituting the test values in equation (41) shows that the initial reflected wave changes from a positive value to a negative value for a tube diameter of 0.124 inch. (See also fig. 14.)

To check the experimental results on the effect of tube diameter, tests were run at a pump speed of 470 r. p. m. with injection tubes above and below the critical tube diameters. (Fig. 16.) Again it is seen that for the injection tube diameter below the critical diameter, the stem motion is ragged. It is seen that with either of the injection tubes the injection period at the discharge orifice is less than the period at the pump. This has been discussed in the section on the "Effect of Injection Valve Closing Pressure."

The general conclusion to be drawn from these figures is that, in designing a pump injection system, care must be taken to have the injection tube diameter and the diameters of all other flow passages, with the exception of the discharge orifice, not less than the critical tube diameter, in order to prevent turbulent flow.

Effect of load.—The effect of load or pump throttle setting on the instantaneous pressures is shown in Figure 17. Since the injection tube diameter was less than the critical diameter, the record of the stem movement is ragged. The curves show that the throttle

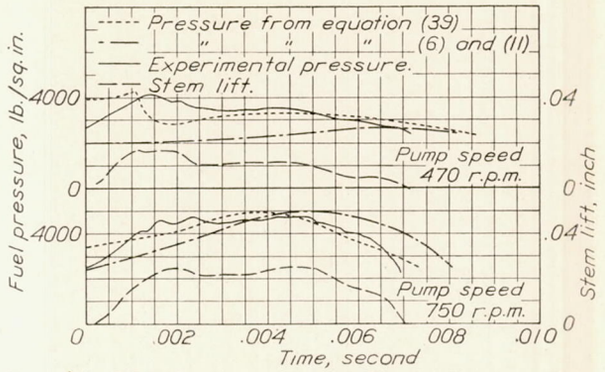

FIGURE 18.—Effect of pump speed on stem lift and fuel pressure. Tube length=34 inches; inside tube diameter=0.138 inch; valve closing pressure=2,500 lb./sq. in.

setting had no effect on the instantaneous pressures up to the point of cut-off. The throttle settings designated do not refer to the fuel quantity delivered but to the fraction of the throttle setting. It can be concluded from the figure that with a constant-area discharge orifice and with a constant-stroke fuel pump, the injection characteristics during the injection period are independent of the throttle setting, and that once the injection characteristics are determined for full load they are determined for all loads. This is in contradiction to the opinion of Joachim and Foster in the report on an annular orifice injection valve (reference 25), in which they state that at part loads with a spring-loaded automatic injection valve there will be throttling between the injection valve stem and seat.

Effect of pump speed.—From the previous figures the effect of pump speed on the injection characteristics can be studied. Additional test results are shown in Figure 18. It is seen that as the pump speed increased the pressures during injection increased. As has been stated before, this increase results in an increase in rate of penetration and in atomization at the higher speeds. In the adaptation of equation (39) to this particular set of conditions, it was found that the initial wave was not sufficient to open the injection valve, unless the reflection was complete. Consequently, complete reflection of the initial wave up to $t=3\ L/s$ was used in the computations. Under this circumstance the reflected wave $-W$ was equal in magnitude to the oncoming wave F. This results in the high rate of pressure rise at the lower speed and the considerable deviation from the curve computed according to equation (6). It is interesting to note

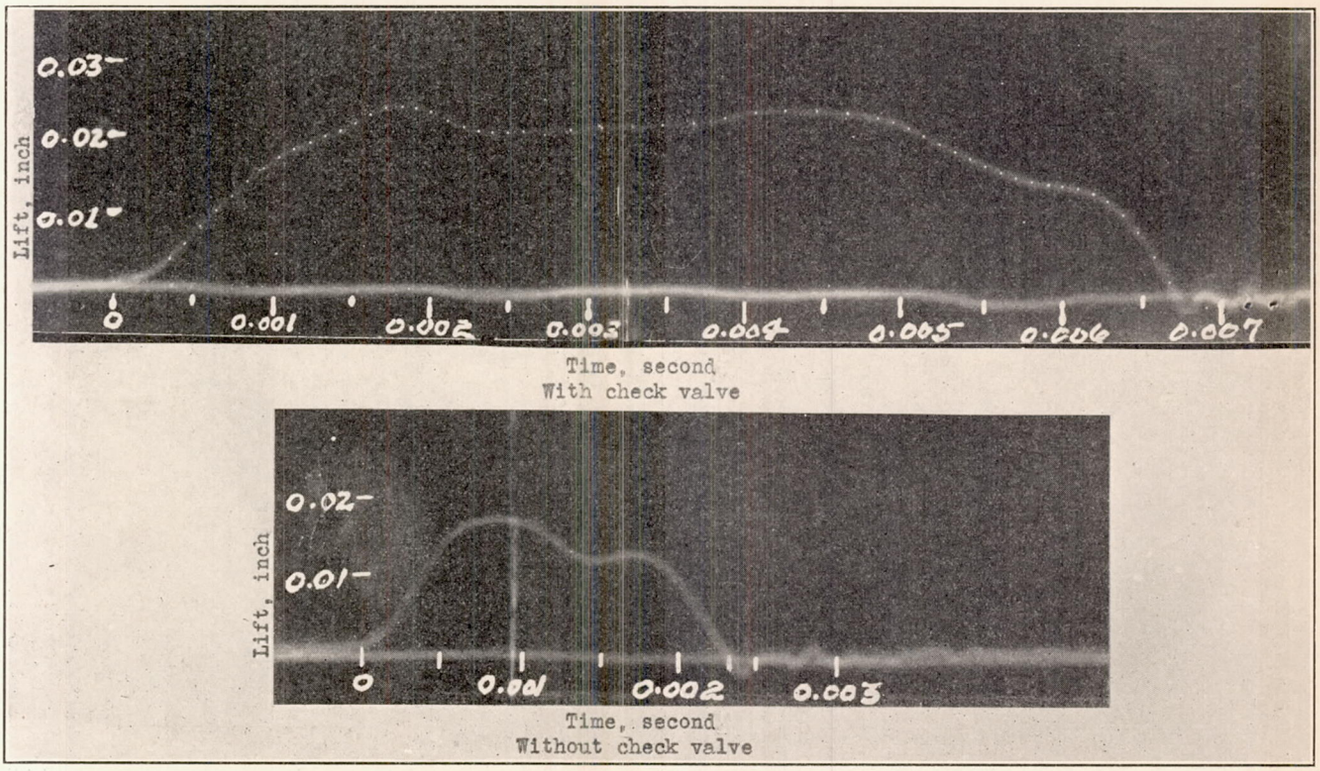

FIGURE 19.—Effect of check valve on stem lift. Tube diameter=0.138 inch; tube length=34 inches; orifice diameter=0.020 inch; pump speed=750 r. p. m.; valve closing pressure=2,600 lb./sq. in.

the drop in pressure after injection started. Alexander (reference 21) also noticed this phenomenon and attributed it to the volume change in the injection valve as the stem lifted. The author of reference 26 drew the same conclusion from the records of the movement

of the stem of an automatic injection valve. Figure 18 shows that the drop in pressure is explained by the pressure-wave phenomena.

Effect of the check valve.—It was found extremely important to have a check valve between the fuel pump and the injection tube, although the type of check valve was not so important provided it was light and did not restrict the fuel flow. At low-speed operation (470 r. p. m.) there was little difference in the injection characteristics with or without the check valve. However, as the speed of the pump was increased, there proved to be a critical speed above which the injection characteristics with and without the check valve were materially different. Figure 19 shows two stem records taken under the same conditions with the exception that the check valve was used in obtaining the upper record, while no check valve was used in obtaining the lower. An examination of the lower record indicates that injection started about 0.001 second before the start of pressure rise designated zero time. With a 70-inch injection tube no injection took place without the check valve, although it did when the check valve was in place as is shown in Figure 14. Three different check valves were employed; first, one with a small collar below the seat, as is shown in Figure 4; then, one with no collar; and finally, an ordinary ball-check valve. The first two gave virtually the same results. The ball-check valve gave an injection period equal to that obtained with the other two check valves, but the maximum stem lift was less, indicating a restriction to fuel flow past the ball. The conclusion to be drawn from the figure is that for high-speed operation some check should be provided to prevent all the fuel under pressure from leaving the injection tube when cut-off occurs at the fuel pump. Although a check valve is the simplest method of accomplishing this, the same results can be obtained by the use of a high primary pressure under which the fuel is fed to the injection pump, or possibly by the use of a restriction to flow in the by-pass valve. The last method is not recommended since the chance of obtaining pressure waves of sufficient magnitude to open the injection valve before the by-pass valve is closed are increased by any restriction to the by-pass valve flow area.

APPLICATION OF THEORY TO PUMP DESIGN

In the following paragraphs the preceding theoretical analysis with the modifications based on the experimental data will be applied to the design of a fuel pump required to meet a definite set of conditions.

(a) TO DESIGN A PUMP TO GIVE THE SAME INJECTION PERIOD IN SECONDS AT MAXIMUM AND MINIMUM PUMP SPEEDS

Assume the following requirements:

Range of pump speeds—250 r. p. m. to 1,000 r. p. m.

Fuel quantity to be injected—0.010 cubic inch.

Period of injection—0.0025 second.

Since it is assumed that the injection period in seconds is to be constant over the speed range, it is necessary to use a variable-velocity pump so that the low velocity range with respect to pump degrees can be used at the high speeds and the high velocity range with respect to pump degrees can be used at the low speeds. If the injection period is to be kept constant, the mean velocity of the pump plunger during the injection period must be kept constant regardless of engine speed. In order to maintain the inertia forces in the pump at a minimum value, a constant-acceleration cam is employed. The volume velocity B with which the fuel is displaced by the pump at any time t is given by the equation

$$B = Aft \tag{50}$$

in which f is the acceleration of the pump plunger in units of length per second per second and A the area of the pump plunger. Since

$$t = \theta/6n \tag{51}$$

$$f = 36n^2\alpha \tag{52}$$

in which α is the pump-plunger acceleration in units of length per degree per degree and θ is the angular rotation of the pump in the time t. Substituting in equation (50)

$$B = 6nA\alpha\theta \tag{53}$$

Since α is constant, the mean velocity between any two angles θ_1 and θ_2 is given by

$$B_m = \frac{1}{2}6nA\alpha\ (\theta_1 + \theta_2) \tag{54}$$

Let θ_1 represent the angular position for the start of injection and θ_2 the position for the stop of injection. Then, since the time of injection is to be maintained constant,

$$\frac{\theta_2 - \theta_1}{6n} = k \tag{55}$$

in which k represents the injection period in seconds. Solving equation (55) for θ_2 and substituting in equation (54)

$$B_m = \frac{1}{2}6nA\alpha\ (2\theta_1 + 6nk) \tag{56}$$

Solving for θ_1 and θ_2

$$\theta_1 = \frac{B_m}{6\ nA\alpha} - 3nk \tag{57}$$

$$\theta_2 = \frac{B_m}{6\ nA\alpha} + 3nk \tag{58}$$

Equations (57) and (58) give the cam positions for the start and stop of injection at any pump speed n. The value of α is determined by the maximum acceleration permissible in units of length per second per second for the highest speed at which the pump is to be driven.

Let M be the maximum pump speed and N the minimum pump speed. Let b be the highest permissible acceleration in units of length per second per second. Then

$$b=36M^2\alpha \tag{59}$$

The maximum angular displacement θ_m of the cam during the upstroke of the pump plunger is θ_2 for the minimum r. p. m.

$$\theta_m=\frac{B_m}{6\ NA\alpha}+3Nk \tag{60}$$

Substituting for α the value obtained from equation (59)

$$\theta_m=\frac{6B_mM^2}{N\ A\ b}+3Nk \tag{61}$$

The lift of the plunger H for θ_m is

$$H=\frac{1}{2}\alpha\theta_m^2 \tag{62}$$

If it is assumed that the deceleration of the pump plunger is equal in magnitude to the acceleration, the total lift of the pump plunger is equal to 2 H.

Assume that the maximum permissible acceleration of the pump plunger is 10,000 inches per second per second. Substituting in equation (59)

$$10{,}000=36\times1000^2\times\alpha$$

$$\alpha=2.78\times10^{-4}\text{ inches per degree}^2$$

Assume that θ_1 for the maximum speed is 5°. The value of B_m is equal to the total fuel quantity divided by the time of injection.

$$B_m=\frac{0.010}{0.0025}$$

$$=4.00\text{ cu. in. per second}$$

Substituting in equation (57)

$$5=\frac{4.00}{6\times1000A\times2.78\times10^{-4}}-3\times1000\times0.0025$$

$$A=0.1918\text{ sq. in.}$$

The diameter of the pump plunger is, therefore, 0.494 in. The value of θ_m is now obtained from equation (61)

$$\theta_m=\frac{6\times4\times1{,}000^2}{250\times0.1918\times10{,}000}+3\times250\times0.0025$$

$$=51.9°$$

The lift of the plunger at H is given by equation (62)

$$H=\frac{1}{2}2.78\times10^{-4}\times51.9^2=0.375\text{ in.}$$

The total lift of the pump plunger, assuming that the deceleration is equal in magnitude to the acceleration, is $2H$ or 0.75 inch. The dimensions of the pump are now determined.

The next step is to compute the discharge-orifice diameter. Assume that the mean injection pressure is to be 4,000 pounds per square inch. From the conventional flow formula

$$Q=ac\sqrt{\frac{2p}{\rho}}\ t \tag{63}$$

in which Q is the total quantity discharged. Assume that the coefficient of discharge of the orifice is 0.80. Substituting in equation (63)

$$0.010=a\times0.80\sqrt{\frac{2\times4{,}000}{0.795\times10^{-4}}}\times0.0025$$

$$a=0.000498\text{ square inch.}$$

The diameter of the discharge orifice is, therefore, 0.0252 inch.

The minimum diameter of the injection tube is determined from equation (46)

$$D_k=\frac{6nVA}{500\pi\nu} \tag{46}$$

in which $6nVA$ is replaced by B_m. The value of ν is determined from Figure 28, Appendix III. At 4,000 pounds per square inch pressure the coefficient of viscosity is shown to be 0.100 poise which must be converted into English units. Following the method given in the section on the "Investigation of the Resistance to Flow in the Injection Tube:"

$$\eta=\frac{\mu g}{\gamma}$$

$$=0.0182\text{ inch}^2\text{ second}^{-1}.$$

Substituting in equation (46)

$$D_k=\frac{4.00}{500\times3.14\times0.0182}$$

$$=0.140\text{ inch.}$$

The length of the injection tube depends on the length of tubing required to connect the injection pump to the injection valve mounted farthest from the pump. It will be assumed that this length is 30 inches.

The test results have shown that a high injection valve closing pressure eliminates secondary discharges from the system. If the injection valve opening pressure and closing pressure differ by a small amount, there will be less chance of the initial pressure waves proving insufficient to open the injection valve. The difference between the injection valve opening and closing pressures should be such that in every case the initial wave will open the injection valve. Consequently, the difference should be less than the mini-

mum value of $\rho s v_1$. The minimum value occurs at the start of injection at the maximum speed and is equal to

$$\rho s v_{1_m} = 0.795 \times 10^{-4} \times 5.96 \times 10^5 \times v_1$$
$$= 4.74\, v_1$$

But v_1 is given by

$$v_1 = 6nV \times \frac{A}{T}$$

in which V is given by

$$V = \alpha\, \theta$$
$$= 2.78 \times 10^{-4} \times 5$$
$$= 1.390 \times 10^{-3}$$
$$v_1 = 6 \times 1000 \times 1.39 \times 10^{-3} \times \frac{0.1918}{0.0154}$$
$$= 104 \text{ in./sec.}$$
$$\rho s v_1 = 4.74 \times 104$$
$$= 493 \text{ lb. per sq. in.}$$
$$\fallingdotseq 500 \text{ lb. per sq. in.}$$

The maximum value of $\rho s v_1$ occurs at θ_2 for the maximum r. p. m. The value is equal to $\frac{\theta_2}{\theta_1} \times \rho s v_{1_{\theta_1}} = \frac{20}{5} \times 493$ or 1,970 pounds per square inch. The mean value of $\rho s v_1$ is, therefore, approximately $\frac{1{,}970 + 493}{2} = 1{,}230$ pounds per square inch. The mean injection pressure has been assumed to be 4,000 pounds per square inch. The injection valve closing pressure, assuming that a check valve is employed that maintains the closing pressure in the injection tube at the end of injection will be $4{,}000 - 1{,}200 = 2{,}800$ pounds per square inch. The injection valve opening pressure will, therefore, be $2{,}800 + 500 = 3{,}300$ pounds per square inch.

The value of θ_1 was assumed to be 5° at 1,000 r. p. m. From equation (55) it is seen that θ_2 equals $\theta_1 + 6nk$ or 20°. At 250 r. p. m. θ_2 has already been determined (51.9°). Consequently, since θ_1 equals $\theta_2 - 6nk$, θ_1 at 250 r. p. m. is 48.1°.

The known conditions are now:

Pump plunger diameter—0.498 in.
Pump plunger acceleration—2.78×10^{-4} in. per degree per degree.
Injection tube diameter—0.140 in.
Injection tube length—30 in.
Discharge orifice diameter—0.0252 in.
Coefficient of discharge of discharge orifice—0.80.
Injection valve opening pressure—3,300 lb. per sq. in.
Injection valve closing pressure—2,800 lb. per sq. in.
Injection start—5° at 1,000 r. p. m.; 48.1° at 250 r. p. m.
Injection stop—20° at 1,000, r. p. m.; 51.9° at 250 r. p. m.
Check valve employed between pump and injection tube.

The instantaneous pressures are next determined. Since the operation covers the high-speed range, equation (39) is used, neglecting all pressure waves after the second reflection at the discharge orifice.

The value of L/s for the 30-inch tube is 30/59,600 or 0.000504 second. At 1,000 r. p. m. this corresponds to an interval of 3.02° and at 250 r. p. m. to an interval of 0.756°. In column 1 of Tables I and II for 1,000 r. p. m. and 250 r. p. m., respectively, are tabulated the values of time in seconds; in column 2, the values of time in L/s seconds; and in column 3, the values of time in pump degrees. In column 4 the total angular displacements are tabulated. The velocity of the pump plunger v_o for corresponding pump angles is equal to $6n\alpha\theta$. The velocities are tabulated in column 5 in units of inches per degree, and in column 6, in units of inches per second. The values of v_1 are equal to $v_o A/T$. They are tabulated in column 7. The waves originating at the pump plunger are equivalent to $\rho s v_1$. (Column 8.) Since these waves reach the discharge orifice L/s seconds later, the same values are tabulated in column 9 for $\rho s v_{1_{t-\frac{L}{s}}}$ but displaced a time interval of L/s seconds.

TABLE I

INJECTION PRESSURES AT 1,000 PUMP R. P. M.

1	2	3	4	5	6	7	8	9	10		11		12		13
t sec.$\times 10^4$	t L/s sec.	t deg.	t total deg.	V_o (in./deg.) $\times 10^3$	v_o in./sec.	v_1 in./sec.	$\rho s v_1$ lb./in.^{2}	$\rho s v_1 \, t-\frac{L}{a}$ lb./in.^{2}	$p_k+\rho s v_1 \, t-\frac{L}{a}$ lb./in.^{2}		$p_k+2s\rho v_1 \, t-\frac{L}{a}$ lb./in.^{2}		p_2 lb./in.^{2}		$-W$ lb./in.^{2}
									A	B	A	B	A	B	
0	0	0	5	0 1.39	0 8.34	0 104	0 490		2,800				2,800		
2.52	0.5	1.51	6.51	1.81	10.9	136	640		2,800				2,800		
5.04	1.0	3.02	8.02	2.23	13.4	167	790	490	2,800 3,290		2,800 3,780		2,800 2,680		0 −610
7.56	1.5	4.53	9.53	2.65	15.9	198	940	640	3,440		4,080		2,950		−490
10.08	2.0	6.04	11.04	3.07	18.4	229	1,090	790	3,590		4,380		3,200		−390
12.60	2.5	7.55	12.55	3.49	20.9	261	1,240	940	3,740		4,660		3,460		−280
15.12	3.0	9.06	14.06	3.91	23.5	293	1,390	1,090	3,890	3,280	4,980	3,760	3,750	2,670	−140
17.64	3.5	10.57	15.57	4.34	26.1	325	1,540	1,240	4,040	3,550	5,280	4,300	4,040	3,150	0
20.16	4.0	12.08	17.08	4.75	28.5	355	1,680	1,390	4,190	3,800	5,530	4,750	4,300	3,550	160
22.68	4.5	13.59	18.59	5.17	31.0	386	1,830	1,540	4,340	4,060	5,880	5,320	4,600	4,100	260
25.20	5.0	15.10	20.10	5.59 0	33.6 0	419 0	1,990 0	1,680	4,480	4,340	6,160	5,880	4,900	4,630	420
27.81	5.5	16.61	21.61	0	0	0	0	1,830	4,630	4,630	6,460	6,460	5,200	5,200	570
30.24	6.0	18.12	23.12	0	0	0	0	1,990	4,790 2,800	4,950 2,960	6,780 2,800	7,100 3,120	5,500 1,900	5,850 2,150	700
32.76	6.5	19.63	24.63	0	0	0	0	0 0	2,800	3,060	2,800	3,320	1,900	2,350	−900
35.28	7.0	21.15	26.15	0	0	0	0	0	2,800	3,220	2,800	3,640	1,900	2,580	−900
37.80	7.5	22.66	27.65	0	0	0	0	0	2,800	3,370	2,800	3,940	1,900	2,850	−900
40.32	8.0	24.16	29.16	0	0	0	0	0	2,800	3,500	2,800	4,200	1,900	3,100	−900
42.84	8.5	25.67	30.67	0	0	0	0	0	2,800	1,900	2,800	1,000	1,900	600	

TABLE II

INJECTION PRESSURES AT 250 R. P. M.

1	2	3	4	5	6	7	8	9	10		11		12		13
t sec.$\times 10^4$	t L/s sec.	t deg.	t total deg.	V_o (in./deg.) $\times 10^2$	v_o in./sec.	v_1 in./sec.	$\rho s v_1$ lb./in.^{2}	$\rho s v_1 \, t-\frac{L}{a}$ lb./in.^{2}	$p_k+s\rho v_1 \, t-\frac{L}{a}$ lb./in.^{2}		$p_k+2s\rho v_1 \, t-\frac{L}{a}$ lb./in.^{2}		p_2 lb./in.^{2}		$-W$ lb./in.^{2}
									A	B	A	B	A	B	
0	0	0	48.1	1.34	20.2	252	1,190	0	2,800		2,800		2,800		
2.52	0.5	.38	48.5	1.35	20.3	253	1,200	0	2,800		2,800		2,800		
5.04	1.0	.75	48.9	1.36	20.4	254	1,200	1,190	2,800 3,900		2,800 5,180		2,800 3,960		−30
7.56	1.5	1.14	49.2	1.37	20.6	256	1,210	1,200	4,000		5,200		3,980		−20
10.08	2.0	1.52	49.6	1.38	20.7	258	1,220	1,200	4,000		5,200		3,980		−20
12.60	2.5	1.90	50.0	1.39	20.9	260	1,230	1,210	4,010		5,220		4,000		−10
15.12	3.0	2.28	50.4	1.40	21.0	262	1,240	1,220	4,020	4,050	5,240	5,300	4,020	4,050	0
17.64	3.5	2.66	50.8	1.41	21.2	264	1,250	1,230	4,030	4,050	5,260	5,300	4,040	4,050	10
20.16	4.0	3.09	51.2	1.42	21.3	266	1,260	1,240	4,040	4,060	5,280	5,320	4,060	4,070	20
22.68	4.5	3.45	51.5	1.43	21.5	268	1,270	1,250	4,050	4,060	5,300	5,320	4,080	4,070	30
25.20	5.0	3.80	51.9	1.44 0	21.6 0	270 0	1,280 0	1,260	4,060	4,060	5,320	5,320	4,100	4,070	40
27.81	5.5	4.18	52.3	0	0	0	0	1,270	4,070	4,060	5,340	5,320	4,120	4,070	50
30.24	6.0	4.56	52.7	0	0	0	0	1,280 0	4,080 2,800	4,060 4,080	5,360 2,800	5,320 2,760	4,140 1,900	4,070 1,850	60
32.76	6.5	4.94	53.0	0	0	0	0	0	2,800	4,070	2,800	2,740	1,900	1,840	−900
35.28	7.0	5.32	53.4	0	0	0	0	0	2,800	4,060	2,800	2,720	1,900	1,830	−900
37.80	7.5	5.70	53.8	0	0	0	0	0	2,800	4,050	2,800	2,700	1,900	1,800	−900

To determine the values of the back-rushing waves, the graphical method is used. The range of values for v_1 is from 104 inches per second to 416 inches per second. From equation (29), neglecting p_z,

$$p_2 = \frac{\rho}{2} v_2^2 \left(\frac{T}{a\ c}\right)^2 \qquad (29a)$$

$$= \frac{0.795 \times 10^{-4}}{2} \times \left(\frac{0.0154}{0.000498 \times 0.80}\right)^2 v_2^2$$

$$= 0.0597\ v_2^2$$

In Table III are tabulated the values of v_2, p_2, $s\rho v_2$, and $p_2 + s\rho v_2$.

TABLE III

COMPUTATION OF p_2 & $s\rho v_2$

1	2	3	4
v_2 in./sec.	p_2 lb./in.²	$s\rho v_2$ lb./in.²	$p_2+s\rho v_2$ lb./in.²
100	600	470	1,070
200	2,390	950	3,340
300	5,380	1,420	6,800
400	9,560	1,900	11,460
500	14,940	2,370	17,310

From Table III the curve of p_2 against $p_2 + s\rho v_2$ is plotted. (Fig. 20.) It is also the curve of $p_k + 2s\rho v''_{1\ t-\frac{L}{s}}$ in which $v''_{1\ t-\frac{L}{s}}$ is considered as the effective velocity of all onrushing waves.

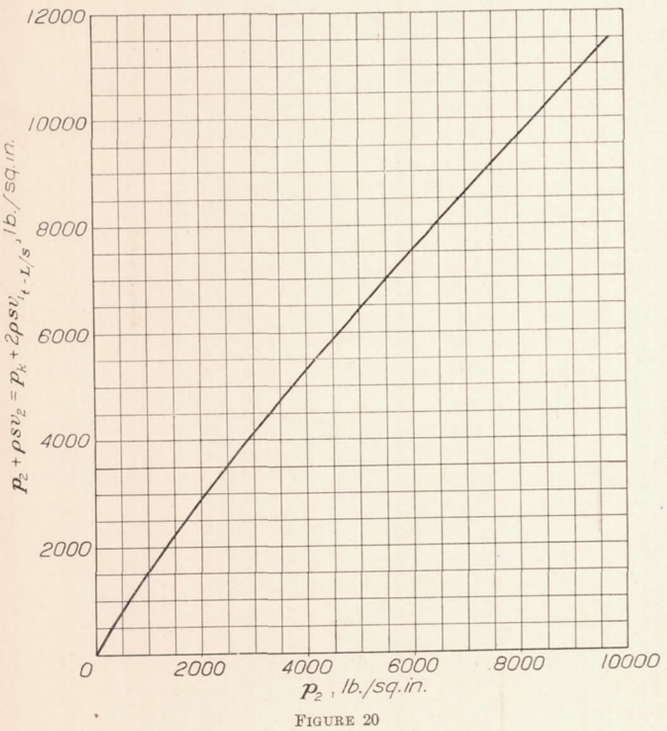

FIGURE 20

In column 10–A, Tables I and II are tabulated the values of $p_k + s\rho v_{1\ t-\frac{L}{s}}$. This column is completed for all time intervals, since the waves are considered as being destroyed after the second reflection. In column 11–A are tabulated the values of $p_k + 2s\rho v_{1\ t-\frac{L}{s}}$

From column 11–A and Figure 20 the values of p_2 are determined. (Column 12–A.) The reflected waves $-W$ are equal to column 10–A minus column 12–A. They are tabulated in column 13. The reflected waves are then added to $p_k + s\rho v_{1\ t-\frac{L}{s}}$ at a time $2L/s$ seconds after they appear in column 13. (Column 10–B.) Twice the values of the reflected waves are added to column 11–A in the same manner to determine $p_k + 2\ (s\rho v_{1\ t-\frac{L}{s}} + s\rho v'_{1\ t-\frac{L}{s}})$, equation (40) which is the same as $p_k + 2\left(F\left(t-\frac{L}{s}\right) - W\left(t-\frac{L}{s}\right)\right.$ (Column 11–B.) The corresponding values of p_2 are entered in column 12–B. Column 12–B represents the instantaneous pressures.

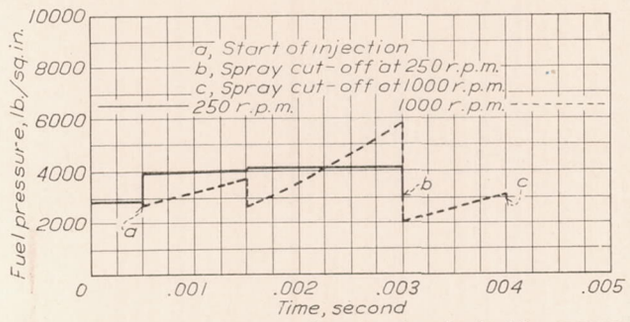

FIGURE 21.—Pressures at discharge orifice at maximum and minimum pump speeds

In Figure 21 the instantaneous pressures are plotted against time for 1,000 r. p. m. and 250 r. p. m. It is seen that the curves are not the same, since the acceleration of the pump plunger with respect to time varies as the square of the pump speed. (Equation

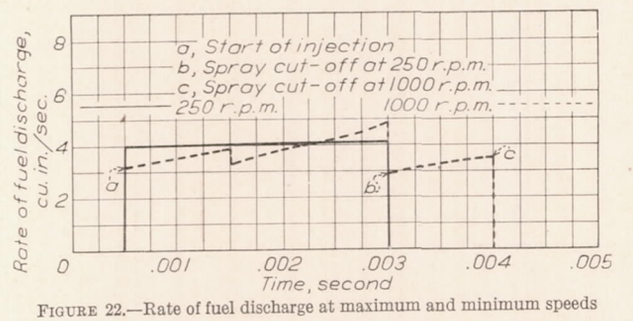

FIGURE 22.—Rate of fuel discharge at maximum and minimum speeds

(52).) Furthermore, the time of discharge is greater at 1,000 r. p. m. because the pressure at the end of injection at the pump is higher at 1,000 r. p. m. than at 250 r. p. m. Since the pressure returns to the injection valve closing pressure, that is p_k, the fuel quantity discharged is equal to the fuel quantity displaced less the losses due to leakage, which are included in the assumption that the waves are dissipated after the second reflection. The results show that although the desired conditions are not exactly obtained they are closely enough approached for practical purposes.

At 1,000 pump r. p. m. the pressures during the start of injection fall below the injection valve closing pressure. Under these circumstances the injection valve might or might not close, depending on the inertia and on the period of vibration of the injection valve stem and spring. However, in order to avoid a possible closing, it would be better to retard the start of injection at 1,000 r. p. m. a few degrees past the original start position of 5°, and also to retard the stop of injection accordingly. It must be remembered that the by-pass valve does not open instantaneously at the end of injection, as is assumed in the computations, so that the abrupt drops shown in the two curves do not occur. Instead, the phenomenon is affected by the rate of opening of the by-pass valve, so that, although the pressure falls rapidly, there is an appreciable time required for the effect of the pump plunger motion at cut-off to disappear.

Figure 22 shows the rates of fuel discharge at the maximum and minimum pump speeds. Since the rate of discharge varies as the square root of the pressure, the curves show less variation than the pressure curves.

(b) TO DESIGN A PUMP TO GIVE A DEFINITE RATE OF FUEL DISCHARGE

Assume the following conditions:

Pump r. p. m.—1,500.
Fuel quantity to be injected—0.00030 lb.
Average injection pressure—4,000 lb. per sq. in.
Injection period—15° pump rotation.
Injection tube length—20 in.
Coefficient of discharge of discharge orifice—0.80.
Rate of fuel injection—see Figure 23.

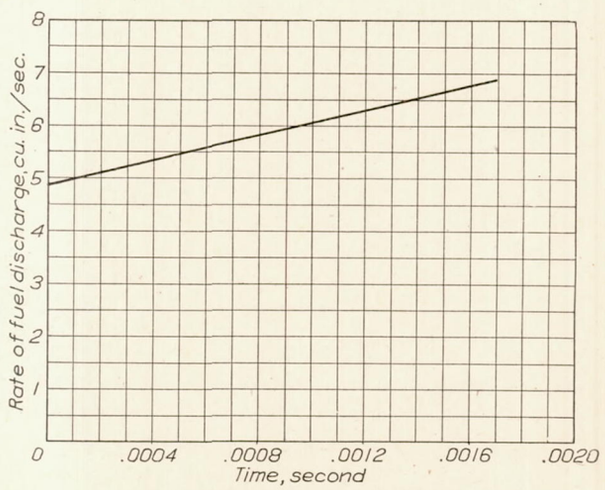

FIGURE 23.—Assumed rate of fuel discharge

The diameter of the discharge orifice is determined by equating the mean velocity of flow through the discharge orifice multiplied by the time of injection to the total quantity discharged. Since the total quantity Q is equal to the total weight m, divided by the density

$$\frac{m}{\gamma}=ac\sqrt{\frac{2p}{\rho}}t \tag{63}$$

$$a=\frac{m}{\gamma ct\sqrt{\frac{2p}{\rho}}} \tag{64}$$

Substituting the numerical values

$$a=\frac{3.0\times10^{-4}}{0.0307\times0.80\times\frac{15}{6\times1500}\sqrt{\frac{2\times4000}{0.795\times10^{-4}}}}$$

$$=7.32\times10^{-4}\text{ in.}^2.$$

Solving for d, the diameter of the orifice,

$$d=0.031\text{ in.}$$

The diameter of the injection tube is obtained from equation (45)

$$D_K=\frac{2000\nu}{v_2} \tag{45a}$$

But v_2 the velocity in the injection tube at the discharge orifice, is given by

$$v_2=\frac{ac}{T}\sqrt{\frac{2p_2}{\rho}} \tag{65}$$

The maximum value of v_2 occurs at the end of the injection period at which time $ac\sqrt{2p/\rho}$ is given from Figure 23 as 6.87 cubic inches per second. Substituting in equation (45a) and since $T=\frac{\pi}{4}D^2$

$$D=\frac{2000\times0.0251}{\frac{6.87}{\frac{\pi}{4}D^2}}$$

$$=0.175\text{ in.}$$

$$T=0.0241\text{ sq. in.}$$

in which 0.0251 is the kinematic viscosity at 4,000 pounds per square inch in units of inches^2 seconds^{-1} obtained by the method given in Appendix III. Although the maximum pressure in the injection tube will be greater than 4,000 pounds per square inch, the tube diameter determined from the average pressure will be sufficiently accurate. It is noticed that D is determined from v_2 instead of v_1, the velocity relative to the pump plunger as is given in Appendix III. Consequently, when the maximum value of v_1 is determined, it will be necessary to determine the pressure losses from equation (47). If the losses are large the computations must be repeated for a new value of the injection tube diameter.

The velocity v_1 at the entrance of the injection tube is determined from equation (25)

$$p_2+\rho s v_2=p_k+2\rho s v''_{1\,t-\frac{L}{s}} \tag{25a}$$

in which v''_1 is the sum of the velocity originating at the pump plus that of the reflected wave. Solving for v''_1

$$v''_{1\,t-\frac{L}{s}}=\frac{1}{2}\left[\frac{1}{\rho s}(p_2-p_k)+v_2\right] \tag{66}$$

In column 1 of Table IV the time of injection is divided into intervals of L/s, 20/59,600, seconds. The corresponding times in pump degrees are tabulated in column 2. The corresponding rates of discharge obtained from Figure 23 are displaced L/s seconds and tabulated in column 3. Column 4 contains the values of v_2 obtained by dividing the rates of discharge by the area of the injection tube. Column 5 contains the values of p_2 obtained from Figure 23 and equation (63). The value of p_k—the injection valve closing pressure—depends on the value of the injection valve opening pressure. An opening pressure of 2,600 pounds per square inch is chosen, 150 pounds per square inch less than the initial discharge pressure. The closing pressure should be sufficiently high so that the values of v_1 are not excessive, but at the same time the closing pressure must be low enough so that the difference in the forces on the injection valve stem before and after the injection valve has opened is sufficient to assure a rapid movement of the injection valve stem. A value of 2,000 pounds per square inch will be used.

The values of v'_1 are now computed and tabulated in column 6.

The velocities v_1 at the entrance to the injection tube are determined from the values of v'_1 and equation (32)

$$W=s\rho v_2-s\rho v'_{1\,t-\frac{L}{s}} \tag{32a}$$

in which W represents the wave reflected from the discharge orifice at the time under consideration. The value of W also represents the reflected wave which again reaches the discharge orifice $2L/s$ seconds later. The values of $-W$ are entered in column 7. The computations show that $-W$ is negative at times of 1.0 and 1.5 L/s seconds, since at both these times $v'_{1\,t-L/s}$ is less than v_2 This negative value would result in an irregular cam to compensate for the wave of rarefaction. To avoid this it is advisable to start injection later. At the time of 1.5 L/s seconds the negative wave is negligible so that injection will be started at this point; that is, at 0.5 L/s seconds at the pump. Substitution in equation 41 shows that the value of v_1 for no reflection is 212 inches per second, approximately the value of v_2 at 1.5 L/s seconds. The values of $v_{1\,t-L/s}$, column 8, are obtained by dividing the value $-W$ which occurs $2L/s$ seconds earlier by ρs and subtracting from the values of $v''_{1\,t-L/s}$

$$v_{1_{4.5L/s}}=405-\frac{210}{4.74}=361 \text{ in./sec.}$$

The values of v_1 are equal to the values of $v_{1\,t-L/s}$ but occurs L/s seconds earlier. They are correspondingly

TABLE IV

COMPUTATIONS TO DETERMINE v_1

1	2	3	4	5	6	7	8	9	10
t L/s sec.	θ deg.	R in.³/sec.	v_2 in./sec.	p_2 lb./in.²	$v'_{1\,t-L/s}$ in./sec.	$-W$ lb./in.²	$v'_{1\,t-L/s}$ in./sec.	v_1 in./sec.	t sec.$\times 10^4$
0	0	0	0	2,000	0	0			0
0.5	1.5	0	0	2,000	0	0	0	210	1.68
1.0	3.0	4.87	202	2,750	180	−100	0	240	3.36
1.5	4.6	5.07	211	2,990	210	−5	210	271	5.03
2.0	6.1	5.28	219	3,240	240	100	240	302	6.71
2.5	7.6	5.48	227	3,490	271	210	271	337	8.39
3.0	9.2	5.68	236	3,740	302	320	302	351	10.06
3.5	10.7	5.89	244	4,030	336	440	337	360	11.78
4.0	12.3	6.09	256	4,310	372	550	351	373	13.42
4.5	13.8	6.29	261	4,600	405		361	386	15.10
5.0	15.3	6.50	270	4,900	441		373	394	16.78
5.5	16.8	6.70	278	5,220	478		386	0	18.45
6.0	18.3	6.90	286	5,530	510		394	0	20.13

The values of v_1 are equal to the values of $v_{1\,t-L/s}$ but occurs L/s seconds earlier. They are correspondingly

entered in column 9. In Figure 24 the values of v_1 are plotted against time in seconds.

The diameter of the pump plunger is determined from the permissible acceleration and from the curve of v_1 against time. To determine the acceleration relative to the velocity in the injection tube, the

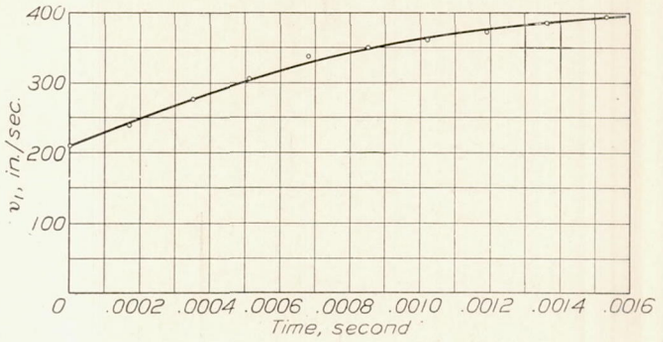

FIGURE 24

equation of the curve in Figure 24, in which zero time equals 0.5 L/s, is determined by assuming that the curve is of the general form

$$v_1 = A\,t^3 + C\,t^2 + G\,t + \mathrm{I} \qquad (67)$$

in which I is the value of v_1 for $t=0$. The solution of equation (67) is obtained by solving three simultaneous equations in A, C, and G. A fourth equation is not needed since I is determined directly from the curve. Any three sets of values for v_1 and t may be chosen. It is, however, advisable to choose values fairly well distributed along the curve. For values of time of 0.0004, 0.0008, and 0.0012 second the equations become

$$285 = 64\times10^{-12}A + 16\times10^{-8}C + 4\times10^{-4}G + 210$$

$$340 = 512\times10^{-12}A + 64\times10^{-8}C + 8\times10^{-4}G + 210$$

$$375 = 1728\times10^{-12}A + 144\times10^{-8}C + 12\times10^{-4}G + 210$$

Solving for A, C, and G

$$A = 0$$

$$C = -0.625\times10^{8}$$

$$G = 21.3\times10^{4}$$

Substituting in equation (67)

$$v_1 = -0.625\times10^{8}t^2 + 21.3\times10^{4}t + 210 \qquad (67a)$$

The equation for the acceleration is obtained by taking the first derivative of v_1 with respect to t

$$\frac{dv_1}{dt} = -0.313\times10^{8}\,t + 21.3\times10^{4} \qquad (68)$$

The maximum value of acceleration occurs at $t=0$ and is equal to 213,000 inches per second per second. Assume that the maximum permissible acceleration of the pump plunger is 24,000 inches per second per second. The ratio of the pump plunger area to the area of the injection tube must be 213,000/24,000 or 8.87. The plunger area is, therefore, $8.87\times\frac{\pi}{4}\,0.175^2$ or 0.213 square inch. The diameter of the pump plunger is 0.521 inch.

The equation of the lift of the pump plunger is obtained by dividing equation (67a) by 8.87 and integrating between the limits t_o and t

$$v_o = -0.705\times10^{7}\,t^2 + 2.40\times10^{4}\,t + 23.7 \qquad (69)$$

$$S = -2.35\times10^{6}\,t^3 + 1.20\times10^{4}\,t^2 + 23.7\,t + S_o \qquad (70)$$

in which v_o is the velocity of the pump plunger, S the lift at any time t, and S_o the lift at the start of injection. The lift of the plunger during injection is obtained by letting t equal 16.7×10^{-4} second

$$S = 0.0621 \text{ inch}$$

The total fuel quantity displaced during injection is

$$Q = 0.213\times0.0621$$

$$= 0.0132 \text{ cubic inch}$$

APPENDIX I

SAMPLE CALCULATIONS CONSIDERING COMPRESSIBILITY BUT NEGLECTING PRESSURE WAVES

Consider the following experimental conditions:

p_t—2,850 lb. per sq. in.
L—34 in.
T—0.0148 sq. in. − 0.138 in. diameter.
A—0.0985 sq. in. − 0.354 in. diameter.
n—750 r. p. m.
γ—0.0307 lb. per cu. in.
ρ—$0.0307/(32.2\times12)=0.795\times10^{-4}$ lb. sec.^{2} in.$^{-4}$.
a—0.000314 sq. in. − 0.020 in. diameter.
c—0.94.
E—284,000 lb. per sq. in.

Let the motion of the injection pump plunger be given by Figure 5. The volume of the injection tube is 0.509 cu. in. The displacement volume of the pump from the start of the injection to the top of the pump stroke is 0.027 cu. in. The total volume is 0.536 cu. in. This volume will be considered to be 0.552 cu. in. to correspond with the experimental results already presented. As the tube volume is considerably greater than the pump volume, equation (6) is used. The value of $\theta_b-\theta_a$ is taken as 2°. First the constants of equation (6) are derived.

$$ac\sqrt{\frac{2}{\rho}}=3.14\times10^{-4}\times0.94\sqrt{\frac{2}{0.795\times10^{-4}}}=4.69\times10^{-2}$$

$$\frac{2a^2c^2}{\rho}=2.20\times10^{-3}$$

$$\frac{12n}{\theta_b-\theta_a}\frac{R_\theta}{E}=\frac{12\times750\times0.552}{2\times284{,}000}=0.875\times10^{-2}$$

$$\frac{144n^2AVR_\theta}{(\theta_b-\theta_a)E}=\frac{12nR_\theta}{(\theta_b-\theta_a)E}\times12\ nAV=0.875\times10^{-2}\times9.000\times10^3\times0.985\times10^{-1}V=7.76V$$

$$\frac{144\ n^2R_\theta^2}{(\theta_b-\theta_a)^2E^2}p_a=4(0.875\times10^{-2})^2p_a=0.765\times10^{-4}p_a$$

$$\sqrt{p_b}=\frac{-4.69\times10^{-2}+\sqrt{2.20\times10^{-3}+7.76V+0.765p_a\times10^{-4}}}{0.875\times10^{-2}}=-5.36+\sqrt{2.88\times10+1.015V\times10^5+p_a}\qquad(6)$$

The difference in R_θ at the start of injection and R_θ at the end of injection is 0.024 cu. in.; this difference of 4 per cent of the total volume is negligible.

Equation (6) is now solved for the various values of p_b in terms of V and p_a. First tabulate in column 1 of Table V the values of θ taken at 2° intervals. In column 2 tabulate the total pump displacement, column 1 plus 132°. In column 3 tabulate the values of V obtained from Figure 5 and column 2. Column 4 is the product of V and 1.015×10^5. To column 4 is added 30 (30 is used in place of 28.8, since the values are computed to the closest 10 lb. per in.^{2}), the first term under the radical in equation (6), column 5. To column 5 is added p_a, remembering that p_a is equal to p_b for the time interval 2° earlier than that under consideration. Column 6 for $\theta=0$ is the injection valve opening pressure, which is also p_b for $\theta=0$, so the actual calculations start at $\theta=2°$. Column 6 at 2° is, therefore, 2,850 lb. per sq. in. plus 730 lb. per sq. in. or 3,580 lb. per sq. in. In column 7 is tabulated the square root of column 6. In column 8, 5 is subtracted from column 7 (5 is used in place of 5.36 since the accuracy of the computations does not warrant the extra figures). Column 8 is, therefore, the square root of p_b. The values of column 8 squared are entered as p_b in column 9. This process is repeated in each case, using for p_a the preceding value of p_b until the injection process is completed. The results of Table V are plotted in Figure 25.

The total fuel quantity discharged up to the point of cut-off at the pump is equal to the total fuel quantity displaced less the fuel absorbed by compression. The fuel quantity displaced is 0.0985 in.$^2\times0.24$ in. = 0.0234 cu. in. The fuel absorbed by compression is equal to the final pressure minus the initial pressure multiplied by the total volume divided by E. Assuming the initial pressure was 2,000 lb. per sq. in., $Q_c=(3{,}360-2{,}000)\times\frac{0.536}{284{,}000}=0.0026$ cu. in. The total quantity discharged is $0.0234-0.0026=0.0208$ cu. in.

In the calculation of Table V it was assumed that the pressure in the injection tube before the start of injection was close to the injection valve opening pressure, and, consequently, after the by-pass valve closed, a negligible part of the motion of the pump plunger was necessary to raise the pressure to the injection valve opening pressure. Under these conditions it is necessary to have a check valve between the entrance

to the injection tube and the fuel pump so that the pressure in the injection tube can not drop to atmospheric when cut-off occurs. Evaluating equation (11) for the conditions under consideration,

$$p=\left[\sqrt{4750}-\frac{2.84\times10^{5}\times2.95\times10^{-4}}{0.529\times1.26\times10^{-2}}t\right]^{2}$$

$$=[69.0-1.26\times10^{4}t]^{2}$$

Taking t in intervals of 2 pump degrees (0.00044 second), Table VI is obtained. If it is further assumed that the closing pressure of the injection valve is 2,000 lb. per sq. in., the discharge from the valve stops approximately 8 pump degrees after cut-off at the pump. The results of Table VI are also plotted in Figure 25. Since, at the end of injection, the pressure has dropped to the initial pressure, the total discharge is equal to the total fuel quantity displaced, but the injection period at the discharge orifice is 8° longer than at the pump.

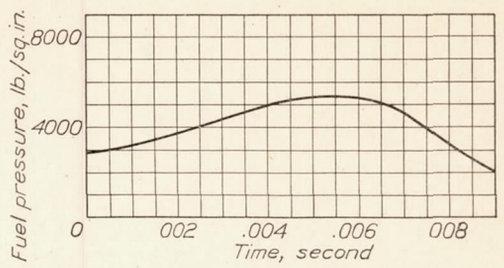

FIGURE 25.—Instantaneous pressures computed from equations (6) and (11). Tube length=34 inches; pump speed=750 r. p. m.; orifice diameter=0.020 inch

TABLE V

COMPUTATIONS ACCORDING TO EQUATION (6)

1	2	3	4	5	6	7	8	9	10
θ	Total deg.	V (in./deg.)$\times10^{3}$	$\frac{1.015\times10^{5}}{V}$	(4)+30	p_a+(5)	$\sqrt{(6)}$	$\sqrt{p_b}$	p_b lb./in.^{2}	Time sec.$\times10^{4}$
0	132	6.6	670	700				2,850	0
2	134	6.9	700	730	3,580	60	55	3,010	4.4
4	136	7.3	740	770	3,780	61	56	3,140	8.9
6	138	7.8	790	820	3,960	63	58	3,360	13.3
8	140	8.4	850	880	4,240	65	60	3,600	17.8
10	142	8.9	900	930	4,530	67	62	3,840	22.2
12	144	9.4	950	980	4,820	69	64	4,100	26.6
14	146	9.8	990	1,020	5,120	72	67	4,500	31.1
16	148	9.8	990	1,020	5,520	74	69	4,750	35.5
18	150	9.5	960	990	5,740	76	71	5,050	40.0
20	152	8.9	900	930	5,980	77	72	5,200	44.4
22	154	8.2	830	860	6,060	78	73	5,350	48.8
24	156	7.2	730	760	6,110	78	73	5,350	53.3
26	158	6.3	640	670	6,020	78	73	5,350	57.7
28	160	5.4	550	580	5,930	77	72	5,200	62.2
30	162	4.6	470	500	5,700	76	71	5,050	66.6
32	164	3.8	390	420	5,470	74	69	4,750	71.1

TABLE VI

COMPUTATIONS ACCORDING TO EQUATION (11)

1	2	3	4	5	6
Sec.$\times10^{4}$	Deg.	Total deg.	$1.26\times10^{4}t$	$\sqrt{p_3}$ −(4)	p lb./in.^{2}
0	0	164	0		4,750
4.4	2	166	5	63	3,900
8.8	4	168	11	58	3,400
13.2	6	170	17	52	2,700
17.6	8	172	22	47	2,200
22.0	10	174	28	41	1,700

TABLE VII

COMPUTATIONS OF INJECTION PRESSURES ACCORDING TO EQUATION (15)

	1	2	3	4	5	6	7	8	9	10	11							12							
	$\frac{t}{L/s}$	$t\times10^4$ sec.	t deg.	Total deg.	V_0 (in./deg.) $\times10^3$	v_0 in./sec.	v_1 in./sec.	$F(t)$ $s\rho v_1$	$F\left(t-\frac{L}{s}\right)$	$P_k+F\left(t-\frac{L}{s}\right)$	$p_k+s\rho v_1{}_{t-\frac{L}{s}}+s\rho v_1'{}_{t-\frac{L}{s}}$★, lb./in.²							$p_k+2\left(s\rho v_1{}_{t-\frac{L}{s}}+s\rho v_1'{}_{t-\frac{L}{s}}\right)=p_2+s\rho v_2$, lb./in.²							
											A	B	C	D	E	F	G	A	B	C	D	E	F	G	
1	0	0	0	132	6.6	29.7	197	930	0	2,000	2,000														1
2	0.5	2.85	1.5	133.5	6.8	30.6	202	950	0	2,000	2,000														2
									0	2,000	2,000							2,000							
3	1.0	5.70	2.5	134.5	7.0	31.5	209	990	930	2,930	2,930							3,860							3
4	1.5	8.56	4.0	136.0	7.3	32.9	218	1,040	950	2,950	2,950							3,900							4
5	2.0	11.4	5.0	137.0	7.6	34.2	226	1,070	990	2,990	2,990							3,980							5
6	2.5	14.3	6.5	138.5	8.0	36.0	238	1,130	1,040	3,040	3,040							4,080							6
												3,070+120													
7	3.0	17.1	7.5	139.5	8.3	36.9	244	1,150	1,070	3,070	3,070	3,190						4,140	4,380						7
8	3.5	20.0	9.0	141.0	8.6	38.7	256	1,210	1,130	3,130	3,130	3,270						4,260	4,540						8
9	4.0	22.8	10.5	142.5	9.0	40.5	268	1,270	1,150	3,150	3,150	3,320						4,300	4,640						9
10	4.5	25.7	11.5	143.5	9.3	41.9	277	1,310	1,210	3,210	3,210	3,410						4,420	4,820						10
													3,270+320												
11	5.0	28.5	13.0	145.0	9.6	43.2	286	1,350	1,270	3,270	3,270	3,490	3,590					4,540	4,980	5,180					11
12	5.5	31.4	14.0	146.0	9.8	44.2	293	1,390	1,310	3,310	3,310	3,580	3,700					4,620	5,160	5,400					12
13	6.0	34.2	15.5	147.5	9.9	44.6	295	1,400	1,350	3,350	3,350	3,640	3,780					4,700	5,280	5,560					13
14	6.5	37.1	17.0	149.0	9.7	43.6	289	1,370	1,390	3,390	3,390	3,730	3,890					4,780	5,460	5,780					14
														3,400+640											
15	7.0	39.9	18.0	150.0	9.5	42.8	283	1,340	1,400	3,400	3,400	3,790	3,960	4,040				4,800	5,580	5,920	6,080				15
16	7.5	42.8	19.5	151.5	9.1	40.9	271	1,280	1,370	3,370	3,370	3,790	4,000	4,090				4,740	5,600	6,000	6,180				16
17	8.0	45.7	20.5	152.5	8.7	39.2	260	1,230	1,340	3,340	3,340	3,790	4,020	4,120				4,680	5,580	6,040	6,240				17
18	8.5	48.5	22.0	154.0	8.2	36.9	244	1,160	1,280	3,280	3,280	3,760	4,030	4,150				4,560	5,520	6,060	6,300				18
															3,230+990										
19	9.0	51.4	23.0	155.0	7.7	34.7	230	1,090	1,230	3,230	3,230	3,710	4,020	4,160	4,220			4,460	5,420	6,040	6,320	6,440			19
20	9.5	54.2	24.5	156.5	7.0	31.5	209	990	1,160	3,160	3,160	3,620	3,970	4,120	4,190			4,320	5,240	5,940	6,240	6,380			20
21	10.0	57.0	26.0	158.0	6.3	28.4	188	890	1,090	3,090	3,090	3,530	3,880	4,070	4,150			4,180	5,060	5,760	6,140	6,300			21
22	10.5	60.0	27.0	159.0	5.8	26.1	173	820	990	2,990	2,990	3,380	3,760	3,970	4,070			3,980	5,760	5,520	5,940	6,140			22
																2,890+1,140									
23	11.0	62.8	28.5	160.5	5.2	23.4	155	730	890	2,890	2,890	3,240	3,630	3,870	3,980	4,030		3,780	4,480	5,260	5,740	5,960	6,060		23
24	11.5	65.6	29.5	161.5	4.8	21.6	143	680	820	2,820	2,820	3,120	3,480	3,760	3,880	3,940		3,640	4,240	4,960	5,520	5,760	5,880		24
25	12.0	68.5	31.0	163.0	4.2	18.9	125	590	730	2,730	2,730	2,980	3,320	3,600	3,750	3,820		3,460	3,960	4,640	5,220	5,500	5,640		25
26	12.5	71.3	32.0	164.0	3.8	17.1	113	540	680	2,680	2,680	2,850	3,150	3,450	3,620	3,680		3,360	3,700	4,300	4,900	5,240	5,380		26
					3.2	14.4	95	450									2,590+990								
27	13.0	74.2	33.5	165.5	0	0	0	0	590	2,590	2,590	2,680	2,950	3,260	3,450	3,540	3,580	3,180	3,360	3,900	4,520	4,900	5,080	5,160	27
28	13.5	77.0	34.5	166.5	0	0	0	0	540	2,540	2,540	2,590	2,810	3,090	3,310	3,410	3,450	3,080	3,180	3,620	4,180	4,620	4,820	4,900	28
									450	2,450	2,450	2,420	2,610	2,870	3,110	3,210	3,270	2,900	2,840	3,220	3,740	4,220	4,420	4,540	
29	14.0	79.9	36.0	168.0	0	0	0	0	0	2,000	2,000	1,970	2,160	2,420	2,660	2,760	2,820	2,000	1,980	2,320	2,840	3,320	3,520	3,640	29
30	14.5	82.8	37.5	169.5	0	0	0	0	0	2,000	2,000	1,940	2,060	2,290	2,530	2,660	2,730	2,000	1,880	2,120	2,580	3,060	3,320	3,460	30
31	15.0	85.6	38.5	170.5	0	0	0	0	0	2,000	2,000	1,870	1,940	2,140	2,380	2,520	2,600	2,000	1,740	1,880	2,280	2,760	3,040	3,200	31
32	15.5	88.4	40.0	172.0	0	0	0	0	0	2,000	2,000	1,820	1,860	2,030	2,240	2,410	2,470	2,000	1,640	1,720	2,060	2,480	2,820	3,040	32
33	16.0	91.3	41.0	173.0	0	0	0	0	0	2,000	2,000	1,450	1,430	1,570	1,740	1,920	2,000	2,000	900	860	1,140	1,480	1,840	2,000	33

★v_1'=Velocities of reflected waves reaching pump plunger at $t-\frac{L}{s}$.

TABLE VII—Continued

COMPUTATIONS OF INJECTION PRESSURES ACCORDING TO EQUATION (15)—Continued

	13							14							15	16	17	18	19	20	21	
	p_2, lb./sq.²							$spu2$, lb./in.²							$W(t)$ lb./in²	$V(t)$ lb./in.²	$Y(t)$ lb./in.²	$R(t)$ lb./in.²	$M(t)$ lb./in.²	$N(t)$ lb./in.²	$S(t)$ lb./in.²	
	A	B	C	D	E	F	G	A	B	C	D	E	F	G								
1																						1
2																						2
	2,000							0							0							
3	3,050							810							−120							3
4	3,090							810							−140							4
5	3,160							820							−170							5
6	3,240							840							−200							6
7	3,290	3,510						850	870						−220	−320						7
8	3,400	3,660						860	880						−270	−390						8
9	3,440	3,750						860	890						−290	−430						9
10	3,550	3,910						870	910						−340	−500						10
11	3,660	4,050	4,230					880	930	950					−390	−560	−640					11
12	3,730	4,210	4,420					890	950	980					−420	−630	−720					12
13	3,800	4,320	4,560					900	960	1,000					−450	−680	−780					13
14	3,870	4,480	4,760					910	980	1,020					−480	−750	−870					14
15	3,880	4,580	4,890	5,030				920	1,000	1,030	1,050				−480	−790	−930	−990				15
16	3,830	4,600	4,960	5,120				910	1,000	1,040	1,060				−460	−810	−960	−1,030				16
17	3,780	4,580	5,000	5,180				900	1,000	1,040	1,060				−440	−790	−980	−1,060				17
18	3,670	4,530	5,010	5,230				890	990	1,050	1,070				−390	−770	−980	−1,080				18
19	3,580	4,450	5,000	5,250	5,360			880	970	1,040	1,070	1,080			−350	−740	−980	−1,090	−1,140			19
20	3,460	4,280	4,910	5,180	5,310			860	960	1,030	1,060	1,070			−300	−660	−940	−1,060	−1,120			20
21	3,340	4,120	4,750	5,090	5,240			840	940	1,010	1,050	1,060			−250	−590	−870	−1,020	−1,090			21
22	3,160	3,850	4,530	4,910	5,090			820	910	990	1,030	1,050			−170	−470	−770	−940	−1,020			22
23	2,980	3,600	4,300	4,730	4,930	5,020		800	880	960	1,010	1,030	1,040		−90	−360	−670	−860	−950	−990		23
24	2,870	3,390	4,030	4,530	4,750	4,850		770	850	930	990	1,010	1,030		−50	−270	−550	−770	−870	−910		24
25	2,700	3,140	3,740	4,260	4,510	4,640		760	820	900	960	990	1,000		+30	−160	−420	−660	−760	−820		25
26	2,620	2,910	3,440	3,980	4,280	4,410		740	790	860	920	960	970		+60	−60	−290	−530	−660	−730		26
27	2,460	2,620	3,090	3,640	3,970	4,140	4,210	720	740	810	880	930	940	950	+130	+60	−140	−380	−520	−600	−630	27
28	2,360	2,450	2,840	3,330	3,720	3,880	3,990	720	730	780	850	900	940	930	+180	+140	−30	−240	−410	−470	−520	28
	2,220	2,170	2,490	2,950	3,370	3,550	3,660	680	670	730	790	850	870	880	+230	+250	+120	−130	−260	−340	−390	
29	1,450	1,400	1,730	2,160	2,580	2,760	2,860	550	540	590	680	740	760	780	+550	+570	+430	+260	+80	0	−40	29
30	1,450	1,360	1,560	1,950	2,360	2,580	2,700	550	520	560	630	700	740	760	+550	+580	+500	+340	+170	+80	+30	30
31	1,450	1,240	1,350	1,690	2,100	2,340	2,480	550	500	530	590	660	700	720	+550	+630	+590	+450	+280	+180	+120	31
32	1,450	1,150	1,210	1,480	1,840	2,140	2,330	550	490	510	580	640	680	710	+550	+670	+650	+550	+400	+270	+140	32
33	1,450	560	540	750	1,030	1,320	1,450	550	340	320	390	450	520	550	+550	+890	+890	+820	+710	+600	+550	33

APPENDIX II

SAMPLE CALCULATION CONSIDERING PRESSURE WAVES

Consider the conditions under which equations (6) and (11) were evaluated:

p_k—2,000 lb. per sq. in.
L—34 in.
T—0.01498 sq. in.
A—0.0985 sq. in.
$\frac{A}{T}$—6.6.
n—750 r. p. m.
γ—0.0307 lb. per cu. in.
ρ—0.795 x 10^{-4} lb. sec.^{2} in.$^{-4}$.
a—0.000314 sq. in.
c—0.94.
$\frac{T}{ac}$—50.8.
s—59,600 in. per sec.

Using equations (14) and (15):

Tabulate in Table VII, column 1, the time in units of 0.5 L/s in which

$$\frac{L}{s}=\frac{34}{59,600}\text{ sec.}=0.000572\text{ sec.}$$

(any multiple of L/s less than 1 could be used.) In column 2 tabulate the time in units of seconds. In column 3 tabulate the time in units of pump degrees from the equation

$$\theta=6\ nt \qquad (51a)$$

in which θ is the rotation of the pump in degrees and n the pump r. p. m. From Figure 5 it is seen that the by-pass valve closes at 132 pump degrees; consequently the total pump rotation—tabulated in column 4—for any time is 132, plus the corresponding value in column 3. From column 4 and Figure 5 the pump plunger velocity is obtained in units of in. per degree, and is tabulated in column 5. The velocity is changed to units of in. per second by multiplying the values in column 5 by $6n$, column 6. By multiplying the values in column 6 by A/T, equation (19), the corresponding values of v_1 are obtained, column 7. The values in column 7 are multiplied by $s\rho$ to obtain the values of the waves originating at the pump plunger at each time ordinate, column 8. Since each wave reaches the discharge orifice L/s seconds after it originates at the pump plunger, the values in column 8 are tabulated in column 9, but displaced by a time interval of L/s seconds. Column 9, therefore, represents the values of $F(t-L/s)$ in equations (21). By adding these values to p_k the effect of the oncoming wave originating at the pump plunger plus the static pressure in the injection tube is obtained, column 10. The values are tabulated again in column 11–A. The next step is to obtain the value of the back-rushing wave W. The graphical method is used. From equation (29)

$$p_2-p_z=\frac{\rho}{2}v_2^2\left(\frac{T}{a\ c}\right)^2 \qquad (29)$$

Neglecting p_z

$$p_2=\frac{0.795\times10^{-4}}{2}\ 50.8^2\ v_2^2=0.1027\ v_2^2.$$

From Table VII it is seen that the maximum value of v_1 is 295 in. per second. Consequently, p_2 is evaluated for values of v_2 up to 300 in. per second. From these values corresponding values of $p_2+s\rho v_2$ are obtained.

TABLE VIII

COMPUTATIONS OF

$p_2+s\rho v_2$

1	2	3	4
v_2 in./sec.	p_2 lb./sq. in.	$s\rho v_2$ lb./sq. in.	$p_2+s\rho v_2$ lb./sq. in.
100	1,026	437	1,499
150	2,310	710	3,020
200	4,100	950	5,050
250	6,410	1,180	7,390
300	9,230	1,420	10,650

(Table VIII.) The curve in Figure 26 for $s\rho v_2$ against $p_2+s\rho v_2$ is plotted from Table VIII. Since $p_2+s\rho v_2=p_k+2s\rho v_{1_{t-\frac{L}{s}}}$ (equation 25), this is also a curve of $s\rho v_2$ against $p_k+2s\rho v_{1_{t-\frac{L}{s}}}$. In column 12–A are tabulated the values of $p_k+2s\rho v_{1_{-\frac{L}{s}}}$ from the sum of column 11 plus column 9. With these values of $p_k+2s\rho v_{1_{t-\frac{L}{s}}}$ the corresponding values of $s\rho v_2$ are obtained from the curve in Figure 26 and tabulated in column 14–A. Column 14–A represents the part of the oncoming wave $\rho s v_1$ which is lost to discharge through the discharge orifice. Therefore, the reflected part of the oncoming wave is column 14–A minus column 9. (Equation (32).) These values are entered in column 15. The value of

p_2 (column 13–A) can now be obtained by subtracting column 14 from column 12, or by subtracting column 15 from column 11. (Equation (25)). Column 14 can be eliminated from the computations entirely by plotting a curve of p_2 against $p_2+s\rho v_2$ from Table VIII. The values of $s\rho v_2$ are incorporated in Table VII to show the amount of the oncoming wave energy that is lost to discharge. On the completion of the process, the values of p_2 in column 13–A represent the first three terms in the right-hand member of equations (14) and (15). At the end of the third phase, $t=3L/s$ seconds, the reflected wave from the first phase (column 15) has again reached the discharge orifice and must be added to the values of column 11. This is done in column 11–B, so that column 11–B represents the oncoming wave during the fourth phase, and can be treated as a single wave. Consequently, a corresponding series of values for column 12 must be

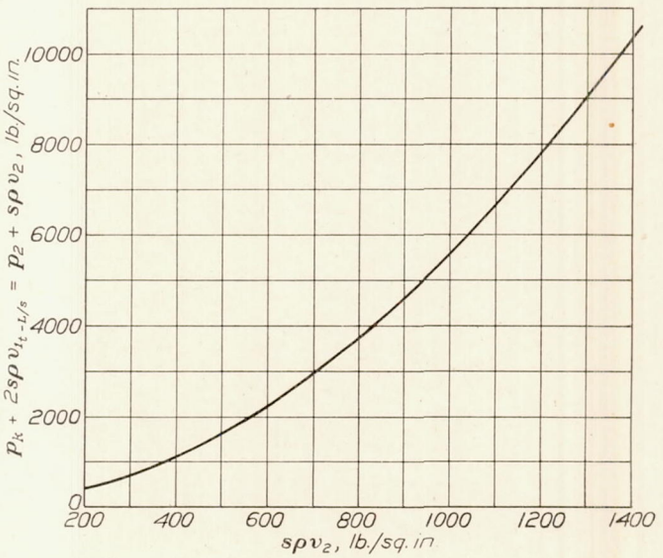

FIGURE 26.

obtained (column 12–B) which start at a time of $3L/s$ seconds. From columns 12–B and 11–B, columns 14–B and 16 are obtained. Column 16 represents the reflected portion of the wave originating in the phase under consideration plus the reflected portion of the wave reflected at the discharge orifice $2L/s$ seconds earlier. Consequently, if column 15 is subtracted from column 16, the result is the portion of column 15, phase of $2L/s$ seconds earlier, that is now reflected. Therefore, the difference between column 16 and column 15 must always be less than the value of column 15 for a time of $2L/s$ seconds earlier.

This process is continued until the injection process is completed. From Table VII it is seen that the bypass valve in the fuel injection pump opens, stopping the injection process at the pump at $t=13L/s$ seconds, so that after 14 L/s seconds, the values of column 9 become zero. If the check valve at the entrance to the fuel injection tube closes instantaneously, the pressure waves that are oscillating in the injection tube continue, although there is no reenforcement from the fuel pump plunger. The injection process continues until the energy of these waves at the discharge orifice becomes less than the injection valve closing pressure, in this case, 2,000 lb. per sq. in. The total fuel quantity discharged during the injection process is obtained, as before, by subtracting from the fuel quantity displaced by the pump plunger the fuel lost to compression. Since, in this particular case the valve closing pressure is equal to p_k, no fuel is lost to compression.

To find how an individual wave originating at the pump plunger loses its energy because of the discharge through the discharge orifice, consider the initial wave originating at $t=0$. The intensity of this wave is 930 lb. per sq. in. However, 810 lb. per sq. in. of it are lost because of discharge when the wave first reaches the discharge orifice at $t=L/s$ seconds. The remaining 120 lb. per sq. in. is reflected to the pump plunger, and is again reflected to the discharge orifice, reaching it at $t=3L/s$ seconds. Its reflected intensity is column 16 minus column 15 for $t=3L/s$ seconds, 100 lb. per sq. in. When it again reaches the discharge orifice, $t=5L/s$ seconds the reflected portion, column 17 minus column 16, is 80 lb. per sq. in. On its next reflection it is reduced to 60 lb. per sq. in., then to 40 lb. per sq. in., until at $t=13L/s$ seconds the original wave of 930 lb. per sq. in. has been reduced to 30 lb. per sq. in. because of the energy lost to discharge. From this point on the wave is neglected as being negligible.

From Table VII a series of curves may be drawn representing the pressures at the discharge orifice caused by the various pressure waves as expressed in equations (14) and (15). First, the static pressure in the injection tube, p_k is plotted. (Fig. 27.) To this is added the values of $F(t-L/s)$ from column 9 of Table VII. This curve is designated $F(t-L/s)$. The reflected portion of this curve is added $W(t-L/s)$. (Column 15.) The values of $W(t-L/s)$ again reach the injection valve $2L/s$ seconds after they left it. Consequently, the values of $W(t-L/s)$ are again added to the curve but offset a time of $2L/s$ seconds and designated $U(t-3L/s)$. The reflected portion of $U(t-3L/s)$, designated $V(t-3L/s)$, is obtained by subtracting column 15 from column 16. This process is continued until the injection process is completed. The addition of all the waves constitutes the total pressure, and is indicated in Figure 27 by the uppermost line. It is seen that the curve jumps at all values of $\eta L/s$ where η is an odd number, but that the jump continually decreases in intensity. At L/s seconds after the end of the injection process at the pump, $F(t-L/s)$ becomes equal to zero, and the curve has an instantaneous drop. The injection process at the discharge orifice continues, however, until the

other waves in the injection tube have decreased so that the pressure at the discharge orifice becomes less than 2,000 lb. per sq. in., the injection valve closing pressure.

The solution of the instantaneous pressure according to equation (39) is given in Table IX. Columns 1 to 10 are the same as columns 1 to 10 of Table VII. Column 10, however, contains in a single column the sum of all the onrushing waves. In column 11 for the time interval from $t=0$ to $t=3L/s$ seconds the values of $p_k+F(t-L/s)$ are tabulated as before, and the results in columns 12, 13, 14, and 15 for the same interval are tabulated as in Table VII. However, at $t=3L/s$ the jump in the curve occurs, so to column 10 is added the value of $-W$ obtained from column 14 for the time $2L/s$ seconds before the time under consideration. These values are entered in column 11 with the two values shown at $t=3L/s$ seconds. Column 12 is now column 11 plus the difference between column 11 and p_k. Column 14, as in Table VII, is obtained from Figure 26. Column 13, p_2, is column 12 minus column 14. In the completed table column 13 contains only the final pressures and not the individual pressures from the various waves. As is seen, the calculations are much shorter and simpler to handle than those given in Table VII.

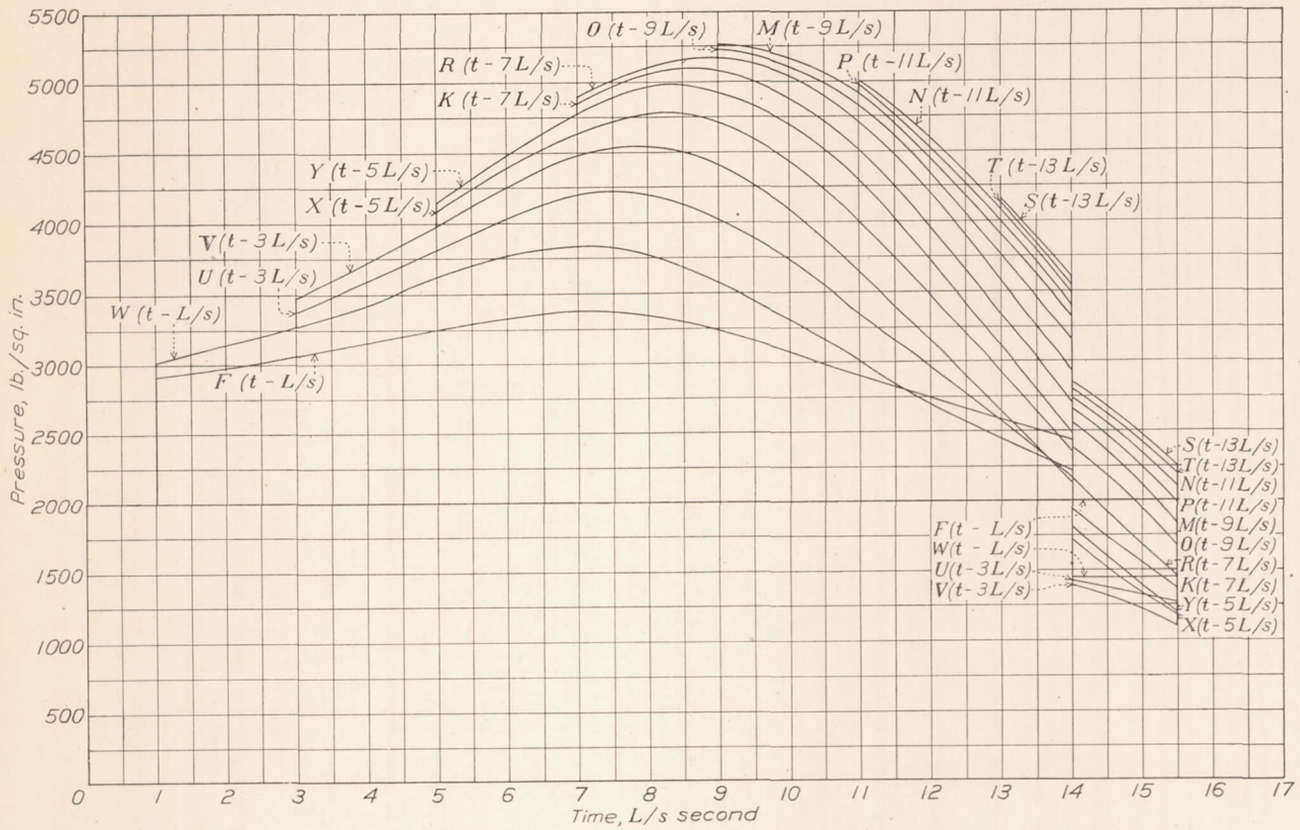

FIGURE 27.—Instantaneous pressures computed from equation (39)

W= Reflected portion of F	$U\left(t-3\frac{L}{s}\right)=W\left(t-\frac{L}{s}\right)$
V= " " " U	$X\left(t-5\frac{L}{s}\right)=V\left(t-3\frac{L}{s}\right)$
Y= " " " X	$K\left(t-7\frac{L}{s}\right)=Y\left(t-5\frac{L}{s}\right)$
R= " " " K	$O\left(t-9\frac{L}{s}\right)=R\left(t-7\frac{L}{s}\right)$
M= " " " O	$P\left(t-11\frac{L}{s}\right)=M\left(t-9\frac{L}{s}\right)$
N= " " " P	$T\left(t-13\frac{L}{s}\right)=M\left(t-11\frac{L}{s}\right)$
S= " " " T	

TABLE IX

COMPUTATIONS ACCORDING TO EQUATION (39)

1	2	3	4	5	6	7	8	9	10	11	12	13	14	15
t L/s	$t\times10^4$ sec.	t deg.	Total deg.	Vo (in./deg.) $\times10^3$.	vo in./sec.	v_1 in./sec.	$F(t)$ $s\rho v_1$	$F(t-L/s)$	$p_k+F(t-L/s)$	$p_k+F(t-L/s)$ $-W(t-2\ L/s)$	$p_k+2F(t-L/s)$ $-2W(t-2\ L/s)$	p_2 lb./in.^{2}	$s\rho v_2$	W'
0	0	0	132	6.6	29.7	197	930	0	2,000	2,000				
0.5	2.85	1.5	133.5	6.8	30.6	202	950	0	2,000	2,000				
1.0	5.70	2.5	134.5	7.0	31.5	209	990	0 930	2,000 2,930	2,000 2,930	2,000 3,860	2,000 3,050	0 810	0 −120
1.5	8.56	4.0	136.0	7.3	32.9	218	1,040	950	2,950	2,950	3,900	3,090	810	−140
2.0	11.4	5.0	137.0	7.6	34.2	226	1,070	990	2,990	2,990	3,980	3,160	820	−170
2.5	14.3	6.5	138.5	8.0	36.0	238	1,130	1,040	3,040	3,040	4,080	3,240	840	−200
3.0	17.1	7.5	139.5	8.3	36.9	244	1,150	1,070	3,070	3,070 3,190	4,140 4,380	3,290 3,510	850 870	−220 −320
3.5	20.0	9.0	141.0	8.6	38.7	256	1,210	1,130	3,130	3,270	4,540	3,660	880	−390
4.0	22.8	10.5	142.5	9.0	40.5	268	1,270	1,150	3,150	3,320	4,640	3,750	890	−430
4.5	25.7	11.5	143.5	9.3	41.9	277	1,310	1,210	3,210	3,410	4,820	3,910	910	−500
5.0	28.5	13.0	145.0	9.6	43.2	286	1,350	1,270	3,270	3,490 3,590	4,980 5,180	4,050 4,230	930 950	−560 −640
5.5	31.4	14.0	146.0	9.8	44.2	293	1,390	1,310	3,310	3,700	5,400	4,420	980	−720
6.0	34.2	15.5	147.5	9.9	44.6	295	1,400	1,350	3,350	3,780	5,560	4,560	1,000	−780
6.5	37.1	17.0	149.0	9.7	43.6	289	1,370	1,390	3,390	3,890	5,780	4,760	1,020	−870
7.0	39.9	18.0	150.0	9.5	42.8	283	1,340	1,400	3,400	3,960 4,040	5,920 6,080	4,890 5,030	1,030 1,050	−930 −990
7.5	42.8	19.5	151.5	9.1	40.9	271	1,280	1,370	3,370	4,090	6,180	5,120	1,060	−1,030
8.0	45.7	20.5	152.5	8.7	39.2	260	1,230	1,340	3,340	4,120	6,240	5,180	1,060	−1,060
8.5	48.5	22.0	154.0	8.2	36.9	244	1,160	1,280	3,280	4,150	6,300	5,230	1,070	−1,080
9.0	51.4	23.0	155.0	7.7	34.7	230	1,090	1,230	3,230	4,160 4,220	6,320 6,440	5,250 5,360	1,070 1,080	−1,090 −1,140
9.5	54.2	24.5	156.5	7.0	31.5	209	990	1,160	3,160	4,190	6,380	5,310	1,070	−1,120
10.0	57.0	26.0	158.0	6.3	28.4	188	890	1,090	3,090	4,150	6,300	5,240	1,060	−1,090
10.5	60.0	27.0	159.0	5.8	26.1	173	820	990	2,990	4,070	6,140	5,090	1,050	−1,020
11.0	62.8	28.5	160.5	5.2	23.4	155	730	890	2,890	3,980 4,030	5,960 6,060	4,930 5,020	1,030 1,040	−950 −990
11.5	65.6	29.5	161.5	4.8	21.6	143	680	820	2,820	3,940	5,880	4,850	1,030	−910
12.0	68.5	31.0	163.0	4.2	18.9	125	590	730	2,730	3,820	5,640	4,640	1,000	−820
12.5	71.3	32.0	164.0	3.8	17.1	113	540	680	2,680	3,680	5,380	4,410	970	−730
13.0	74.2	33.5	165.5	3.2 0	14.4 0	95 0	450 0	590	2,590	3,540 3,580	5,080 5,160	4,140 4,210	940 950	−600 −630
13.5	77.0	34.5	166.5	0	0	0	0	540	2,540	3,450	4,900	3,970	930	−520
14.0	79.9	36.0	168.0	0	0	0	0	450 0	2,450 2,000	3,270 2,820	4,540 3,640	3,660 2,860	880 780	−390 −40
14.5	82.8	37.5	169.5	0	0	0	0	0	2,000	2,730	3,460	2,700	760	+30
15.0	85.6	38.5	170.5	0	0	0	0	0	2,000	2,600	3,200	2,480	720	+120
15.5	88.4	40.0	172.0	0	0	0	0	0	2,000	2,470	3,040	2,330	710	+140
16.0	91.3	41.0	173.0	0	0	0	0	0	2,000	2,000	2,000	1,450	550	+550

APPENDIX III

SAMPLE CALCULATIONS FOR DETERMINING CRITICAL INJECTION TUBE DIAMETER AND LOSSES IN TUBE

As an example, consider the fuel injection pump already under consideration. Let V equal 0.0079 in. per degree, approximately the average value for V from Figure 5. Let the discharge orifice be 0.020 in. in diameter, 0.000314 sq. in. in area, with a discharge coefficient of 0.94. In order to determine the value of μ the pressure of the fuel must be determined. This pressure is obtained from equation (2).

$$p_m = \frac{18\,(AnV)^2\rho}{(ac)^2} \tag{2}$$

$$= \frac{18(0.0985 \times 750 \times 0.0079)^2 \times 0.795 \times 10^{-4}}{(0.000314 \times 0.94)^2} = 5{,}600 \text{ lb. per sq. in.}$$

Having determined the value of p, the value of μ is determined from a pressure-viscosity curve. Figure 28 shows the pressure-viscosity curve obtained by

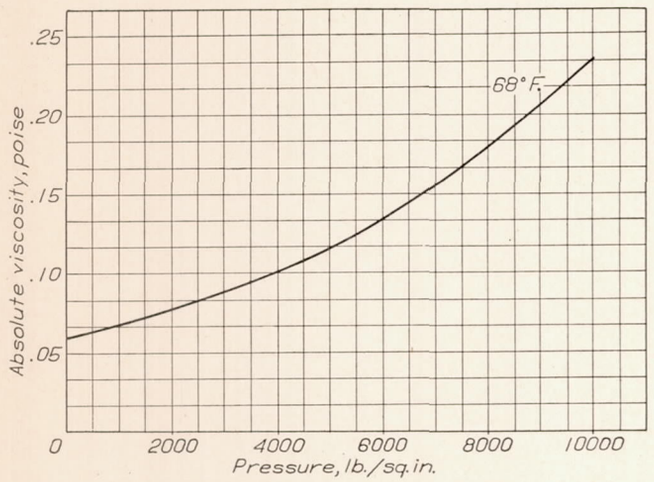

FIGURE 28.—Effect of pressure on viscosity of fuel oil

Hersey (reference 20) for Diesel oil with a Saybolt Universal viscosity of 45 seconds at 80° F. and atmospheric pressure. The viscosity at 5,600 lb. per sq. in. pressure is 0.130 poise, that is, 0.130 dyne cm.$^{-2}$ sec. This must be converted into the English system. The process is

$$\mu g = \frac{0.130 \text{ dyne sec. cm.}^{-2}}{981 \text{ dyne g.}^{-1}} \times 981 \text{ cm. sec.}^{-2}$$

$$= 0.130 \text{ g. cm.}^{-1} \text{ sec.}^{-1}$$

$$= \frac{0.130 \text{ g. cm.}^{-1} \text{ sec.}^{-1} \times 2.54 \text{ cm. in.}^{-1}}{454 \text{ g. lb.}^{-1}}$$

$$= 0.000728 \text{ lb. in.}^{-1} \text{ sec.}^{-1}$$

The kinematic viscosity is obtained from

$$\nu = \frac{\mu}{\rho} = \frac{\mu g}{\gamma} = \frac{0.000728 \text{ lb. in.}^{-1} \text{ sec.}^{-1}}{0.0307 \text{ lb. in.}^{-3}}$$

$$= 0.0237 \text{ in.}^2 \text{ sec.}^{-1}$$

The critical velocity at 750 r. p. m. is obtained from equation (45)

$$v_k = \frac{2{,}000 \times 0.0237 \text{ in.}^2 \text{ sec.}^{-1}}{D \text{ in.}}$$

$$= \frac{47.4}{D} \text{ in. sec.}^{-1}$$

which expresses v_k as a function of the injection tube diameter. In the case under consideration

$$D_k = \frac{6nVA}{500\nu\pi} \tag{46}$$

$$= \frac{4500 \times 0.0079 \times 0.0985}{\pi \times 500 \times 0.0237}$$

$$= 0.094 \text{ in.}$$

Expressed as a function of pump speed equation (46) becomes

$$D_k = \frac{6n \times 0.0079 \times 0.0985}{500 \times \pi \times 0.0237}$$

$$= 2.99 \times 10^{-5} n$$

In Fgure 29 the effect of the pump speed on the critical injection tube diameter is shown, and it is seen that the maximum value of D_k occurs at 600 r. p. m.

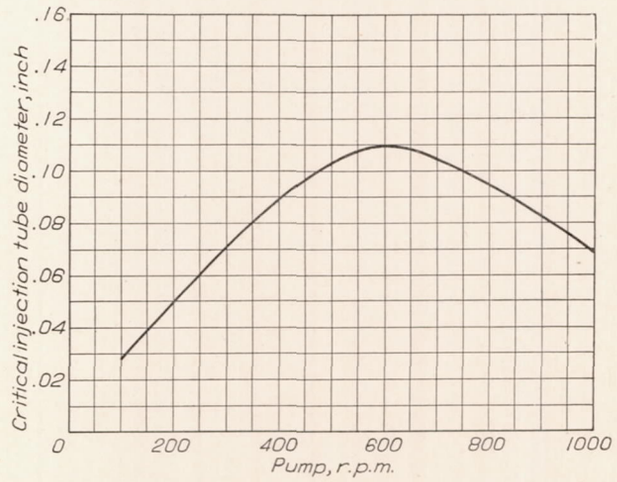

FIGURE 29.—Effect of pump r. p. m. on critical injection tube diameter

For the pump speed of 750 r. p. m. the effect of injection-tube diameter on the friction loss is obtained as

follows: The average velocity through the injection tube is expressed by the relationship

$$v_{1_m}=\frac{A}{\frac{\pi}{4}D^2}\,6nV=\frac{\frac{\pi}{4}0.354^2}{\frac{\pi}{4}D^2}\times 6\times 750\times 0.0079$$

$$=\frac{4.46}{D^2}\text{ in. sec.}^{-1}$$

where D is in inches. The coefficient of friction is obtained from equation (48). Substituting the values obtained in the previous equations

$$f=0.00714+0.6104\left(\frac{4.46}{D^2}\,D\,\frac{1}{0.0237}\right)^{-0.35}$$

$$=0.00714+0.6104\left(\frac{188.3}{D}\right)^{-0.35}$$

The value of f is determined for each value of D. The average value of v_1 expressed as a function of D is substituted in equation (47) which becomes

$$p=fL\left(\frac{4.46}{D^2}\right)^2\frac{\rho}{2D}.$$

The coefficient f is dimensionless because it is a function of Reynolds Number. Substituting the dimensions of the factors

$$p=\text{in. in.}^2\text{ sec.}^{-2}\frac{\text{lb. in.}^{-3}}{\text{in. sec.}^{-2}\text{ in.}}$$

$$=\text{lb. in.}^{-2}$$

Substituting the values already determined and assuming an injection tube 34 inches in length

$$p=\frac{f\times 34\times 19.9\times 0.0307}{2\times D^5\times 386}$$

$$=\frac{0.0269}{D^5}\left[0.00714+0.614\left(\frac{188.3}{D}\right)^{-0.35}\right]$$

The curve of this equation, together with the values of v_m and v_k are shown in Figure 30. It is seen that v_k and v_m intersect at an injection tube diameter of

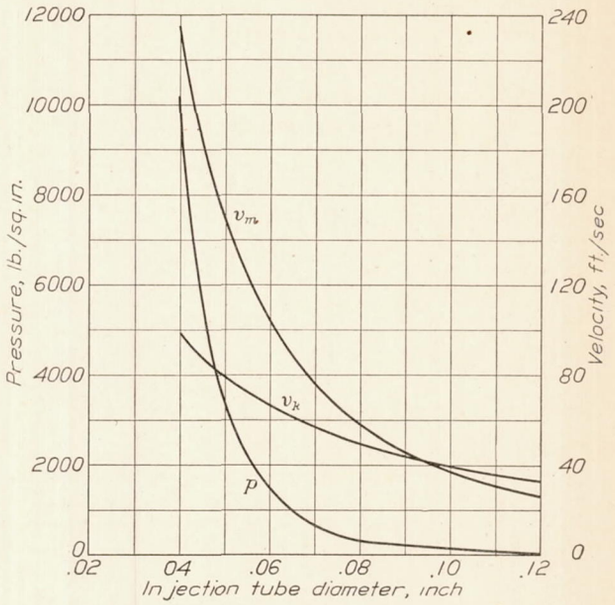

FIGURE 30.—Effect of injection tube diameter on pressure losses, maximum velocity, and critical velocity. Orifice diameter=0.020 inch; pump speed=750 r. p. m.; tube length=33.75 inches

0.094 inch. The figure shows the high pressure losses that can occur in the injection tube for small tube diameters.

APPENDIX IV

WORK OF OTHER INVESTIGATORS

Work of Matthews and Gardiner (reference 27).—Matthews and Gardiner investigated the injection characteristics of an impact pump by means of spraying the fuel onto a target attached to the flywheel of the engine. They claimed that this type of pump would give injection characteristics that were independent of engine speed because the discharge was controlled by the return of the pump plunger when released by a cam with a radial drop. Their results showed that the time of injection for a constant stroke decreased with an increase in the discharge-orifice diameter. This was due to the lower end-pressure of injection, and is in accord with the results presented in this report. They found that the discharge interval decreased with an increase in valve opening pressure, and correctly attributed it to the additional time necessary to build up the pressure in the injection tube to the valve opening pressure. They also found that for a given valve opening pressure the injection lag increased with an increase in discharge-orifice area. This is rather difficult to explain, unless with the larger orifices the initial discharge was not of sufficient intensity to record on the paper targets.

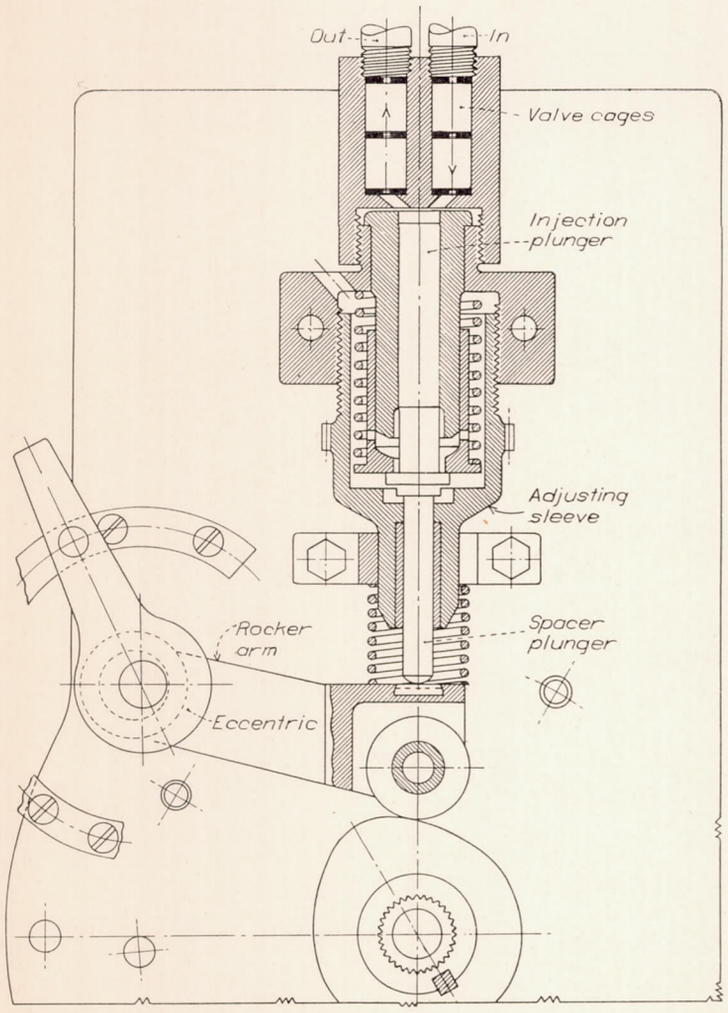

FIGURE 31.—Fuel pump used by Matthews

Matthews and Gardiner's attempt to design an injection system that was independent of engine speed is interesting. The chief difficulty with the system they suggested would lie in the pump plunger not returning under its spring force entirely, but being affected by the cam follower overtraveling the drop of the cam at the high speeds. Furthermore, the cam would be subjected to severe impact loads.

Work of Matthews (reference 28.)—Matthews investigated the spray characteristics of a cam-operated variable stroke pump (fig. 31) by means of spray targets. He found that the maximum injection pressures varied with pump r. p. m. Matthews did not use a check valve at the entrance to the injection tube, since he believed that it would restrict the fuel flow. This belief is not in accordance with the results presented in this report. Matthews stated that any pressure waves caused by the initial impact of the cam against the cam follower were probably dissipated. Actually, in his injection system, in which there was an initial clearance between the cam and the cam follower, there were probably pressure waves of a rather violent nature. He noted secondary discharges and attributed them to the bouncing of the stem. He recorded a slight increase in injection lag with injection valve opening pressure. Matthews correctly attributed discharge that took place after the pump plunger had passed through the top center of its stroke to the compressibility and elasticity of the fuel. The time lag of injection that Matthews obtained shows that his injection was probably more of a wave phenomenon than a displacement phenomenon. The lag (fig. 32) is virtually independent of engine speed, varying from 0.0013 second to 0.0012 second for a speed range from 600 to 1,600 r. p. m. Since the time lag remained virtually independent of engine speed over the range investigated, the start of injection at least was apparently controlled by the elasticity and inertia of the fuel and not by the rate of displacement of the pump

plunger. Matthews attributed too many of the characteristics that he observed to the motion of the automatic injection valve stem. The apparent time interval between the start of injection and the high rate of injection, which he based on the opening of the injection valve, is probably due more to the pressure-wave phenomenon such as is observed in Figure 19. As he has stated, investigations with spray targets must be supplemented by additional research on the rates of discharge from the injection valves in order to interpret fully the target data.

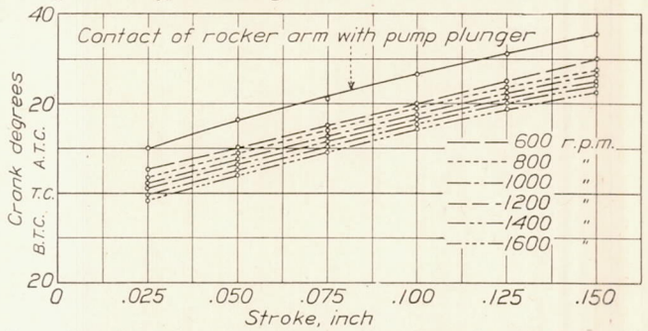

FIGURE 32.—Effect of r. p. m. on time lag of jet. Two orifices 0.022 inch; valve opening pressure=1,000 lb./sq. in.; primary pressure=225 lb./sq. in.

Work of Hicks and Moore (reference 29).—Hicks and Moore, by means of an oscilloscope, investigated the spray characteristics of the same variable-stroke fuel pump tested by Matthews. Their data, however, are for a constant fuel quantity and not constant stroke so that the data are difficult to interpret. They recorded a negative injection lag (fig. 33) at speeds over

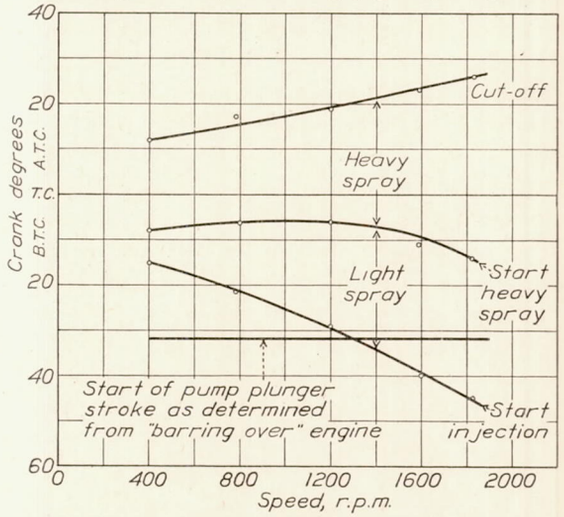

FIGURE 33.—Effect of engine speed on injection lag, spray characteristics, and duration of injection. Orifice diameter=0.025 inch; fuel quantity constant at 2.5×10^{-4} lb./cycle; valve opening pressure=6,000 lb./sq. in.

1,300 r. p. m. Matthews did not record negative lags even at speeds as high as 1,600 r. p. m. By means of the oscilloscope Hicks and Moore found that the pump cam had become irregular because of excessive use; consequently, the rocker arm left the cam at high speeds, causing it to strike the pump plunger at an earlier position than that obtained from barring the engine over.

Work of Joachim.—During the process of the development of the N. A. C. A. single-cylinder pump for use on the N. A. C. A. Universal test engine, Joachim recorded the injection lag by means of spray targets. The injection pump that he employed was eccentric-operated. The injection valve has been described in reference 25. He found that the injection lag increased with the injection valve opening pressure (fig. 34) but that at a valve opening pressure of 2,750 lb. per sq. in. the curve became discontinuous. At opening pressures above this the lag curve, while remaining parallel to the original portion of the curve, was offset from it. At the lower valve opening pressures the initial pressure waves from the pump were apparently sufficient to open the injection valve, but the maximum intensity of this wave was 2,750 lb. per sq. in. Consequently,

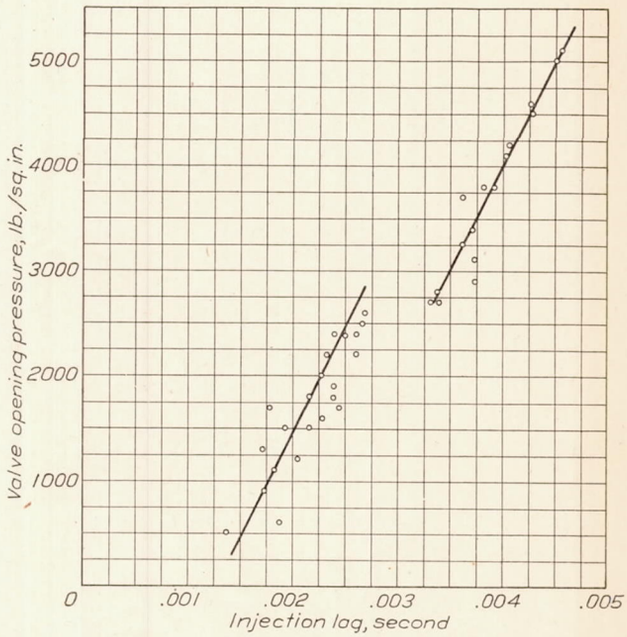

FIGURE 34.—Effect of valve opening pressure on injection lag. Pump speed=750 r. p. m.; tube length=44 inches; inside diameter=0.125 inch; outside diameter=0.250 inch; primary pressure=200 lb./sq. in.

when a higher valve opening pressure was used, the injection valve did not open until a reenforced wave reached it.

Work of Alexander (reference 21).—Alexander recorded the instantaneous pressures in a fuel injection system by means of a Hopkinson optical indicator, and the motion of the injection valve stem by means of a Cosby indicator. The pump tested is shown in Figure 35. The load control was obtained by means of the spill valve which by-passed a portion of the fuel during the injection. Alexander investigated the effect of valve opening pressure and load on the pressures in the injection system. He found that increasing the valve opening pressure increased the injection pressures throughout the injection period. (Fig. 36.) This is in accord with the mathematical analysis and the experimental work presented in this report. He also found

that because of the compressibility of the fuel the pressures did not reach the maximum pressure of 2,000 lb. per sq. in. as given in equation (2) of this report unless the valve opening pressure exceeded this amount. When this was so, the pressure dropped steadily after the injection valve opened. Alexander correctly concluded that the injection characteristics of an injection system can be materially altered by changing the injection valve opening pressure.

The effect of load on the instantaneous pressures with the type of pump he employed is shown in Figure 37. It is seen that as the load decreased, the instantaneous pressures, after injection started, decreased at a more rapid rate because of the fuel quantity by-passed through the spill valve. The use of the spill valve as a load control is the same as the use of a variable-stroke pump for load control. In each case, the instantaneous injection pressures, and, consequently, the fuel atomi-

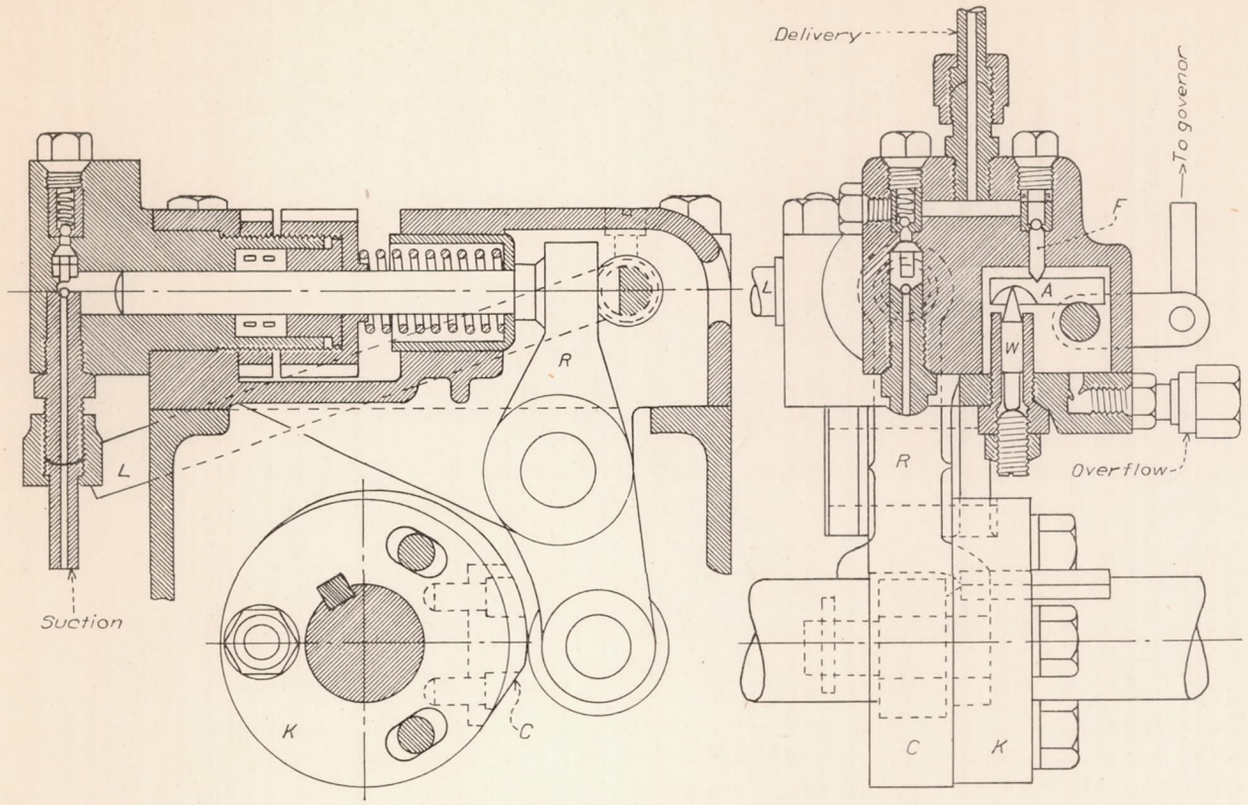

FIGURE 35.—Fuel pump used by Alexander

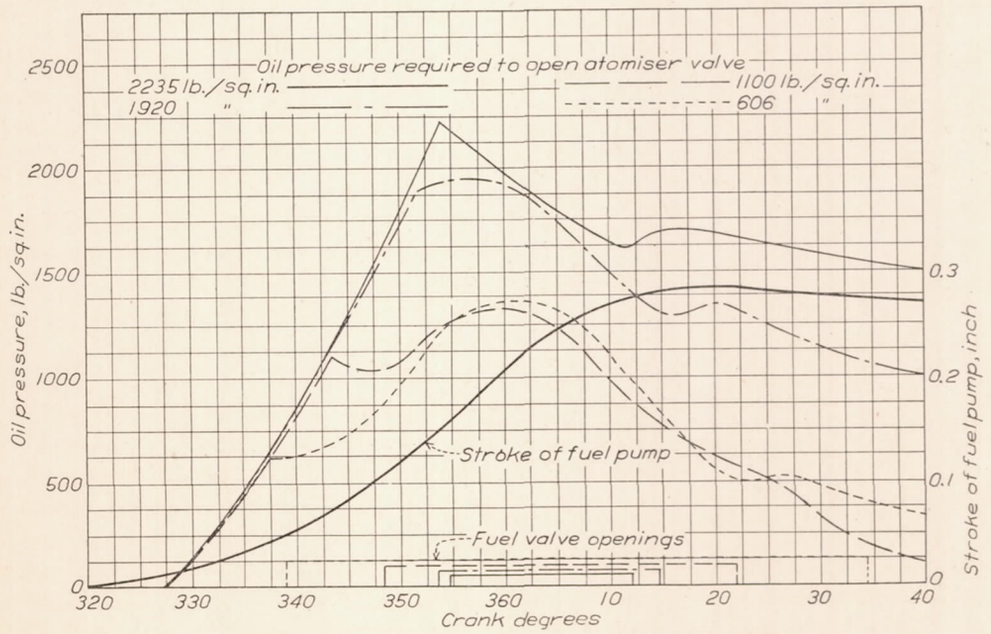

FIGURE 36.—Effect of injection valve opening pressure on instantaneous pressures

zation and distribution vary with the load. Consequently, the type of combustion in the combustion chamber of the engine will vary with load. This constitutes the chief objection to the variable-stroke injection pump.

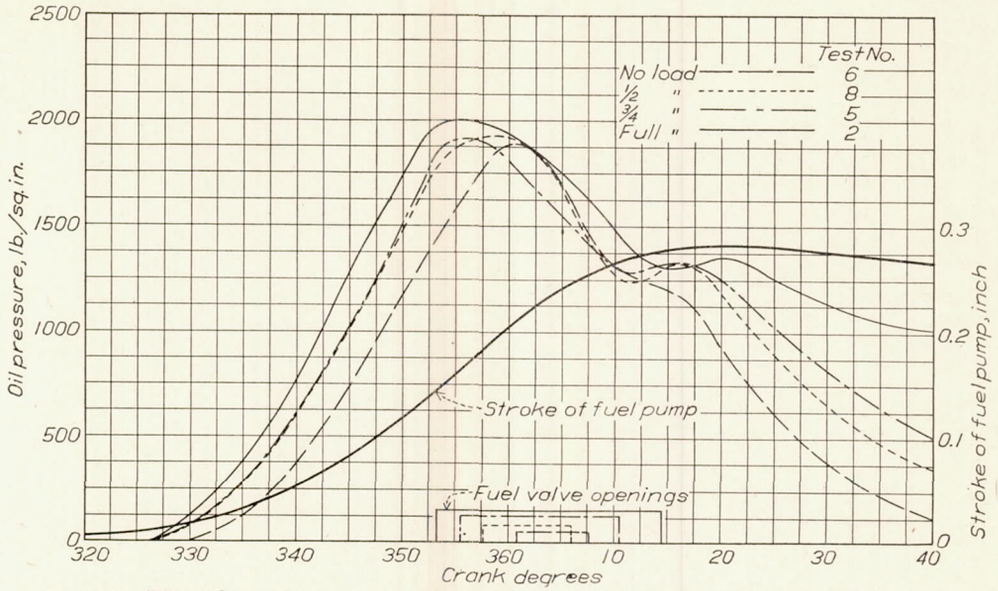

FIGURE 37.—Effect of load on instantaneous pressures. Pressure required to open atomizer valve=1,920 lb./sq. in.

Work of Wild (reference 1).—In a paper presented before the Society of Automotive Engineers, Wild has given a discussion of the operation of various types of fuel injection pumps. He correctly states that the instantaneous pressures delivered by a fuel injection pump are less than the values obtained by equating

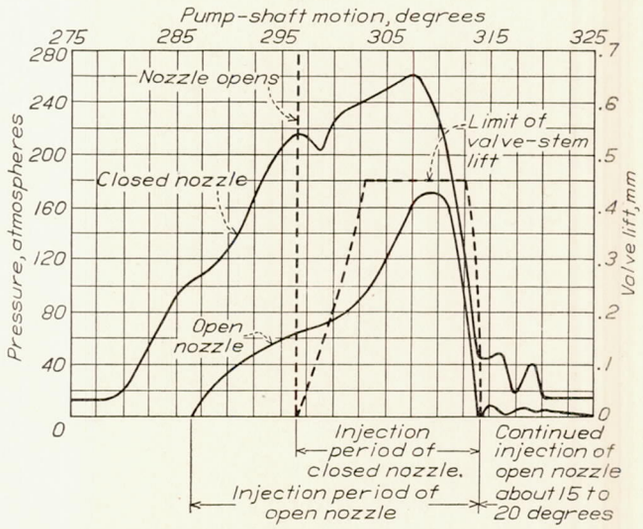

FIGURE 38.—Comparison of pressures with open and closed nozzles

the rate of displacement at the fuel pump to the rate of discharge through the discharge orifice because of the compressibility of the fuel, but he does not consider methods of correcting for the compressibility. He presents a comparison of open and closed nozzles and gives data on the instantaneous pressures with both types. (Fig. 38.) It is not stated how the data were obtained. He states that with an open nozzle when cut-off occurs the fuel under pressure in the fuel injection line continues to discharge through the discharge orifice until the pressure has reached the pressure in the combustion chamber. This is correct, but since most of the fuel under pressure will flow out through the by-pass valve of the pump, the rate of pressure drop will be extremely rapid, as was shown in reference 18, and only a small part of the fuel left under compression will continue to discharge through the discharge orifice. The case that Wild cites compares to the case presented in this report where it is considered that there is a by-pass valve at the entrance to the injection tube which closes instantaneously when cut-off occurs. As has been pointed out, this is an extreme condition and will not occur in practice, because the check valve does not close instantaneously. Wild concludes that the fuel volume under pressure should be as small as possible. The present investigation has shown that injection tubes for small high-speed engines can be as long as 30 to 40 in. without presenting any disadvantages to the injection of the fuel, and that it is more important to employ a tube diameter sufficiently large to insure laminar flow through it, than it is to decrease the fuel volume under pressure to a minimum. Wild has correctly stated that the speed of the injection pump materially affects the injection pressure and the atomization and dispersion of the fuel jet. He states that to compensate for this variation it is necessary to employ injection pressures at high speeds considerably higher than are necessary for good atomization. This is, at best, a compromise method that must result in the injection characteristics being correct for only one speed. For constant-speed operation this will prove satisfactory,

but for variable-speed operation either a variable-velocity-cam pump with a constant time of injection, an injection system similar to that described by the author in reference 18, or a system similar to that described by Rosen in reference 30, in which the initial opening of the injection valve is cam-controlled, will probably prove more satisfactory. Wild's value for the compressibility of fuel oil, 0.0001 part of the original volume per atmosphere, gives a value of 147,000 lb. per sq. in. for the bulk modulus. This value is probably too low. Hersey gives a value of 284,000 lb. per sq. in. (reference 20) chosen from the values for fuel of similar properties, and Alexander (reference 21) determined the value experimentally to be 296,000 lb. per sq. in.

Work of Gerrish and Voss (reference 32).—Gerrish and Voss have done some preliminary work at the Langley Memorial Aeronautical Laboratory on the rates of fuel discharge from an automatic injection valve. The injection valve and the fuel pump were the same as employed by Spanogle and Foster (reference 6) in their investigation on the effect of multi-orifice nozzles on engine performance. The apparatus that Gerrish and Voss employed was similar to that used by De Juhasz. (Reference 31.) The method consisted of intercepting the fuel discharge from the injection valve for an interval of 0.5° rotation of the fuel pump. The results, though brief, are extremely interesting. The start and stop of the fuel spray from the injection valve was also observed with an oscilloscope. (Reference 29.) Figure 39 shows the total displacement of the pump plunger and also the rate of displacement obtained by drawing tangents to the total displacement curve. Figure 40 shows the

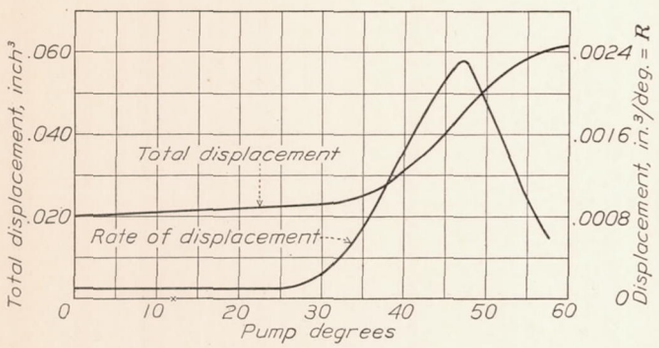

FIGURE 39.—Displacement curves for fuel pump used by Gerrish. Injection valve opening pressure=3,000 lb./sq. in.; pump speed=750 r. p. m.; total area of discharge orifices=0.0113 sq. in.; injection tube diameter=0.120 in.; injection tube length=36 in.; by-pass valve closes at 6°; by-pass valve opens at 41.5°

start and stop of injection as measured with the oscilloscope, the rate of discharge from the injection valve measured with the apparatus, the rate of discharge computed according to the Allievi theory, and the record of the movement of the stem of the automatic injection valve. The curve shows that there was no appreciable discharge until 10° after the start of injection. The discharge before this time, though plainly visible with the oscilloscope, was barely sufficient to be measured. The rate of discharge increased rapidly from 34 to 45 pump degrees. At this point, cut-off occurred and the discharge dropped to a small amount, and dwindled to zero. The motion of the injection valve stem was recorded by the same method as shown in Figure 6. Because of the light spring used in the injection valve it was necessary to limit the lift of the

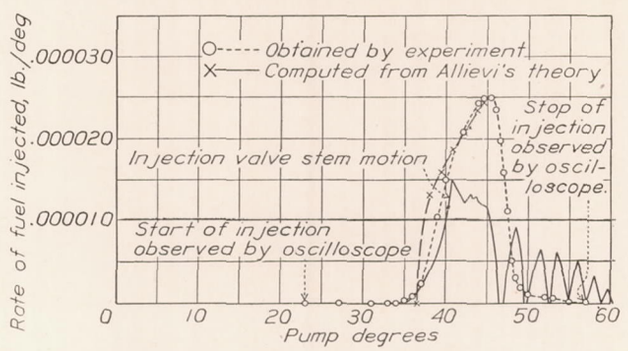

FIGURE 40.—Injection valve opening pressure=3,000 lb./sq. in.; pump speed =750 r. p. m.; total area of discharge orifices=0.0113 sq. in.; injection tube diameter=0.120 in.; injection tube length=36 in.; by-pass valve closes at 6°; by-pass valve opens at 41.5°

stem to 0.20 in. in order to prevent oscillations of the stem that would open and close the injection valve during the injection period. Consequently, the record can not be used for a pressure analysis. The stem movement record was not synchronized with the rate-of-discharge data. It is seen, however, that the period during which the injection valve remained opened corresponds closely to the period during which there was an appreciable discharge from the injection valve. The afterdischarge apparently took place during the bouncing of the stem. An explanation of the fact that the oscilloscope showed a discharge from the injection valve, even though no lift was recorded on the stem, is found in the rate of displacement of the fuel pump and in the instantaneous pressures computed according to the Allievi theory. (Table X.) The primary pressure maintained in the injection tube between injections was 150 lb. per sq. in. There was no check valve between the pump and the injection tube. At the point in the plunger stroke at which the by-pass valve closed, the plunger was moving at a velocity that was not sufficient to maintain either the injection valve opening pressure (3,000 lb. per sq. in.) or the injection valve closing pressure (1,600 lb. per sq. in.). Consequently, the injection valve did not open until there was sufficient pressure on the stem to equal the valve opening pressure. This opening occurred between 39.4° and 40.8°, Table X. There was, however, sufficient leakage through the injection valve before this time so that a spray was formed which was sufficient to be observed by the oscilloscope but was scarcely sufficient to be weighed. A comparison of the computed and measured rates of discharge shows a close agreement, particularly for the time at which the main discharge started and the time at which it stopped.

TABLE X

COMPUTATION OF PRESSURES FOR RATES OF DISCHARGE SHOWN IN FIGURE 40

1	2	3	4	5	6	7	8	9		10		11		12
t L/s sec.	t deg.	t deg. total	V_0 (in./deg.) x10^3	v_1 in./sec.	$F(t)$ $\rho s v$ lb./sq. in.	$F(t-L/s)$ lb./sq. in.	p_k+ $F(t-L/s)$ lb./sq. in.	$p_k+s\rho v_{1\,t-L/s}$ lb./sq. in.		$p_k+2s\rho v_{1\,t-L/s}$ lb./sq. in.		p_2 lb./sq. in.		$-W$
0	0	6.0	0.10	39.7	188	0	150	150		150		150		
.5	1.5	7.5	.10	39.7	188	0	150	150		150		150		
1.0	2.9	8.9	.10	39.7	188	188	350	350		550		550		200
1.5	4.4	10.4	.10	39.7	188	188	350	350		550		550		200
2.0	5.8	11.8	.10	39.7	188	188	350	350		550		550		200
2.5	7.3	13.3	.10	39.7	188	188	350	350		550		550		200
3.0	8.7	14.7	.10	39.7	188	188	350	350	550	550	950	550	950	200
3.5	10.2	16.2	.10	39.7	188	188	350	350	550	550	950	550	950	200
4.0	11.6	17.6	.10	39.7	188	188	350	350	550	550	950	550	950	200
4.5	13.1	19.1	.10	39.7	188	188	350	350	550	550	950	550	950	200
5.0	14.5	20.5	.10	39.7	188	188	350	350	550	550	950	550	950	200
5.5	16.0	22.0	.10	39.7	188	188	350	350	550	550	950	550	950	200
6.0	17.4	23.4	.10	39.7	188	188	350	350	550	550	950	550	950	200
6.5	18.9	24.9	.10	39.7	188	188	350	350	550	550	950	550	950	200
7.0	20.3	26.3	.11	43.7	207	188	350	350	550	550	950	550	950	200
7.5	21.8	27.8	.15	59.5	282	188	350	350	550	550	950	550	950	200
8.0	23.2	29.2	.20	79.4	371	207	350	350	550	550	950	550	950	200
8.5	24.7	30.7	.29	115.2	545	282	450	450	650	750	1,150	750	1,150	300
9.0	26.1	32.1	.39	155.0	734	371	500	500	700	850	1,250	850	1,250	350
9.5	27.6	33.6	.52	207.0	980	545	700	700	900	1,250	1,650	1,250	1,650	550
10.0	29.0	35.0	.70	278.0	1,315	734	900	900	1,100	1,650	2,050	1,650	2,050	750
10.5	30.5	36.5	.90	358.0	1,695	980	1,050	1,050	1,350	1,950	2,550	1,950	2,550	900
11.0	31.9	37.9	1.13	449.0	2,125	1,315	1,450	1,450	1,800	2,750	3,450	2,750	1,850	1,300
11.5	33.4	39.4	1.38	548.0	2,595	1,695	1,850	1,850	2,400	3,550	4,650	1,900	2,650	
12.0	34.8	40.8	1.63	647.0	3,060	2,125	2,300	2,300	3,050	4,450	5,950	2,500	3,650	
12.5	36.3	42.3	0	0	0	2,595	2,750	2,750	3,650	5,350	7,150	3,200	4,650	
13.0	37.7	43.7	0	0	0	3,060	3,200	3,200	4,500	6,250	8,850	3,850	5,800	

Work of Gasterstädt (reference 33).—Gasterstädt has published some interesting information relative to the injection system of the Junkers-Diesel aircraft engine. The injection system consists of four injection valves and two injection pumps. Each pump supplies fuel to two valves. The pumps have the same method of fuel control as that illustrated in Figure 4. Open nozzles are employed, and a ball-check valve is mounted between the pump and the short injection tubes. He has correctly stated that the degree of atomization of the fuel spray increases with a decrease in the size of the discharge orifice. (Reference 17.) The use of short tubes is recommended, since, according to Gasterstädt, it causes the resistance to flow to be small and minimizes after-dribbling. The present investigation has shown that the resistance to flow can be made negligible by the use of the correct injection tube diameter, even though the injection tube is of sufficient length to permit the mounting of the fuel pumps in a single unit instead of mounting each fuel pump as close to the combustion chamber as possible, as is the case in the Junkers engine. It is possible that after-dribbling may be more marked with long injection tubes, if the check valve at the entrance to the injection tube closes instantaneously. However, the work of the author on the common-rail system (reference 18), has shown that even with an injection tube 70 in. in length the drop of pressure at the discharge orifice is extremely rapid when cut-off occurs. In fact, the rate of pressure drop was shown to be virtually independent of the injection tube length for tubes from 13 in. to 70 in. in length. These results showed that the effect of injection tube length on after-dribbling has been overestimated.

Gasterstädt has measured the maximum recorded injection pressures at the injection pump and at the discharge orifice for various speeds and loads. His results are shown in Figure 41. It is noticed that the maximum injection pressures recorded at the fuel pump vary as the 1.64 power of the engine speed at full load and as the 1.60 power at half load. (Compare with equation (2).) Consequently, as has been

stated before, the rate of spray penetration and the spray atomization both vary with engine speed. With the Junkers injection system, it is also noted that there is an appreciable pressure drop between the fuel pump and the discharge orifice. This may be caused either by pressure-wave phenomena or by resistance to flow in the injection tube.

Work of "Oil Engine Designer" (reference 26).—An anonymous investigator who signs himself "Oil Engine Designer" has presented experimental records of the lift of an automatic injection valve stem, together with an analysis of the instantaneous pressure occurring at the discharge orifice of the injection valve. The record he obtained is shown in Figure 42. His analysis is based on the assumption that the compressibility of the fuel is negligible. He states that as the injection valve stem starts to rise the volume of fuel around the stem is increased and the fuel pressure drops. This continues until the stem having reached its maximum lift starts toward the seat again, actually strikes the seat and causes the pressure to build up and reopen the valve. The cycle repeats itself so that the pressures appear as plotted in the lower half of Figure 42. Actually, as has been shown by the present work, this is not the case. In the first place, any analysis based on the assumption that the fuel is not compressible is fundamentally in error. In practice the additional volume in the injection valve caused by the lift of the valve stem is too small to affect the pressure conditions. The conditions shown in Figure 42 indicates that the stem lift of the injection valve was not sufficiently limited and consequently the same phenomenon occurred as is shown in Figure 10, in which the rate of pressure rise was sufficiently great to cause the valve stem and spring to oscillate at the free period of the system. This does not result in the pressure at the discharge orifice dropping to zero, unless the size of the injection valve stem is out of proportion to the rest of the injection system. Figure 10 shows that the maximum pressure may occur at the maximum stem lift which is contrary to the assumed pressure diagram given by the investigator. (Fig. 42.) If detrimental oscillations of the injection valve stem do occur, they can be eliminated by stopping the stem at a lift which is less than that which the injection pressures will impart to the stem, as is the case in Figure 40.

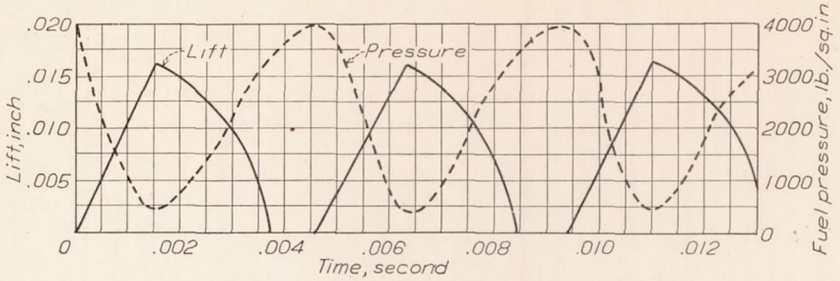

FIGURE 42.—Injection valve stem record as recorded and assumed pressure

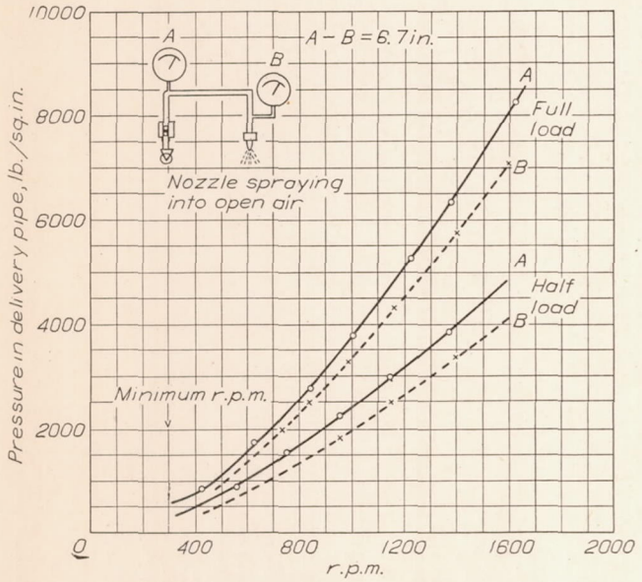

FIGURE 41.—Effect of engine r. p. m. on maximum injection pressures for Junkers aircraft Diesel engine

LANGLEY MEMORIAL AERONAUTICAL LABORATORY,
NATIONAL ADVISORY COMMITTEE FOR AERONAUTICS,
LANGLEY FIELD, VA., *March 6, 1931.*

REFERENCES

1. Wild, J. E.: Combustion Chambers, Injection Pumps, and Spray Valves of Solid-Injection Oil Engines. S. A. E. Journal, May, 1930.
2. Joachim, W. F.: Combustion in High-Speed Oil Engines. Paper Presented at the Second National Oil and Gas Power Conference at the Pennsylvania State College, June, 1929.
3. Hausfelder, Ludwig: High-Speed Oil Engines for Vehicles, Part III. N. A. C. A. Technical Memorandum No. 410. May, 1927.
4. Hausfelder, Ludwig: Injection Systems for High-Speed Diesel Engines, Parts IV and V. Diesel Power, April, 1930, pp. 202–204; June, 1930, pp. 311–313.
5. Woolson, L. M.: The Packard Diesel Aircraft Engine. S. A. E. Journal, April, 1930.
6. Spanogle, J. A., and Foster, H. H.: Performance of a High-Speed Compression-Ignition Engine Using Multiple Orifice Fuel Injection Nozzles. N. A. C. A. Technical Note No. 344, June, 1930.
7. Ricardo, H.: Compression Ignition Aero Engines. The Characteristics, Present Position, and Future Possibilities of Heavy Oil Engines for Aircraft Propulsion Duties. Aircraft Engineering (England). Vol. 1, No. 3, May, 1929, pp. 83–88.
8. Neumann, Kurt: The Diesel as a Vehicle Engine. N. A. C. A. Technical Memorandum No. 467, June, 1928.
9. Rheim, Dr. W.: Untersuchungen über den Einspritzvorgang bei Dieselmaschinen. Zeitschrift des Vereines Deutscher Ingenieure, June, 1924.
10. Schweitzer, P. H.: Factors in Nozzle Design in the Light of Recent Oil-Spray Research. Paper Presented before the Third National Oil and Gas Power Conference at the Pennsylvania State College, June, 1930.
11. Miller, H. E., and Beardsley, E. G.: Spray Penetration with a Simple Fuel Injection Nozzle. N. A. C. A. Technical Report No. 222, 1926.
12. Gelalles, A. G.: The Effect of Orifice Length-Diameter on Spray Characteristics. N. A. C. A. Technical Note No. 352, October, 1930.
13. Sass, Dr. F.: Kompressorlose Dieselmaschinen. Berlin, Verlag von Julius Springer, 1929; 395 pp., 328 fig., 29 tables, pp. 207–235.
14. Triebnigg, Heinrich: Der Einblase- und Einspritz-vorgang bei Dieselmaschinen, Julius Springer, Vienna, 1925.
15. Woltjen, Alfred: Ueber die Feinheit der Brennstoffzerstaübung in Oelmaschinen. Technische Hochuschule, Darmstädt, 1925.
16. Kuehn, Dr. R.: Atomization of Liquid Fuels, Part III. N. A. C. A. Technical Memorandum, No. 331, September, 1925.
17. Sass, Dr. F.: Kompressorlose Dieselmaschinen. Berlin, Verlag von Julius Springer, 1929; 395 pp., 328 fig., 29 tables, pp. 41–49.
18. Rothrock, A. M.: Pressure Fluctuations in a Common-Rail Fuel Injection System. N. A. C. A. Technical Report No. 363, 1930.
19. Allievi, Lorenzo: Theory of Water Hammer. Translated by Eugene E. Halmos. Rome, Tipographia Riccardo Garroni. Piazza Mignelli, 23, 1925.
20. Hersey, Mayo D.: Viscosity of Diesel Engine Fuel Oil under Pressure. N. A. C. A. Technical Note No. 315, September, 1929.
21. Alexander, D. H.: Airless Injection and Combustion of Fuel in the High-Compression Heavy Oil Engine. Volume 39 of Transactions of the Institute of Marine Engineers (England), Sessions 1927–28, pp. 366–414.
22. Rothrock, A. M.: Injection Lags in a Common-Rail Fuel Injection System. N. A. C. A. Technical Note No. 332, February, 1930.
23. A. S. M. E.: Report of American Society of Mechanical Engineers—Special Committee on Fluid Meters. Second Edition, 1927. "Fluid Meters—Their Theory and Applications."
24. Gelalles, A. G.: Coefficients of Discharge of Fuel Injection Nozzles for Compression-Ignition Engines. N. A. C. A. Technical Report No. 373, 1931.
25. Joachim, W. F., Hicks, C. W., and Foster, H. H.: The Design and Development of an Automatic Injection Valve with an Annular Orifice of Varying Area. N. A. C. A. Technical Report No. 341, 1930.
26. Anon.: Oil Engine Designer. Design of Airless Injection Engines—An Examination of the Operation of Fuel Injectors. British Motorship, July, 1929, pp. 154–157.
27. Matthews, Robertson, and Gardiner, A. W.: The Time Lag and Interval of Discharge with a Spring Actuated Fuel Injection Pump. N. A. C. A. Technical Note No. 159, September, 1923.
28. Matthews, Robertson: Discharge Characteristics of a High Speed Fuel Injection System. N. A. C. A. Technical Note No. 213, February, 1925.
29. Hicks, C. W., and Moore, C. S.: The Determination of Several Spray Characteristics of a High-Speed Oil Engine Injection System with an Oscilloscope. N. A. C. A. Technical Note No. 298, September, 1928.
30. Rosen, C. G. A.: The Diesel Engine Tractor and Excavator. Paper Presented before the Third National Oil and Gas Power Conference at the Pennsylvania State College, June, 1930.
31. De Juhasz, K. J.: Some Results of Oil-Spray Research. Paper Presented before the Second National Oil and Gas Power Conference at the Pennsylvania State College, June, 1929.
32. Gerrish, Harold C., and Voss, Fred: Investigation of the Discharge Rate of a Fuel-Injection System. N. A. C. A. Technical Note No. 373, April, 1931.
33. Gasterstädt, Dr.: Development of the Junkers-Diesel Aircraft Engine. N. A. C. A. Technical Memorandum No. 565, May, 1930.

U. S. GOVERNMENT PRINTING OFFICE: 1931

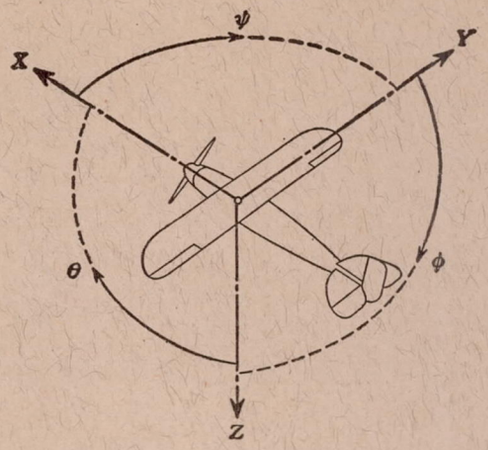

Positive directions of axes and angles (forces and moments) are shown by arrows

Axis		Force (parallel to axis) symbol	Moment about axis			Angle		Velocities	
Designation	Symbol		Designation	Symbol	Positive direction	Designation	Symbol	Linear (component along axis)	Angular
Longitudinal	X	X	rolling	L	$Y \longrightarrow Z$	roll	ϕ	u	p
Lateral	Y	Y	pitching	M	$Z \longrightarrow X$	pitch	θ	v	q
Normal	Z	Z	yawing	N	$X \longrightarrow Y$	yaw	ψ	w	r

Absolute coefficients of moment

$$C_l = \frac{L}{qbS} \qquad C_m = \frac{M}{qcS} \qquad C_n = \frac{N}{qbS}$$

Angle of set of control surface (relative to neutral position), δ. (Indicate surface by proper subscript.)

4. PROPELLER SYMBOLS

D, Diameter.

p, Geometric pitch.

p/D, Pitch ratio.

V', Inflow velocity.

V_s, Slipstream velocity.

T, Thrust, absolute coefficient $C_T = \frac{T}{\rho n^2 D^4}$

Q, Torque, absolute coefficient $C_Q = \frac{Q}{\rho n^2 D^5}$

P, Power, absolute coefficient $C_P = \frac{P}{\rho n^3 D^5}$.

C_s, Speed power coefficient $= \sqrt[5]{\frac{\rho V^5}{P n^2}}$.

η, Efficiency.

n, Revolutions per second, r. p. s.

Φ, Effective helix angle $= \tan^{-1}\left(\frac{V}{2\pi r n}\right)$

5. NUMERICAL RELATIONS

1 hp = 76.04 kg/m/s = 550 lb./ft./sec.
1 kg/m/s = 0.01315 hp
1 mi./hr. = 0.44704 m/s
1 m/s = 2.23693 mi./hr.

1 lb. = 0.4535924277 kg.
1 kg = 2.2046224 lb.
1 mi. = 1609.35 m = 5280 ft.
1 m = 3.2808333 ft.